

ABSTRACT

Title of Dissertation: Single and Multiresponse Adaptive Design of Experiments with Application to Design Optimization of Novel Heat Exchangers

Vikrant Chandramohan Aute
Doctor of Philosophy, 2009

Directed By: Shapour Azarm, Professor
Department of Mechanical Engineering

Engineering design optimization often involves complex computer simulations. Optimization with such simulation models can be time consuming and sometimes computationally intractable. In order to reduce the computational burden, the use of approximation-assisted optimization is proposed in the literature. Approximation involves two phases, first is the Design of Experiments (DOE) phase, in which sample points in the input space are chosen. These sample points are then used in a second phase to develop a simplified model termed as a metamodel, which is computationally efficient and can reasonably represent the behavior of the simulation response. The DOE phase is very crucial to the success of approximation assisted optimization.

This dissertation proposes a new adaptive method for single and multiresponse DOE for approximation along with an approximation-based framework for multi-

level performance evaluation and design optimization of air-cooled heat exchangers. The dissertation is divided into three research thrusts. The first thrust presents a new adaptive DOE method for single response deterministic computer simulations, also called SFCVT. For SFCVT, the problem of adaptive DOE is posed as a bi-objective optimization problem. The two objectives in this problem, i.e., a cross validation error criterion and a space-filling criterion, are chosen based on the notion that the DOE method has to make a tradeoff between allocating new sample points in regions that are multi-modal and have sensitive response versus allocating sample points in regions that are sparsely sampled. In the second research thrust, a new approach for multiresponse adaptive DOE is developed (i.e., MSFCVT). Here the approach from the first thrust is extended with the notion that the tradeoff should also consider all responses. SFCVT is compared with three other methods from the literature (i.e., maximum entropy design, maximin scaled distance, and accumulative error). It was found that the SFCVT method leads to better performing metamodels for majority of the test problems. The MSFCVT method is also compared with two adaptive DOE methods from the literature and is shown to yield better metamodels, resulting in fewer function calls.

In the third research thrust, an approximation-based framework is developed for the performance evaluation and design optimization of novel heat exchangers. There are two parts to this research thrust. First, is a new multi-level performance evaluation method for air-cooled heat exchangers in which conventional 3D Computational Fluid Dynamics (CFD) simulation is replaced with a 2D CFD simulation coupled with an ε -NTU based heat exchanger model. In the second part, the methods

developed in research thrusts 1 and 2 are used for design optimization of heat exchangers. The optimal solutions from the methods in this thrust have 44% less volume and utilize 61% less material when compared to the current state of the art microchannel heat exchangers. Compared to 3D CFD, the overall computational savings is greater than 95%.

Single and Multiresponse Adaptive Design of Experiments with Application to
Design Optimization of Novel Heat Exchangers

By

Vikrant Chandramohan Aute

Dissertation submitted to the Faculty of the Graduate School of the
University of Maryland, College Park, in partial fulfillment
of the requirements for the degree of
Doctor of Philosophy
2009

Advisory Committee:

Dr. Shapour Azarm, Chair and Advisor

Dr. Reinhard Radermacher

Dr. Amr Baz

Dr. Steven Gabriel (Dean's Representative)

Dr. Bao Yang

© Copyright by
Vikrant Chandramohan Aute
2009

Dedication

To all my teachers.

Acknowledgements

I express my sincere gratitude for Dr. Shapour Azarm for accepting me as his graduate student. His continued advice, the constant encouragement for paying attention to details and conducting objective research has brought my dissertation to this stage. I also thank my committee members, Dr. Reinhard Radermacher (Co-advisor), Dr. Amr Baz, Dr. Steven Gabriel (Dean's Representative) and Dr. Bao Yang for their time, efforts and generous comments and suggestions.

I am fortunate to have had the opportunity to work at the Center for Environmental Energy Engineering (CEEE) led by Dr. Radermacher and the Design Decision Support Laboratory (DDSL) led by Dr. Azarm. Special thanks goes to Dr. Radermacher for providing access to enormous computing resources and flexible work hours, without which this dissertation would have not been completed in time. I would also like to thank my colleagues and former colleagues at CEEE & DDSL, namely, Jon Winkler, Varun Singh, Dr. Mian Li, Dr. Genzi Li and Dr. Nathan Williams for their inputs, critique and the wonderful time we spent together working on research projects. A special word of thanks goes to my colleague from CEEE, Mr. Omar Abdelaziz for lending his CFD expertise, insights and his relentless efforts and assistance in conducting CFD simulations.

I would like to acknowledge the financial support for my thesis related research that was provided in part through the Office of Naval Research under contract number N000140710468. Such support does not constitute an endorsement by the funding agency of the opinions expressed in the thesis.

Finally, I thank my wife and kids for their understanding of all the rightful time which I was not able to spend with them.

I am glad that I decided to learn and explore the field of optimization.

Table of Contents

Dedication.....	ii
Acknowledgements.....	iii
Table of Contents.....	v
List of Tables.....	ix
List of Figures.....	x
Nomenclature.....	xiii
Chapter 1 Introduction.....	1
1.1 Motivation.....	1
1.2 Dissertation Objective.....	6
1.3 Assumptions.....	7
1.4 Research Thrusts.....	7
1.4.1 Research Thrust-1: Single Response Adaptive DOE.....	8
1.4.2 Research Thrust-2: Multiresponse Adaptive DOE.....	8
1.4.3 Research Thrust-3: Approximation Based Framework for Design Optimization of Novel Heat Exchangers.....	9
1.5 Organization of the Dissertation.....	9
Chapter 2 Definition and Terminology.....	12
2.1 Introduction.....	12
2.2 Multi-objective Optimization.....	12
2.2.1 Simulation.....	13
2.2.2 Input Space, Experiment and Design.....	13
2.3 Dominance and Pareto Set.....	14
2.4 Methods for solving Multi-objective optimization problems.....	15
2.4.1 Overview.....	15
2.4.2 Genetic Algorithms.....	17
2.4.3 Multiobjective Genetic Algorithm.....	18
2.5 Approximation Assisted Optimization.....	20
2.5.1 Overview.....	20
2.5.2 Maximum Entropy Design.....	23
2.5.3 Kriging Method.....	25
2.5.4 Metamodel Performance Metrics: Errors Verification.....	30
2.5.5 Maximin-Scaled Distance (MSD) Method.....	33
2.5.6 Accumulative Error (ACE) Method.....	34
Chapter 3 Single Response Adaptive Design of Experiments.....	36
3.1 Introduction.....	36
3.2 Related Work.....	37
3.3 Terminology.....	44
3.3.1 Response Characteristics.....	44

3.3.2 Leave-One-Out Cross-validation Error.....	46
3.3.3 Level of Dominance.....	50
3.4 Proposed Cross-Validation Based Approach for Adaptive DOE	51
3.4.1 Overview of Proposed Approach.....	52
3.4.2 Choice of Initial Design.....	53
3.4.3 LOO Error Prediction	54
3.4.4 Space-filling Criterion	55
3.4.5 Choosing Next Sample	56
3.4.6 Design Update.....	63
3.4.7 Stopping Criteria.....	63
3.4.8 Step-by-Step Description of Proposed Approach.....	63
3.5 Application Examples.....	65
3.5.1 Metamodel Comparison: Factor of Improvement.....	67
3.5.2 Results for the Proposed Approach.....	67
3.5.3 Comparison with MED Method.....	71
3.5.4 Comparison with MSD Method.....	78
3.5.5 Comparison with ACE Method	82
3.5.6 Effect of Initial Design.....	85
3.5.7 Scalability to Higher Dimensions	88
3.5.8 Comments on Computational Effort.....	89
3.6 Empirical Procedure for Function Call Allocation	90
3.6.1 Problem Statement.....	90
3.6.2 Proposed Empirical Procedure.....	90
3.6.3 Numerical Experiments	92
3.7 Summary	94
Chapter 4 Multiresponse Adaptive Design of Experiments	97
4.1 Introduction.....	97
4.2 Literature Review.....	98
4.3 Multiresponse Adaptive DOE Approach	102
4.3.1 Overview of the Proposed Approach.....	102
4.3.2 Choice of Initial Design.....	103
4.3.3 LOO Error Calculation	103
4.3.4 Space-filling Criterion	104
4.3.5 Choosing Next Sample	104
4.3.6 Design Update.....	108
4.3.7 Stopping Criteria.....	108
4.3.8 Step-by-Step Description of the MSFCVT Approach.....	108
4.4 Application Examples.....	110
4.4.1 Numerical Example-1	110
4.4.2 Numerical Example – 2	117
4.4.3 Application to Numerical Test Problems.....	122
4.4.4 Comparison Between Formulations.....	127
4.5 Summary.....	129
Chapter 5 Approximation Based Optimization Framework for Design of Novel Heat Exchangers.....	132

5.1 Introduction.....	132
5.2 Background information	134
5.2.1 Tube-Fin Heat Exchangers	134
5.2.2 Microchannel Heat Exchangers	136
5.2.3 CoilDesigner	137
5.3 Literature Review.....	138
5.4 Novel Heat Exchanger Concepts	140
5.4.1 Potential Geometries.....	140
5.4.2 Chosen Geometry.....	141
5.4.3 Performance Evaluation Criteria.....	143
5.5 Performance Evaluation and Design Optimization Approach.....	143
5.5.1 Assumptions.....	144
5.5.2 Hybrid Performance Evaluation Approach.....	145
5.5.3 Geometry Representation and Parameterization.....	147
5.5.4 CFD Analysis.....	149
5.5.5 Verification with 3D CFD	150
5.5.6 Design Optimization Approach	154
5.6 Application of Single Response Adaptive DOE.....	157
5.6.1 Design Variables.....	157
5.6.2 Metamodel Development – SFCVT Method.....	158
5.6.3 Metamodel Development- MSFCVT Method.....	160
5.7 Design Optimization	161
5.7.1 Problem Formulation	161
5.7.2 Pareto Optimal Designs – Approximation Perspective	164
5.7.3 Pareto Optimal Designs – Thermodynamic Perspective	167
5.8 Summary	168
Chapter 6 Conclusion.....	170
6.1 Summary	170
6.2 Conclusions.....	172
6.2.1 Single Response Adaptive DOE	172
6.2.2 Multiresponse Adaptive DOE.....	173
6.2.3 Approximation Based Framework for Design of Novel Heat Exchangers	
.....	174
6.3 Contributions.....	176
6.4 Future Research Directions.....	177
Appendix-A Test Problem Suite.....	180
Bibliography	192

List of Tables

Table 3.1 Test Matrix for Comparison	67
Table 4.1 Test Matrix for Multiresponse Adaptive DOE Method.....	122
Table 5.1 Design variables for metamodel	158
Table 5.2 Optimization problem parameters	162
Table 5.3 MOGA Parameters	162
Table 5.4 Sample Pareto solutions.....	163
Table A.1 Single response test problems.....	181
Table A.2 Multiresponse test problems	190

List of Figures

Figure 1.1 (a) Conventional optimization, and (b) Approximation assisted optimization	3
Figure 1.2 Generic flow chart for (a) Non-adaptive DOE and (b) Adaptive DOE.....	5
Figure 1.3 Organization of Dissertation.....	11
Figure 2.1 Black-box simulations, (a) Single response and (b) Multiresponse	13
Figure 2.2 Dominated points and Pareto points.....	15
Figure 2.3 Genetic Algorithms, (a) design representations and (b) operators	18
Figure 2.4 MOGA flow chart.....	20
Figure 2.5 Approximation, (a) offline and (b) online	23
Figure 2.6 (a) Initial designs and (b) maximum entropy designs	24
Figure 2.7 Correlation vs. Euclidean distance for different θ and p values.....	27
Figure 3.1 Multi-level design problem	44
Figure 3.2 Regions of sensitive response.....	45
Figure 3.3 Highly multimodal response function	46
Figure 3.4 LOO error calculation.....	48
Figure 3.5 LOO Error (a) Response surface for P8, (b) initial design, (c) Actual LOO error and (d) relative LOO error	49
Figure 3.6 (a) Response for Himmelblau’s function, (b) initial design, (c) LOO error surface, (d) MSE response surface , (e) MSE vs. LOO Pareto and (f) new designs based on MSE vs. LOO Pareto	59
Figure 3.7 RMSE for problem P3	60
Figure 3.8 MAE for problem P3	61
Figure 3.9 MAS for problem P3	61
Figure 3.10 Flow chart for the proposed single response adaptive DOE method	64
Figure 3.11 MAS for designs from the proposed SFCVT approach	68
Figure 3.12 MAS for the proposed SFCVT approach	69
Figure 3.13 MAS of the SO and MO formulations, using LoD as selection criterion in MO formulation	70
Figure 3.14 MAS comparison of the SO and MO formulation, using Extreme points criteria in MO formulation.....	70
Figure 3.15 MAS comparison for MED vs. SFCVT	73
Figure 3.16 MAS for MED approach	73
Figure 3.17 RMSE FoI of proposed approach over MED method	74
Figure 3.18 MAE FoI of proposed approach over MED method	74
Figure 3.19 RRMSE FoI of proposed approach over MED method	75
Figure 3.20 RMAE FoI of proposed approach over MED method	75
Figure 3.21 Problem P10, (a) MED design, (b) SFCVT design, (c) absolute error using MED and (d) absolute errors using SFCVT	77
Figure 3.22 Problem P10 with modified initial design, (a) MED design, (b) SFCVT design, (c) absolute error using MED and (d) absolute errors using SFCVT.....	78
Figure 3.23 MAS comparison for MSD vs. SFCVT	79
Figure 3.24 MAS for MSD method	80

Figure 3.25 RMSE FoI of proposed approach over MSD method	80
Figure 3.26 MAE FoI of proposed approach over MSD method	81
Figure 3.27 RRMSE FoI of proposed approach over MSD method.....	81
Figure 3.28 RMAE FoI of proposed approach over MSD method.....	82
Figure 3.29 MAS comparison for ACE vs. SFCVT	83
Figure 3.30 RMSE FoI of proposed approach over ACE method.....	83
Figure 3.31 MAE FoI of proposed approach over ACE method.....	84
Figure 3.32 RRMSE FoI of proposed approach over ACE method	84
Figure 3.33 RMAE FoI of proposed approach over ACE method	85
Figure 3.34 MAS comparison for $5d$ and $10d$ points in initial design.....	86
Figure 3.35 Metamodel RRMSE for $5d$ and $10d$ points in initial design	87
Figure 3.36 Metamodel RMAE for $5d$ and $10d$ points in initial design	87
Figure 3.37 MAS comparison when SFCVT method is applied to higher dimension problems.....	88
Figure 3.38 Points used for developing metamodel.....	93
Figure 3.39 Points used for verification.....	93
Figure 3.40 Resulting MAS for test problems.....	94
Figure 4.1 LOO error tradeoff, (a) Response surface for y_1 , (b) response surface for y_2 , (c) initial design, (d) y_1 vs. y_2 LOO error tradeoff, (e) LOO error surface for y_1 , and (f) LOO error surface for y_2	107
Figure 4.2 Step-by-Step flow chart for MSFCVT approach.....	109
Figure 4.3 Responses for numerical example -1 from Eq. (4.4), (a) Response for y_1 , and (b) Response for y_2	111
Figure 4.4 MED vs. MSFCVT approach, resulting designs and the response surfaces	112
Figure 4.5 DMM vs. MSFCVT, resulting designs and metamodels	115
Figure 4.6 MAS Comparison, (a) Response y_1 and (b) Response y_2	116
Figure 4.7 RRMSE, RMAE and RMSE FoI values for y_1 , from different methods. 116	
Figure 4.8 RMSE for second response y_2	117
Figure 4.9 Error distribution for y_2 , (a) DMM method, and (b) MSFCVT method.. 117	
Figure 4.10 Response surfaces for Numerical Example-2, (a) response y_1 , and (b) response y_2	119
Figure 4.11 Numerical Example-2, (a) MED design, (b) MSFCVT design, (c) MED response y_1 , (d) MSFCVT response y_1 , (e) MED response y_2 , (f) MSFCVT response y_2	120
Figure 4.12 Comparison of RMSE and MAE for response y_1	121
Figure 4.13 Comparison of RMSE and MAE for response y_2	121
Figure 4.14 MAS Comparison for y_1 and y_2 from MED and MSFCVT approaches 121	
Figure 4.15 MAS comparison for MSFCVT method, choosing 1 point vs. 2 points per stage, for problems PM1 - PM4.....	123
Figure 4.16 MAS comparison for MSFCVT method, 1 point vs. 2 points per stage, for problems PM5 – PM8	123
Figure 4.17 MAS for MED vs. MSFCVT method for 2 response case.....	125
Figure 4.18 MED vs. MSFCVT, FoI values for 2 response cases.....	125
Figure 4.19 MAS, MED vs. MSFCVT method for 4 response cases.....	126
Figure 4.20 MED vs. MSFCVT, FoI for 4 response cases.....	127

Figure 4.21 Comparison of MAS for test problems PM1-PM4, for MSFCVT formulation with m objectives vs. $2m$ objectives.....	128
Figure 4.22 Comparison of MAS for test problems PM5-PM8 for MSFCVT formulation with m objectives vs. $2m$ objectives.....	129
Figure 5.1 Schematic of a tube-fin heat exchanger.....	135
Figure 5.2 Schematic of a microchannel heat exchanger	136
Figure 5.3 Concept heat exchanger geometries, Courtesy : NGHX Project (Radermacher et al., 2007), (a) and (b) multiport staggered configurations, (c) circular ports with fin sheet.....	141
Figure 5.4 Proposed NGHX Geometry, (a) 2-D view, (b) 3-D view.....	142
Figure 5.5 Simple shape representation and manipulation	148
Figure 5.6 Different port shapes, (a) simple ports and (b) complex ports	149
Figure 5.7 Automated CFD evaluations	150
Figure 5.8 Air and water pressure drop errors	152
Figure 5.9 Error in predicted outlet temperature	153
Figure 5.10 Errors in outlet temperature vs. Re.....	154
Figure 5.11 Proposed design optimization approach for novel heat exchangers.....	156
Figure 5.12 Metamodel verification results for Air DP and HTC	159
Figure 5.13 Metamodel verification for Air DP and HTC, relative errors	159
Figure 5.14 MSFCVT method verification for air DP and HTC, (a) RMSE, MAE and MAS, (b) RRMSE and RMAE	160
Figure 5.15 Pareto solutions for NGHX approximation assisted optimization	163
Figure 5.16 Sample Pareto designs and their relative volume compared to the baseline microchannel coil volume.....	164
Figure 5.17 CFD vs. Metamodel, percentage errors in predicted performance.....	166
Figure 5.18 Pareto Designs obtained using approximation and verification	166
Figure A.1 Response surface for problem (a) P1 and (b) P2.....	186
Figure A.2 Response surface for problem (a) P3 and (b) P4.....	186
Figure A.3 Response surface for problem (a) P5 and (b) P6.....	187
Figure A.4 Response surface for problem (a) P7 and (b) P8.....	187
Figure A.5 Response surface for problem (a) P9 and (b) P10.....	188
Figure A.6 Response surface for problem (a) P11 and (b) P12.....	188
Figure A.7 Response surface for problem (a) P13 and (b) P14.....	189
Figure A.8 Response surface for problem (a) P15 and (b) P16.....	189

Nomenclature

English Symbols

\hat{y}	Predicted response
\hat{e}_{LOO}	Predicted leave one out error
a_k	k^{th} component of the weight vector
d	dimension,
D	current design
d_{crit}	Cluster threshold
\det	determinant of a matrix
D_{in}	Inner diameter of tube, normalized, [m] or [mm]
D_{out}	Tube outer diameter, [m] or [mm]
ds	Scaled distance
e_{LOO}	Leave one out error
H	Entropy measure
H_s	Horizontal Spacing
I	Identity matrix or vector
K_{max}	Maximum available function calls
L	Tube length, [m] or [mm]
N_{init}	Number of points in initial design for function call allocation procedure
N_v	Number of verifications points
R	Correlation matrix
r	Correlation vector
s	Square root of Mean square prediction error
S	Space-filling metric based on maximin distance
V	Volume, [m ³] or [cm ³]
v	Velocity, [m/s]
V_s	Vertical Spacing
w	Depth of heat exchanger
x	Design variable, input variable
y	True response
Y	random variable, model for local deviations in responses, in Kriging
Z	model of the random process in Kriging

Acronyms

ACE	Accumulative Error
ADP	Air Pressure Drop
AHTC	Air-side Heat Transfer Coefficient [W/m ² K]
CPU	Central Processing Unit (of a computer)
CV	Cross Validation
CVE	Cross Validation Error
CVV	Cross validation variance
DMM	Dependent Meta-Modeling
DOE	Design of Experiments

DP	Pressure drop
HTC	Heat Transfer Coefficient [W/m ² K]
HX	Heat Exchanger
LHC	Latin Hypercubes
LoD	Level of Dominance
LOO	Leave one out
MAE	Maximum Absolute Error
MAS	Metamodel Acceptability Score
MED	Maximum Entropy Design
MO	Multi-Objective
MSD	Maximin Scaled Distance
MSE	Mean Square Error
MSFCVT	Multi-response Space-Filling Cross-Validation Tradeoff
NTU	Number of transfer units
RDP	Refrigerant-side Pressure Drop
RMAE	Relative Maximum Absolute Error
RMSE	Root Mean Square Error
RRMSE	Relative Root Mean Square Error
SFCVT	Space-Filling Cross-Validation Tradeoff
SO	Single Objective

Greek Symbols

ε_{MAS}	Metamodel acceptability threshold
$\hat{\mu}$	Optimal mean from Kriging method
$\hat{\sigma}^2$	Optimal variance from Kriging method
μ	Mean
α	Correlation parameter in the ACE method
ε	Heat exchanger effectiveness
θ	correlation parameter
ρ	Level of dominance
σ^2	Variance

Subscripts and Superscripts

i, j, k	Components of a vector, index
l	Index into a vector
LOO	Leave one out
p	exponent in correlation equations

Chapter 1 Introduction

In this chapter we present the motivation behind this dissertation, the research objectives, and the underlying assumptions, followed by a brief description of the research thrusts.

1.1 Motivation

Real world engineering systems are highly complex in nature and often involve multiple disciplines such as heat transfer analysis, fluid flow analysis, structural analysis, control systems etc. The design of these systems is more complex even considering the recent advances made in the field of distributed and high performance computing. The design and analysis of the individual disciplines is generally carried out with the help of complex simulation models. An example of such a complex simulation is a Computational Fluid Dynamics (CFD) simulation for a heat exchanger. This simulation can take anywhere between a few minutes to several days to execute and converge, not to mention that this is the time required for a single simulation. During optimization in a single or multidisciplinary environment, such a simulation may be invoked by the optimizer several hundred, even several thousand times. Clearly, carrying out a design optimization with such a complex simulation tool is not feasible. Figure 1.1a shows this conventional optimization procedure. A complex engineering simulation such as CFD (Versteeg and Malalasekera, 1995; Anderson, 1995) is used to represent/model the performance of a heat exchanger and is coupled with an optimization or other analysis tools to optimize designs. In order to

alleviate the computational burden associated with the optimization of complex simulations, researchers have proposed a technique called approximation-assisted optimization.

Approximation can generally be summarized as a two-phase process: (a) design of experiments (DOE) phase and (b) development of a metamodel. In the DOE phase, the first step, the complex simulation tool is run for a set of systematically chosen input design points. In the second phase, the inputs design points along with the corresponding simulation results (i.e., response values) are used to develop a metamodel. A metamodel, which is also referred to as a surrogate model, is a simplified numerical model that can reasonably reproduce the simulation results for a set of inputs, but at a fraction of the computational cost. This simplified model is then coupled to (i.e., used by) an optimizer to carry out the design optimization. The optimized design can later be verified by executing the complex simulation using the optimal design variables. The approximation assisted optimization process is shown in Figure 1.1b. Step-1 is the design of experiments process, Step-2 involves the evaluation of the CFD tool for the samples generated in the DOE phase, Step-3 is the development of metamodel and Step-4 is the use of metamodel for optimization and other analysis.

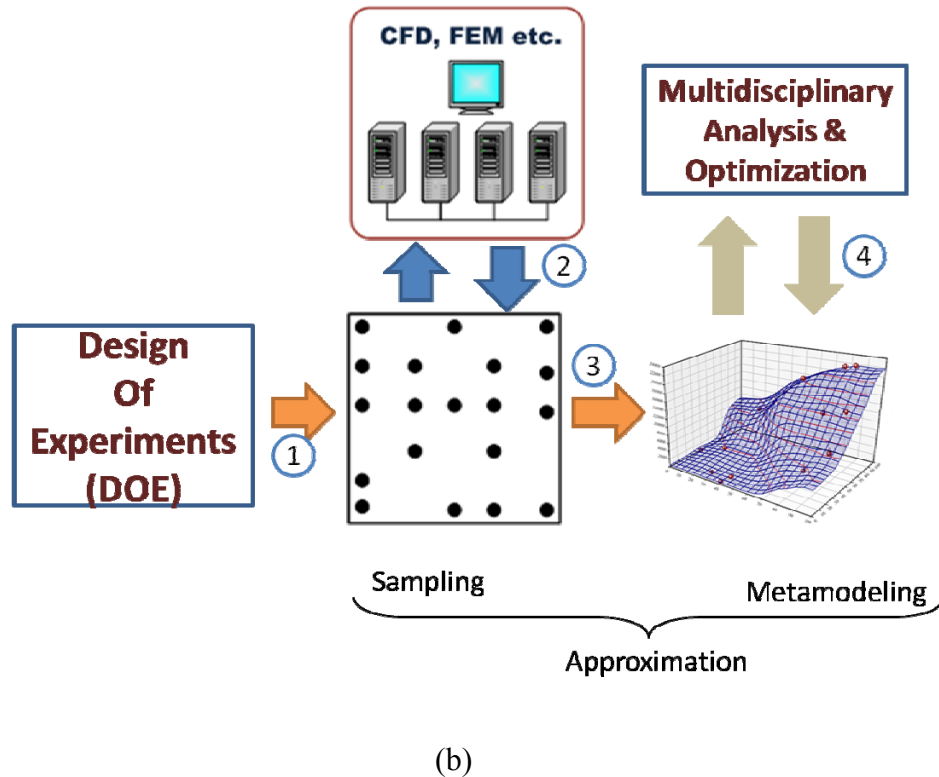
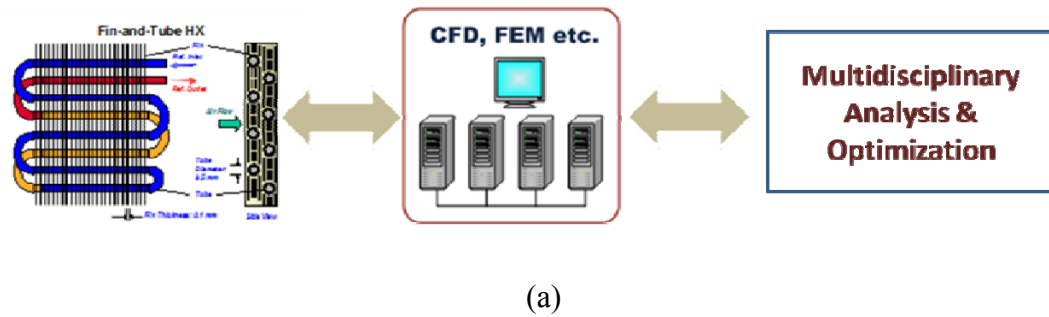


Figure 1.1 (a) Conventional optimization, and (b) Approximation assisted optimization

Several DOE techniques have been introduced in the literature (Myers and Montgomery, 2002; McKay et al., 1979; Currin et al. 1991), such as classical designs, space-filling designs, etc. Examples of metamodeling techniques include response-surface based models (Myers and Montgomery, 2002), statistical methods (Cressie, 1993), radial basis functions (Dyn et al., 1986) and artificial neural networks. Since the metamodel is developed with the (input, output) tuple generated by the simulation

in the DOE phase, clearly this DOE phase has a profound effect on the success or failure of a metamodel. Moreover, the choice of a DOE method also depends upon the metamodeling technique which will be used. For example, classical designs are not suitable for computer simulations and can sometimes result in erroneous models (Sacks et al., 1989; Jin et al., 2001).

Many of the DOE techniques in the literature are such that the design points are generated in a single step, without using any information from the corresponding response or the resulting metamodel. Figure 1.2a shows this non-adaptive approach. Subsequently researchers developed adaptive DOE techniques in which the DOE process was carried out in stages i.e., one or more points were sampled in each stage of the DOE process. In this way, at each stage a metamodel is developed and its performance is evaluated based on relevant criteria and this information is then used to select points in the next stage. It has been shown that in general the adaptive DOE methods are superior (see, e.g., Jin et al., 2002; Li and Azarm, 2006; Lam and Notz, 2007) to non-adaptive methods. Figure 1.2b shows a general flow chart for an adaptive DOE procedure. As shown in Figure 1.2b, the performance of the metamodel is evaluated at each step (or iteration) and new points are sampled based appropriate performance criteria.

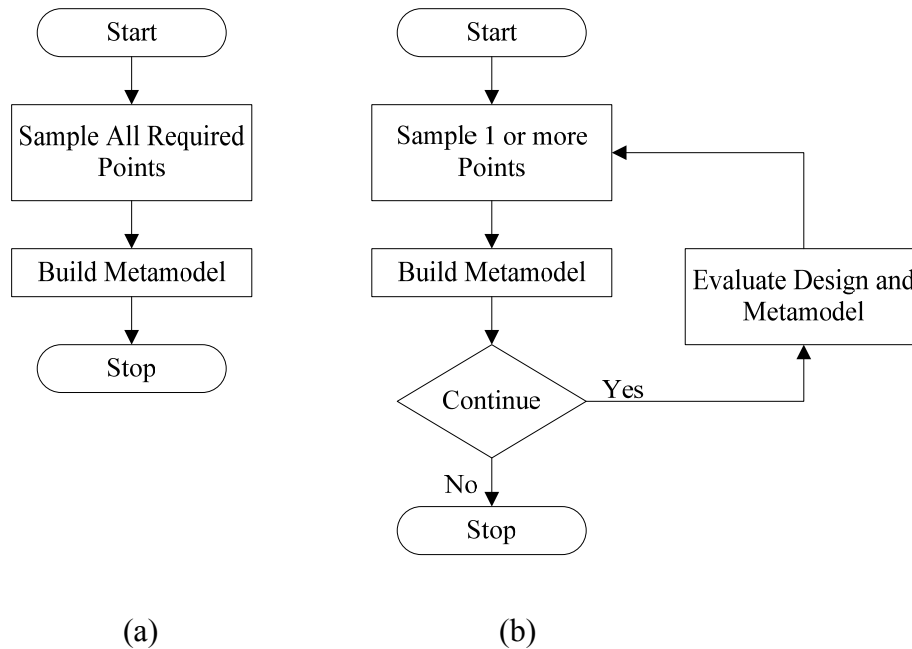


Figure 1.2 Generic flow chart for (a) Non-adaptive DOE and (b) Adaptive DOE

An important aspect of a computer simulation is that it can have multiple outputs. Thus any good approximation method should take into account the multiple responses as well. One could conduct a DOE and develop a metamodel for each individual response, but this would result in excessive simulation runs, probably more than what the designer wants to spare.

A number of adaptive DOE techniques (Jin et al., 2002, Li and Azarm, 2006; Kleijnen, 2004; Li et al., 2006) focus on allocating new points in the input (i.e. design) space based on a space filling criteria, while others focus on metamodel performance metric such as cross-validation only. In terms of approximation for multiple-responses, generally, DOE is seen as an extension of a multiresponse metamodel (Romero et al., 2006, Li et al., 2006) via the use of correlation between responses. This is in contrast to considering the multiple responses individually (i.e.,

developing individual metamodels for each response) in the DOE phase. All of these DOE techniques, except for Jin et al., (2002) have not been applied to design problems with higher dimensions (e.g. 4 - 8 dimensions) nor have been applied to a wide range of test problems to demonstrate their scalability. In some cases (Busby et al., 2007) the resulting statistical metamodels have been compared with response surface methods, which is not a fair comparison. In general, the metamodel performance (i.e., how well the metamodel represents the underlying true function or response) can be improved when the points sampled in the DOE phase systematically cover the entire region of the design space while simultaneously allocating more points in regions that are nonlinear. Moreover, in multiresponse simulations, a good DOE technique should objectively make a tradeoff between multiple responses as well as the space-filling criteria and the metamodel performance and should be scalable to higher than conventional input dimensions and to a wide range of problems.

1.2 Dissertation Objective

The objective of this dissertation is (a) to develop a single-response adaptive design of experiments technique for deterministic black-box computer simulations that is scalable and widely applicable, and an empirical framework for implementing the proposed approach when there is a limit on the computational resources (i.e., the number of simulation calls), (b) to extend the single-response DOE approach to multiresponse adaptive design of experiments technique for deterministic black-box computer simulations, and (c) to develop an approximation-based framework for the performance evaluation and design optimization of novel air-cooled heat exchangers.

1.3 Assumptions

The following assumptions are made in the development of the approach:

- (a) The simulation models are deterministic, i.e., no matter how many times the simulation is invoked, it will always yield the same output for the same inputs.
- (b) The simulation responses are continuous and the models are black-box. In other words, no information about the simulation model or its output is known before hand and no other assumptions are made with regards to its behavior.
- (c) The metamodel developed based on the proposed approach is desired to be globally (i.e. in the entire input space) applicable based on the available computational resources.
- (d) The computational resources available to execute the simulation are limited. In other words, i.e., the number of available simulation calls is fixed and the designer wishes to obtain the best possible metamodel given the DOE points.
- (e) The computational effort for performing a single simulation is much higher than that required for building the DOE and the metamodel.

1.4 Research Thrusts

This dissertation is divided into three research thrusts as discussed in the following sections.

1.4.1 Research Thrust-1: Single Response Adaptive DOE

In this research thrust, an adaptive DOE approach is developed for single response deterministic computer simulations. An adaptive DOE method has to make tradeoffs between allocating new points either in regions of the design space that are sparsely sampled or in regions that correspond to highly sensitive behavior (non-linear and multi-modal) of the response. In this thrust, it is shown how important it is to make a judicious tradeoff between a space-filling criterion and metamodel performance in selecting new experiments. A multiobjective optimization problem is formulated to solve this adaptive DOE problem. The newly developed approach is applied to a suite of 24 test problems to demonstrate its applicability to a wide range of design problems and also its scalability to higher (more than 2) dimensions. The problems in the test suite are compiled from the literature and are challenging (Jin et al., 2002; Li et al., 2006; Busby et al., 2007) problems for adaptive DOE methods.

1.4.2 Research Thrust-2: Multiresponse Adaptive DOE

In this research thrust, an adaptive DOE approach is developed for multiresponse deterministic computer simulations. This is an extension of the approach developed in Research Thrust-1, wherein the problem is viewed as a multi-objective optimization problem of choosing samples while weighing the relative performance of the metamodels for individual responses. This new multiresponse approach is applied to a total of 10 numerical examples from the literature and the results are compared with published results from previous techniques.

1.4.3 Research Thrust-3: Approximation Based Framework for Design Optimization of Novel Heat Exchangers

In this research thrust, a new approach for design optimization and performance evaluation, i.e., heat transfer characteristics and pressure drop, of novel air-cooled heat exchangers in a computationally efficient manner is developed. Conventionally, 3D CFD is used to evaluate the performance of a novel air-cooled heat exchanger such as tube-fin or microchannels. The novel aspect generally refers to a new fin design or a tube bundle design. Due to the computational burden associated with 3D CFD, a small section (i.e., very short length) of the heat exchanger is simulated and the results are assumed to be valid for the entire heat exchanger. Even while simulating a small section of the heat exchanger, the computation time required is in the range of few hours to a few days. A new approach is proposed, in which 2D CFD (instead of 3D CFD) coupled with a ε -NTU heat exchanger model (Jiang et al., 2006) is used to evaluate the performance of heat exchangers in a computationally efficient manner. This new approach is further enhanced with the use of the techniques developed in Research Thrusts-1 and 2 and the resulting metamodels are combined with an optimizer to find optimal heat exchanger design configurations.

1.5 Organization of the Dissertation

The dissertation is organized as shown in Figure 1.3. Chapter 2 provides definitions and terminology used in this dissertation. Also included in Chapter 2 is background information on multiobjective optimization, approximation assisted optimization, and some details on metamodeling and DOE techniques from the literature. Chapter 3 presents the Research Thrust-1, wherein a new approach for

single response adaptive design of experiments is proposed. Chapter-4 presents a new adaptive DOE approach for multiresponse simulations. Chapter-5 presents an approximation based framework for performance evaluation and optimization of air-cooled heat exchangers. Chapter-6 concludes the dissertation with summary, conclusions, research contributions and directions for future research.

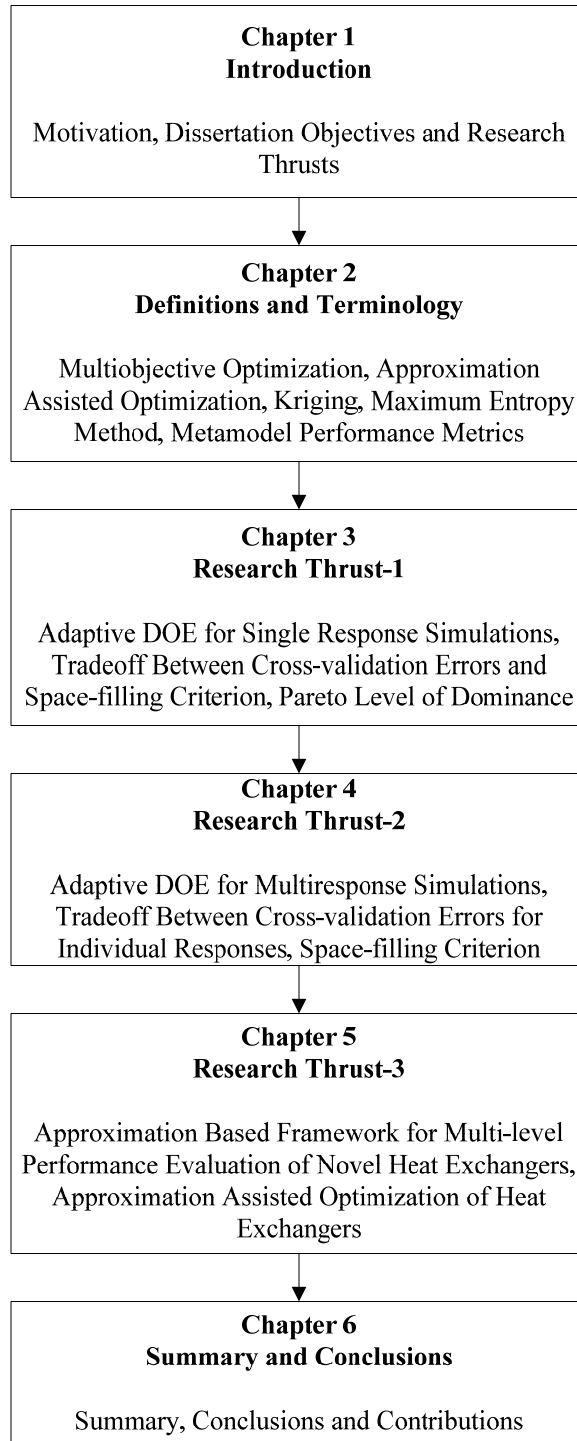


Figure 1.3 Organization of Dissertation

Chapter 2 Definition and Terminology

2.1 Introduction

In this chapter we present several definitions that are used throughout the dissertation. We begin with the formulation of a general multiobjective optimization problem followed by a discussion of the resulting set of solutions and methods to obtain solutions to a multiobjective optimization. This is followed by an introduction to approximation assisted optimization and a short description of relevant design of experiments and metamodeling approaches.

2.2 Multi-objective Optimization

A multi-objective optimization problem (MOOP) can be formulated as follows:

$$\begin{aligned} & \underset{x}{\text{minimize}} && f_i(x) && i = 1, \dots, M \\ & \text{subject to:} && && \\ & && g_j(x) \leq 0 && j = 1, \dots, J \\ & && x_k^L \leq x_k \leq x_k^U && k = 1, \dots, d \end{aligned} \tag{2.1}$$

where f_i refers to the i^{th} objective of the problem, x is a vector of d design variables, i.e., $x = (x_1, x_2, \dots, x_d)^T$, where T indicates a transpose. There are M objectives that are to be minimized. It is assumed that at least two of the M objectives are conflicting in nature. The functions g_1, \dots, g_J are J inequality constraints. The vectors x_k^L and x_k^U indicate the lower and the upper bounds of the variable x_k .

2.2.1 Simulation

A computer program that can calculate the values of f_i and g_j is termed as a *simulation*. In this dissertation we focus on simulations that are reproducible or deterministic. By deterministic we mean that no matter how many times the simulation is invoked, for the same value of input design variables, it always yields the same outputs (i.e., values for f_i and g_j). A simulation can have a closed (explicit) form or can be iterative in nature. In this dissertation the simulation is treated as a black-box object as shown in Figure 2.1, where an example of single response (or output) simulation, Figure 2.1a, and multiresponse simulation, Figure 2.1b is provided.

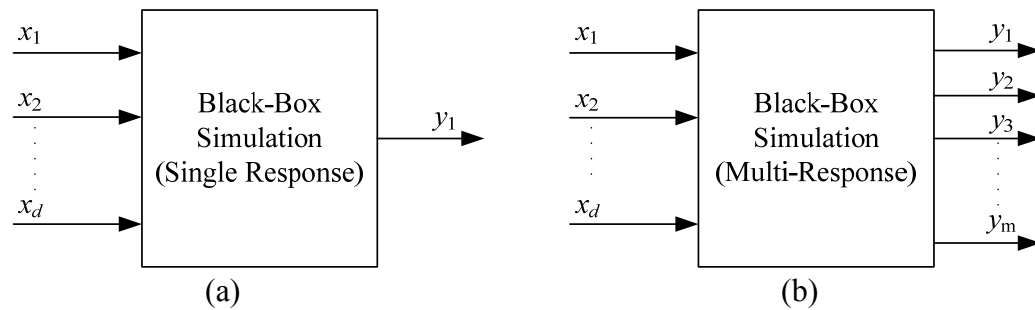


Figure 2.1 Black-box simulations, (a) Single response and (b) Multiresponse

2.2.2 Input Space, Experiment and Design

The d -dimensional space formed by all possible values of $x \in R^d$ is termed as the design variable space or *design space*. Since x is an input to the simulation, its corresponding space is termed as the *input space*. Each element of x in the input space is assumed to be bounded by a lower and an upper bound (see Eq. 2.1) and thus can be linearly normalized in the range $[0,1]$. The output from the simulation is termed as a *true response* when the full (or original model) for the simulation is used. If another

technique such as a metamodel is used to obtain the response for a simulation, the corresponding response is termed as a *predicted response*.

A point x_i , (a specified vector of x_1, \dots, x_d) is referred to as an *experiment* if it has been evaluated (or observed) for its true response, i.e., by invoking the simulation. In contrast, a point that has not been evaluated for its true response is termed as an *unobserved* point.

A set of experiments is termed as a *design*, denoted by D .

The process of choosing the various experiments is termed as sampling.

2.3 Dominance and Pareto Set

In multiobjective optimization, when there are two or more conflicting objectives, there cannot be a single optimum solution which simultaneously optimizes all objectives. Thus the solution obtained from a multiobjective optimization problem is a set of optimal solutions with varying degrees of objective values.

Considering Eq. (2.1), a solution x_1 is said to dominate (Goldberg, 1989; Deb, 2001) a solutions x_2 , when both (a) and (b) below hold:

- (a) Solution x_1 is better than or equal to x_2 in terms of all the objectives and
- (b) Solution x_1 is strictly better than x_2 in at least one of the objectives.

When comparing two solutions, when the first condition is not satisfied, the two solutions are said to be non-dominated with respect to each other. In other words, if a point is not dominated by any other point, it is said to be non-dominated.

Amongst a set of solutions P , the non-dominated set of solutions P' are those that are not dominated by any other point in P . When P is the entire search space, then the resulting non-dominated set P' is termed as the Pareto optimal set and the solutions are said to form a Pareto frontier in the objective space (i.e., f -space). Several algorithms are presented in Deb (2001) to efficiently identify a non-dominated set amongst a given set of solutions.

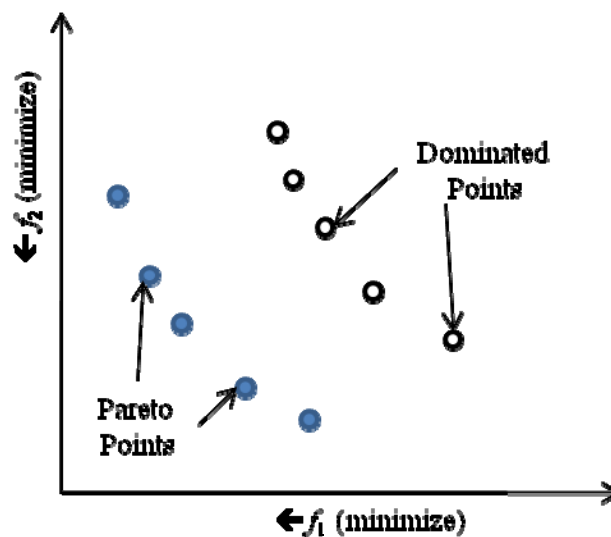


Figure 2.2 Dominated points and Pareto points

Note that in MOOP's where the objectives are not conflicting, the resulting Pareto optimal solution set will contain only one optimal solution (if it is unique).

2.4 Methods for solving Multi-objective optimization problems

2.4.1 Overview

In general there are two classes of methods for solving multi-objective optimization problems. They are: (a) classical methods and (b) non-classical methods. Classical methods are generally gradient-based or direct search methods. These

methods are: weighted-sum method (Cohon, 1978), ϵ -constraint method (Haimes, 1971), weighted metric method (Miettinen, 1999), value function method (Keeny and Raiffa, 1976; Miettinen, 1999), Schaffler's stochastic method (Schaffler et al., 2002; Shukla et al., 2005), normal boundary intersection method (Das and Dennis, 1998), goal programming (Charnes et al., 1955; Ignizio, 1976; Steuer, 1986) etc. Gradient based methods are deterministic in nature and yield Pareto solutions one point at a time.

The second class of methods is non-classical based methods for solving MOOP's. Many of the non-classical methods are based on natural phenomenon. These methods are generally population based such as evolutionary algorithms (Goldberg, 1989; Deb, 2001; Coello Coello et al., 2007), particle swarm optimizers (Coello Coello et al., 2004), multiobjective simulated annealing (Serafini, 1992; Nam and Park, 2000) and Timmel's population based method (Timmel, 1980; Shukla et al., 2005) to name a few.

Several variations of population based multiobjective optimization evolutionary algorithms have been reported in the literature (Fonseca and Fleming, 1993, 1998a, 1998b; Srinivas and Deb, 1994; Horn et al., 1994; Zitzler and Thiele, 1998; Deb et al., 2000, Deb, 2001; Coello Coello et al., 2007). These methods try to assign a goodness or fitness to a design point, based on its objective and constraint values. It is also important to note that population-based methods require numerous function calls, at times several thousands, of the simulation to evaluate the objectives and constraints. In spite of the recent advances in the field of high performance and high

throughput computing, the use of population-based optimization methods for certain complex problems is not feasible.

In this dissertation a multiobjective genetic algorithm (MOGA) is used for solving MOOP's. It is important to point out that even though MOGA is used for solving optimization problems in this dissertation, the approaches proposed are not limited to MOGA and any other suitable multiobjective optimization technique can be used. The details of a genetic algorithm (GA) and a MOGA are discussed in the following section.

2.4.2 Genetic Algorithms

Genetic Algorithms (GA) as defined by Goldberg (1989) are: “search algorithms based on natural selection and natural genetics”. GA maintains a pool of candidate solutions, each of which is assigned a fitness based on its usefulness or ‘payoff’. Fitness is a scalar measure of how well a particular candidate solution satisfies the given problem objectives. At each iteration or generation of GA, candidate solutions are selected for reproduction based on their fitness to form new offspring or solutions. The reproduction process is carried out via the use of genetic operators such as selection, crossover and mutation (Goldberg, 1989; Deb, 2001). A set of probabilistic rules determines whether a candidate solution undergoes crossover or mutation and at what point. A powerful feature of GA's is that they search in multiple directions simultaneously and do not require any gradient information or other supplementary information (convex objective or linear constraints) about the problem at hand, only the usefulness or the payoff value. This makes the GA an ideal tool for optimization of highly non-linear functions involving a combination of continuous and discrete

design variables and black-box functions. A schematic of the GA design representation and operators is shown in Figure 2.3 for a heat exchanger optimization (Aute et al., 2004) example. There are three design variables viz. number of tubes, Nt (discrete), tube length, L (continuous) and fins per inch, FPI (discrete). A chromosome representing one design is shown in Figure 2.3a. The genetic algorithm operators of crossover and mutation are shown in Figure 2.3b.

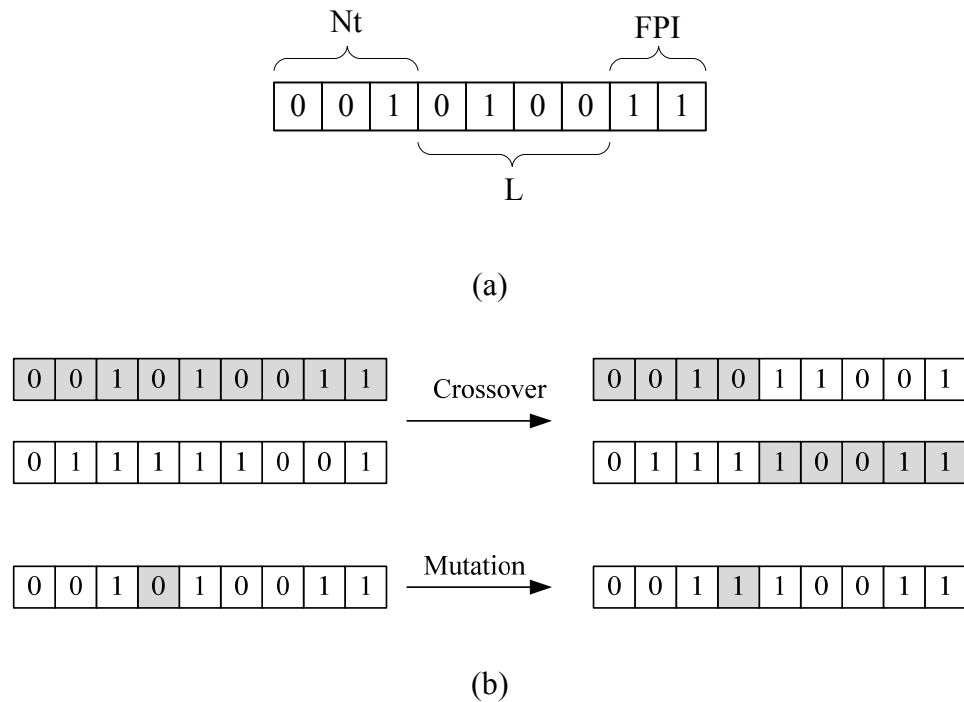


Figure 2.3 Genetic Algorithms, (a) design representations and (b) operators

2.4.3 Multiobjective Genetic Algorithm

Since GA's deal with a scalar fitness value, usually some kind of aggregating method or a utility function is used to assign fitness to solutions. A genetic algorithm that is modified to include multiple objectives is termed as a Multiobjective Genetic Algorithm (MOGA). The main difference between MOGA and GA is the

introduction of the fitness assignment scheme that evaluates the goodness of candidate solutions based their respective objective and constraint values. Typically MOGA considers three criteria in fitness assignment, viz., (a) objective values, (b) constraint values and (c) crowding. The objective values are handled using some kind of non-dominated sorting procedure and address the aspect of reaching as close as possible to the true Pareto frontier. The constraint violations are handled using a penalty or custom selection operator and address the aspect of feasibility. The crowding metric is handled using some form of distance measure such as niche (Goldberg, 1989) or crowding distance (Deb, 2000) and avoids clustering of solutions. Figure 2.4 shows a flowchart for a simple multiobjective genetic algorithm.

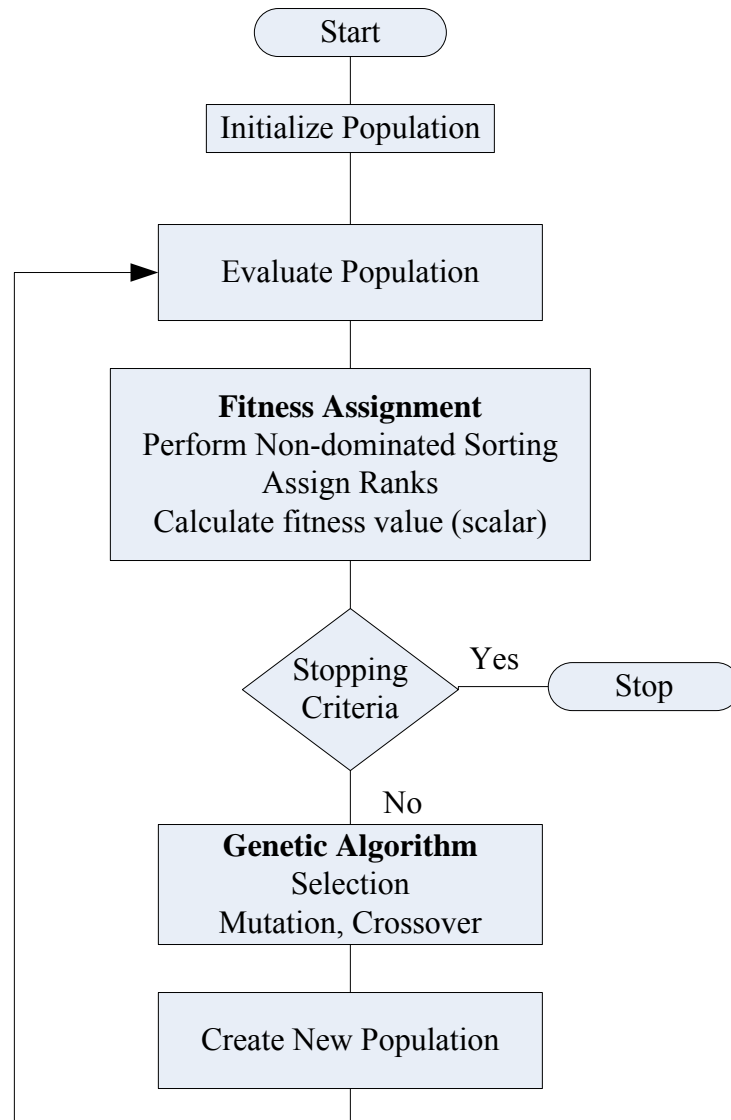


Figure 2.4 MOGA flow chart

2.5 Approximation Assisted Optimization

2.5.1 Overview

As mentioned in Section 2.4.1, optimization requires multiple invocations of the simulation tool to calculate the objectives and the constraints. Thus optimization may not be feasible when the simulation is very complex such as a CFD, which can execute for several days to evaluate one set of inputs. In order to reduce the

computational burden associated with optimization, approximation-assisted optimization is proposed by researchers (see, e.g., Simpson et al., 2001). In approximation-assisted optimization, a simplified model capable of reasonably representing the simulation behavior is used along with the optimizer to carry out the optimization. This simplified model is termed as a metamodel or a surrogate model. As explained in Figure 1.1 earlier, approximation-assisted analysis and optimization in engineering design involves four steps: (1) a design of experiments (DOE) or sampling stage where a design is chosen for conducting an experiment to generate response data, (2) metamodeling stage in which the data from first step is used to build a metamodel, (3) verification of the metamodel to assess how good the metamodel is, and (4) optimization using the metamodel. The metamodel that is developed is computationally more efficient (less expensive) than the actual simulation which it will replace. An important step in approximation-assisted optimization is the verification of the optimum solutions, i.e., comparison of the metamodel predictions with the true responses for the optimum designs. Once a verified metamodel is developed, it can be used for multiple optimization studies.

In the metamodel development phase, the simulation is invoked multiple times for carefully chosen points from the input space. This process is termed as the design of experiments or DOE. These inputs along with their true responses are then used to develop a metamodel. The design of experiments is the structured and organized method for determining the relationship between factors or inputs (to a simulation) and the output of the simulation. The process of choosing the various experiments is

termed as sampling. Different sampling techniques have also been studied and presented in the literature (Jin et al., 2001).

The second step in approximation is to fit the data to a model. These techniques involve the use of response surfaces or other sophisticated stochastic models to approximate the true response. Several computer based meta-modeling approaches are discussed in Simpson et al. (2001) and Wang and Shan (2007). The different approaches can be broadly categorized as (a) response surface based models (b) artificial neural networks (c) statistics based models such as Kriging (d) machine learning and (e) hybrid models. There are several metamodel verification methods proposed in the literature such as random-sample evaluation, cross-validation (Cressie, 1993; Martin and Simpson, 2005) etc. The random sample evaluation method is the most popular and easiest to implement though it requires additional function evaluations. In this method, a random sample of designs is generated and the predicted response from the metamodel is compared with the true response. The results of this comparison can be quantified using statistical metrics which are discussed in Section 2.5.3.

Approximation can be carried out in an offline or online manner. The difference between offline and online approximation is shown in Figure 2.5. In offline approximation, as shown in Figure 2.5a., the design of experiments and the metamodel development is carried out before any optimization is conducted. In online approximation, shown in Figure 2.5b, an existing metamodel is used during optimization, but based on the progress (i.e., design space explored by the optimizer) of the optimizer, new points are sampled in intermediate stages (e.g., between

iterations of the optimizer) and the metamodel is updated. Online approximation has the advantage that as the optimization progresses towards optimal solutions, the accuracy of the metamodels can be selectively improved in the region of the optima.

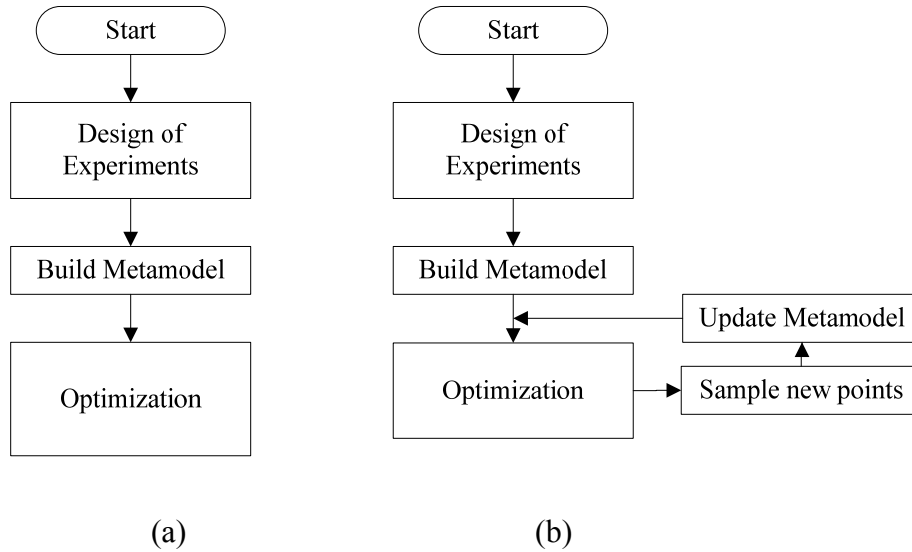


Figure 2.5 Approximation, (a) offline and (b) online

2.5.2 Maximum Entropy Design

The different sampling methods can be broadly grouped (Simpson, 2001) as: classical methods, space filling methods and sequential or adaptive methods. One such relevant spacing filling method is Maximum Entropy Design (MED) method and is discussed in this section.

Entropy as a measure of information content was first introduced by Shannon (Shannon, 1948). Lindley (1956) interpreted Shannon's entropy H as the amount of information retrieved from an experiment. It was then showed (Shewry and Wynn, 1987; Currin et al., 1988) that the entropy criterion H , selects a new experiment as the one that maximizes the expected retrieved information due to the new experiment.

Mathematically, given a current design (x_1, x_2, \dots, x_n) , the new experiment is chosen as follows:

$$x_{n+1} = \arg \max H(x_1, x_2, \dots, x_n; x) \quad (2.2)$$

where (x_1, x_2, \dots, x_n) are the existing n experiments and the “argmax” denotes the optimal solution x_{n+1} of the maximum entropy optimization problem.

Further, under the assumption of normal priors (Shewry and Wynn, 1987; Koehler and Owen, 1996), it was shown that the entropy criterion is the same as maximizing the determinant of the prior covariance matrix R , i.e.,

$$x_{n+1} = \arg \max \det(R) \quad (2.3)$$

where \det indicates a determinant and R is the $((n+1) \times (n+1))$ covariance matrix of x . Each element of R is calculated using the augmented design $(x_1, x_2, \dots, x_n, x_{n+1})$, where there are n existing designs and x_{n+1} is the new candidate design. The details of covariance matrix based on the normal priors are given in Section 2.5.3.

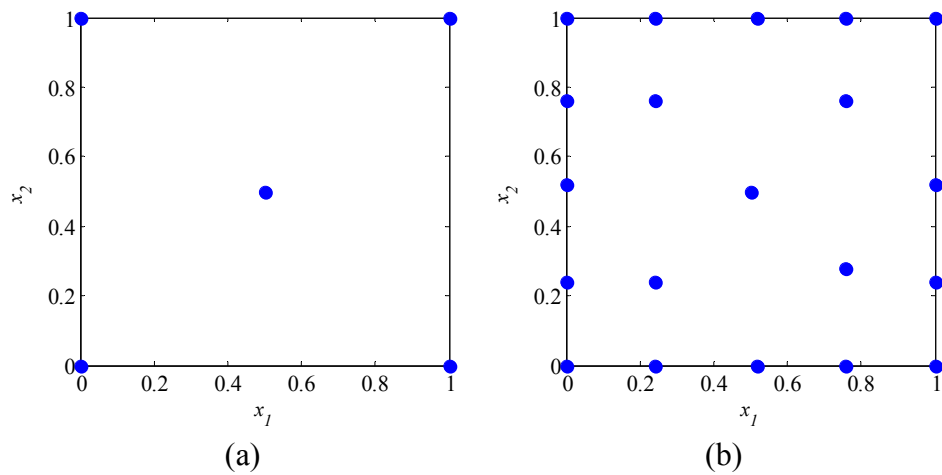


Figure 2.6 (a) Initial designs and (b) maximum entropy designs

Figure 2.6a shows an initial design with 5 points in a two dimensional input space and Figure 2.6b shows 15 additional designs obtained using the maximum entropy criterion. Note that a significant number of designs are on the boundaries of the input space (Currin et al., 1991).

2.5.3 Kriging Method

Kriging is a widely used spatial correlation and prediction technique in the field of Geostatistics (Cressie, 1993; Armstrong 1998) and is named after the South African mining engineer D. G. Krige. The basic idea behind Kriging is to use existing responses at some points x_i , where $i=1, \dots, n$, to predict the response at some unknown point x_0 .

Suppose we want to predict the model response at some point x_0 . Initially, when there are no samples, then there is some assumed uncertainty in this function value. This uncertainty can be modeled as a random variable $Y(x)$ with a mean μ and an associated variance σ^2 . In other words, the function has a typical value of μ but has some local variations in a certain range as we traverse the x -space. Consider two points x_i and x_j . Assuming that the function being modeled is continuous then the corresponding function values $y(x_i)$ and $y(x_j)$ will be close if the distance between x_i and x_j i.e. $\|x_i - x_j\|$ is small. The Kriging approach approximates a true model response $y(x)$ with a stochastic process as follows:

$$y(x) = f(x) + Y(x) \quad (2.4)$$

where $y(x)$ is the unknown function that is being modeled and $Y(x)$ is a normally distributed Gaussian process. Compared to ordinary a least squares method, where we are interested in finding the functional form which best represents the observed data,

in Kriging, we are interested in predicting how the function typically behaves and not the exact functional form. Various functional forms for $f(x)$ and $Y(x)$ are available in the literature (Jones, 2001; Simpson et al., 2001; Martin and Simpson, 2005). The term $f(x)$ is similar to a polynomial model in a response surface method and is equivalent to a global mean μ for the model. The global mean μ is the mean of all the responses in the current design. For simplification purposes $f(x)$ is generally treated as a constant. The $Y(x)$ term represents the local deviations from the global mean obtained by interpolating the available data based on distance between the unobserved point x_0 and the sampled points.

The term $Y(x)$ is represented through the use of one of many correlation functions. One of the widely used correlation functions (Sacks et al., 1989; Jones, 2001) is:

$$\text{Corr}[Y(x_i), Y(x_j)] = \exp\left(-\sum_{l=1}^d \theta_l |x_{il} - x_{jl}|^{p_l}\right) \quad (2.5)$$

In this equation, d is the dimension of vector x , x_{il} and x_{jl} are the l^{th} components of the vectors x_i and x_j , θ_l is the degree of correlation between the responses in the l^{th} coordinate and is termed as the correlation parameter in the l^{th} direction, and p_l controls the smoothness of the function in the l^{th} direction. The terms θ_l and p_l provide a means for adjusting the relative importance in each dimension of the input space. For simplification, a single value of θ is used and the distance term is replaced by the Euclidean distance between x_i and x_j . When one value of θ is used, the model is termed as an isotropic model, which treats all dimensions equally. In Eq. (2.5) when $p=1$, the correlation is known as the exponential correlation.

The effect of θ and p (Jones et al., 1998) on the correlation is shown in Figure 2.7.

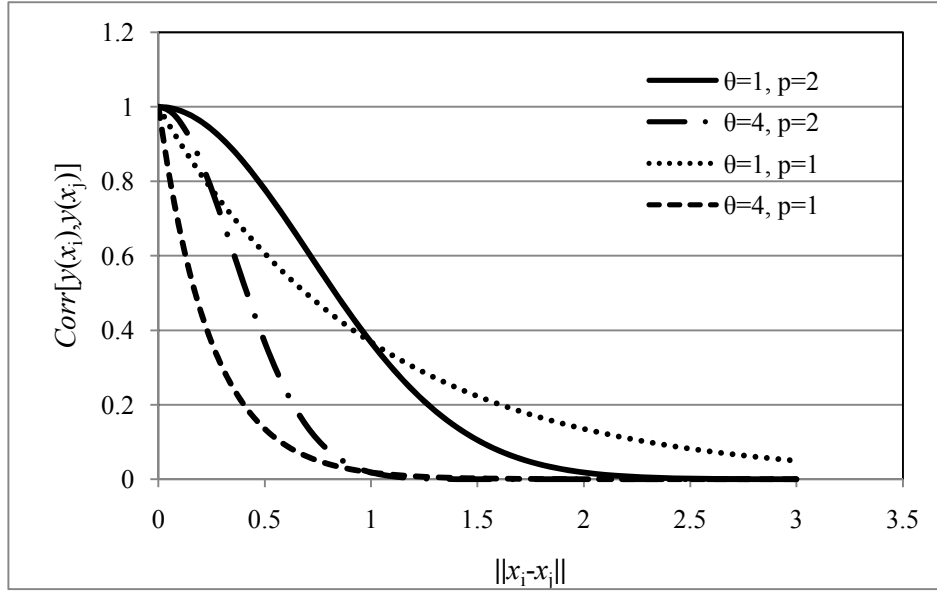


Figure 2.7 Correlation vs. Euclidean distance for different θ and p values

As observed from Figure 2.7, the correlation tends to zero as the distance $\|x_i - x_j\|$ increases. As θ increases, the correlation drops rapidly and p controls the smoothness of the correlation. In practice, θ values are calculated for each dimension in the input space, and thus when the correlation is highly sensitive to one of the dimensions; the corresponding θ value will be higher.

Suppose there are n responses in the current design, then let y represent the set of n observed true responses as given in Eq. (2.6):

$$y = \begin{bmatrix} y(x_1) \\ \cdot \\ \cdot \\ \cdot \\ y(x_n) \end{bmatrix} \quad (2.6)$$

The uncertainty in the function values (local deviations) at the n points can be represented by a vector of random variables $Y(x)$ as:

$$Y(x) = \begin{bmatrix} Y(x_1) \\ \cdot \\ \cdot \\ \cdot \\ Y(x_n) \end{bmatrix} \quad (2.7)$$

This vector has a covariance matrix Cov given by:

$$Cov(Y) = \sigma^2 R \quad (2.8)$$

where R is an $n \times n$ correlation matrix with the (i,j) element given by Eq. (2.5). The diagonal elements of R are always of the form $Corr[Y(x_i), Y(x_i)]$ and thus are always equal to 1. Let I denote an $n \times 1$ vector of ones and r denote the correlation of $Y(x_0)$, the unobserved point, with $Y(x_i)$, the current designs, as

$$r = \begin{bmatrix} Corr[Y(x_0), Y(x_1)] \\ \cdot \\ \cdot \\ \cdot \\ Corr[Y(x_0), Y(x_n)] \end{bmatrix} \quad (2.9)$$

The values of the correlation parameters, such as μ , σ , θ and p_l need to be estimated. They are obtained by maximizing the likelihood function or in other words, to model the functions behavior so that it closely represents the observed data. Maximizing the likelihood function provides an estimate of the optimal values of μ , σ^2 , as functions of R as follows

$$\hat{\mu} = \frac{I^T R^{-1} y}{I^T R^{-1} I} \quad (2.10)$$

and

$$\hat{\sigma}^2 = \frac{(y - I\hat{\mu})^T R^{-1} (y - I\hat{\mu})}{n} \quad (2.11)$$

Then the estimated response for an unobserved point x_0 is given using the Kriging predictor as:

$$\hat{y}(x_0) = \hat{\mu} + r^T R^{-1} (y - I\hat{\mu}) \quad (2.12)$$

In addition to the above predictor, the Kriging measure of uncertainty in the estimated response can be calculated as follows:

$$s^2(x_0) = \hat{\sigma}^2 \left[1 - r^T R^{-1} r + \frac{(1 - r^T R^{-1} r)^2}{IR^{-1}I} \right] \quad (2.13)$$

The derivation for this standard error is provided in Sacks et al. (1989) and Jones (2001). It can be seen that the variance s^2 is zero for an observed point. In utilizing Kriging predictor in approximation assisted optimization (Bakker, 2000; Jones, 2001), this standard error can serve as a basis for making the decision between using the predicted response and invoking the analyzer functions to obtain a true response. The prediction of the standard error is a big advantage of Kriging over other metamodeling methods since the metamodel can then be dynamically updated based on the responses during a given optimization procedure. Furthermore, as mentioned, Kriging does not require a functional form, though the choice of the correlation function is problem dependent. Simpson et al. (2001) found that Kriging is extremely

flexible and suitable for deterministic computer experiments and recommend the use of Kriging metamodels when the number of input variables is less than 50.

2.5.4 Metamodel Performance Metrics: Errors Verification

The performance of a metamodel is generally evaluated by comparing the response obtained using the metamodel with the true response for a given set of points termed as a test sample. This test sample can be chosen randomly or using some systematic method e.g., based on a statistical distribution.

Let $y(x_i)$ be the true response from a simulation and $\hat{y}(x_i)$ be the predicted response for a test sample of size n , where $i=1, \dots, n$. Then we can define a global measure of the accuracy of the metamodel termed as the root mean square error (RMSE) as follows:

$$\text{RMSE} = \sqrt{\frac{1}{n} \sum_{i=1}^n [y(x_i) - \hat{y}(x_i)]^2} \quad (2.14)$$

The maximum absolute error (MAE) represents the maximum deviation of the predicted response from the true response for all the test samples and is given by:

$$\text{MAE} = \max(|y(x_i) - \hat{y}(x_i)|), i = 1, \dots, n \quad (2.15)$$

In addition, we can define RMSE and MAE based on relative errors. The relative error for a sample x_i can be defined as:

$$e_i = \frac{y(x_i) - \hat{y}(x_i)}{y(x_i)} \quad (2.16)$$

Then, the corresponding relative RMSE and relative MAE can be defined as:

$$\text{RRMSE} = \sqrt{\frac{1}{n} \sum_{i=1}^n e_i^2} \quad (2.17)$$

and

$$\text{RMAE} = \max(|e_i|) \quad (2.18)$$

The RMSE and MAE consider only the numerical magnitude of the errors. The relative RMSE and MAE metrics are useful when the numerical range of the response i.e., difference between the minimum and the maximum values differs by several orders of magnitude. RRMSE and RMAE are useful in practical engineering examples as demonstrated in Chapter 5.

Even though the above metrics or RMSE and MAE are widely used in the literature for assessing metamodels, these measures are sensitive to the sample size. Hamad (2006) introduced a new metric termed as metamodel acceptability score (MAS) that is less sensitive to the sample size and is more intuitive in the context of the use of metamodels for global optimization. The designer needs to provide a bound on the acceptable predictor error of the metamodel. Let ε_{MAS} be an acceptability threshold, then a predicted response \hat{y} is said to be acceptable if Eq. (2.19) is satisfied:

$$(1 - \varepsilon_{\text{MAS}}) \leq (\hat{y}_i / y_i) \leq (1 + \varepsilon_{\text{MAS}}) \quad (2.19)$$

If there are n test samples, of which m responses are acceptable as per above equation, then MAS is defined as:

$$\text{MAS} = \frac{m}{n} \times 100 \quad (2.20)$$

The acceptability criteria is a fraction, e.g., $\varepsilon_{\text{MAS}}=0.1$ implies a tolerance of 10% in the predicted response. It should be pointed out that the acceptability criteria need not be symmetric. This is important especially when certain information about the application is known before hand. For example, in an air-cooled heat exchanger design, a metamodel that over predicts the air-side pressure drop (in a reasonable range) could still be acceptable, since this will result in a conservative response and may result in computational savings. A numerical issue with Eq. (2.19) is the case when $y_i = 0$. Hamad (2006) proposes the following remedies: (a) if the number of cases with zero true response is a small fraction of the overall sample size, then these cases can be neglected, (b) if the former is not the case, then a ‘shift-transformation’ can be applied to y_i , i.e., $y_i = y_i + \delta$ to avoid with division with zero. The shift transformation should not affect the overall value of the MAS.

It should be pointed out that in the case of multiple responses, the metrics of MAS, RMSE, MAE, RRMSE and RMAE are calculated individually for each response.

Another method of metamodel verification is the method of cross-validation (CV) error calculation (Cressie, 1993; Meckesheimer et al., 2002). A p-fold cross-validation approach is carried out as follows: (i) the existing design (i.e., inputs and responses) are split into p different mutually-exclusive subsets, (ii) a metamodel is fit p times, each time leaving out one subset, the resulting metamodel is used to predict the response for the omitted subset and an error measure is calculated. This error measure is the cross-validation error (CVE) and is defined in the literature as the absolute difference between the predicted and the actual response. A special case of

cross-validation method is the leave-one-out (LOO) error calculation and this is discussed in more detail in Chapter 3. For Kriging metamodels Meckesheimer et al. (2002) propose to use $0.1n$ or $n^{1/2}$ as the value for p , where n is the number of samples in the current design. We note that while $0.1n$ is a good number for assessing the metamodel performance, it is computationally very expensive as n increases, since each cycle of CV calculation requires the metamodel to be refitted. The advantage of this approach is that it does not require any additional experiments. In statistics a technique called boot-strapping (Cressie, 1993) is also used for model verification, but in contrast to cross-validation, boot-strapping requires additional function calls.

Throughout this dissertation, the metrics of RMSE, MAE, RRMSE, RMAE and MAS are used to evaluate the performance of metamodels.

2.5.5 Maximin-Scaled Distance (MSD) Method

The new adaptive approach proposed in Chapter 3 is compared against two other adaptive DOE methods from the literature. The first of these is the maximin scaled distance method proposed by Jin et al. (2002). The maximin scaled distance (MSD) approach (Jin et al., 2002) is an enhanced version of the original maximin distance approach (Johnson et al., 1990) to make use of the information available from the metamodel. The method chooses the next sample as the point that is farthest from all points in the current design. The distance used for comparison is a scaled distance as given in Eq. (2.21). Mathematically, the next sample x_{n+1} is chosen as the solution of the problem:

$$\begin{aligned}
x_{n+1} &= \arg \max_{x_i \neq x_j} [\min ds(x_i, x_j)] \\
&\text{where} \\
ds(x_i, x_j) &= \sqrt{\sum_{k=1}^d a_k (x_{ik} - x_{jk})^2} \\
x_i, x_j &\in R^d \\
k &= 1, \dots, d \\
i, j &= 1, \dots, n
\end{aligned} \tag{2.21}$$

The weight parameters a_h are chosen to be the same as the correlation parameters θ_l obtained from a Kriging metamodel. These weight parameters reflect the relative importance of the individual design variables. At each stage, a Kriging metamodel is built and the estimated θ_d values are used to solve the optimization problem from Eq. (2.21) to obtain the next sample.

2.5.6 Accumulative Error (ACE) Method

The second adaptive DOE method from literature is the accumulative error (ACE) method proposed by Li and Azarm (2006) and in Li (2007). The new approach proposed in Chapter 3 was inspired in part by the ACE method.

The ACE method develops a metamodel for leave one out cross validation errors using a simple isotropic correlation along with the use of a distance threshold to avoid clustering of points. Isotropic implies that the functional behavior is the same along each dimension of the input space. In the general the cross-validation error metamodel tends to predict higher error values for points that are close to the points in the current design. Let D be the current design with n points, then the new sample is given by:

$$\begin{aligned}
x_{n+1} &= \arg \max \sum_{i=1}^n e_{LOO}^i [\exp(-\alpha \|x_i - x_0\|)] \\
&\text{s.t.} \\
&\|x_i - x_0\| \geq d_{crit}, x_0 \notin D, x_i \in D
\end{aligned} \tag{2.22}$$

where d_{crit} is a cluster threshold distance calculated based on the points in the current design and α is an adaptive correlation parameter. The details of calculation of d_{crit} and α can be found in Li and Azarm (2006) and Li (2007). It should be pointed out that α is a scalar value and as such does not take into account the effect of individual inputs on the response. The cluster threshold d_{crit} is used to ensure that new sample points are sufficiently away of existing points.

In the next chapter, a cross-validation based adaptive design of experiments method for single response deterministic simulations is presented.

Chapter 3 Single Response Adaptive Design of Experiments

3.1 Introduction

This chapter presents a new adaptive design of experiments method for single response deterministic simulations. As introduced in Chapters 1 and 2, any optimization algorithm requires numerous invocations of the simulation tool which calculates the objective and constraint functions of the optimization problem. Often in real engineering design problems these functions (or their corresponding simulations) do not have a closed form expression, i.e., they are iterative in nature and can involve a solution of linear, nonlinear and/or differential equations. An example would be a complex finite element or a computational fluid dynamics simulation. Even when executed on the most sophisticated computing hardware, these simulations may require several minutes to several hours to execute and evaluate for single set of inputs. A technique often used to reduce this computational burden is the use of offline metamodeling. The goal of offline metamodeling is to develop a reasonably accurate metamodel of the entire solution space (objectives and constraints) or a particular region of interest of the solution space using as few experiments as possible.

Developing a reasonable metamodel with the fewest experiments possible clearly emphasizes the importance of design of experiments (DOE) in selecting the experiments. The accuracy of the metamodel will heavily rely on the DOE method used. In this chapter an adaptive DOE approach for multi-input single output (or single response) simulations is presented. We refer to this method as the Space-

Filling Cross Validation Tradeoff (SFCVT) method. In SFCVT, the problem of adaptively generating new experiments at a given point is viewed as a tradeoff between a “space-filling” criterion and a Leave-One-Out (LOO) error criterion.

The remainder of this chapter is organized as follows: Section 3.2 provides an overview of the previous work in the area of adaptive DOE methods. Section 3.3 explains the terminology and definitions used to describe the proposed approach. Section 3.4 describes the proposed approach in detail. In Section 3.5, the proposed approach is applied to suite of 24 numerical test problems and the results are discussed in detail. The proposed approach is also compared with three other DOE methods from the literature. An empirical procedure to allocate available function calls to the proposed adaptive design of experiments and to a random verification of the obtained metamodel is proposed in Section 3.6. The approach and results are summarized in Section 3.7.

3.2 Related Work

Several recent publications (Giunta et al., 2003, Wang and Shan, 2007; Shao and Krishnamurty, 2008) provide an overview of DOE methods suitable for modern computational engineering design. DOE methods can be classified based on two different criteria viz., number of stages or iterations and adaptive vs. non-adaptive criteria.

Based on the number of stages, DOE methods can be classified as single-stage or multi-stage methods. In single-stage methods, all the required experiments are sampled in a single run. In multi-stage methods, also known as sequential designs

methods; one or more points are sampled at each stage. Generally, multi-stage methods with one point per stage are shown to work well overall (Romero et al., 2006).

DOE methods can also be classified as being non-adaptive or adaptive. In non-adaptive DOE methods, only the information from the experiments (i.e., design or input space) is used. Several non-adaptive DOE methods can be found in the literature. Classical designs are used when physical experiments are conducted. Some examples of classical designs (Myers and Montgomery, 2002) include full and fractional factorial designs, central composite designs and Box-Behnken designs. The classical methods tend to allocate points on or near the boundaries of the design space and leave a few points in the centre. Sacks et al. (1989) and Jin et al. (2001) conclude that in the case of deterministic computer simulations, a good experimental design tends to fill the entire design space instead of focusing only on the boundaries or at the center. Examples of space filling designs include Latin Hypercubes (McKay, 1979) abbreviated as LHC, maximum entropy design (Shewry and Wynn, 1987; Koehler and Owen, 1996), mean squared error (Jin et al., 2002), integrated mean squared error (Sacks et al., 1989), maximin distance approach (Johnson et al., 1990), orthogonal arrays (Taguchi, 1987; Owen, 1992), Hammersley sequences (Kalagnanam and Diwekar, 1997) which are also known as low discrepancy sequences (Wang and Shan, 2007) and uniform designs (Fang et al., 2000).

A DOE approach is said to be adaptive when the information from the experiments (inputs and responses) as well as information from the metamodel is used in selecting the next sample. Adaptive approaches are typically superior to non-

adaptive approaches. An adaptive approach generally begins with an initial design chosen randomly or using some space-filling method. A metamodel is constructed using the initial experiments and then new samples are chosen by systematically evaluating the current design and the metamodel.

The adaptive DOE approaches proposed in the literature can be classified into two categories: (a) DOE for globally accurate metamodels and (b) DOE for optimization and/or other analysis. The DOE for globally accurate metamodels are such that they can be used to provide metamodels which give a good estimate of the response in the entire design space. On the other hand, the DOE for the optimization category, involves the use of metamodels but they also add new samples based on progress of optimization, i.e., estimation of an optimum. The various adaptive DOE approaches proposed in the literature use one or both of the two criteria as a basis for selection of new sample points, i.e.,: (a) estimate of an optima and (b) estimate of errors. Methods which use an estimate of the optima include the methods by Cox and John (1997) termed as sequential design for optimization (SDO), Watson and Barnes (1995), Jones et al. (1998), Sasena, 2002, Sasena et al., 2000. These methods try to locate the optimum using the metamodel as each stage and sample points close to the estimated optimum. Methods that are based on the estimate of errors include those by Lin et al. (2004a, 2004b). Lin et al. (2004a, 2004b) propose to use a supplementary metamodel to model the prediction errors of the metamodel based on a test sample. The test sample is generated based on a maximum entropy principle, i.e., maximizing the determinant of a modified covariance matrix. They used Kriging for the response metamodel and multivariate adaptive regression splines for the supplementary

metamodel of prediction errors. Their approach was applied to only one test problem with one design variable and one response. Further tests are necessary to evaluate the general applicability of their method. The method by Jin et al. (2002) is the MSD method and the one by Li and Azarm(2006) is the ACE method described in Chapter 2. Goel et al. (2006) also use the prediction uncertainty in responses along with multiple metamodels. In their approach, multiple metamodels are used to model the response and then the uncertainty in the predicted response from these metamodels is used to choose new samples. The final predicted response is a weighted combination of the responses from the individual metamodels used in the DOE phase. Their approach was presented for single response simulations.

Cross-validation error based methods use either the actual cross-validation error or the cross-validation variance. In general, a metamodel is built using the cross-validation (CV) error or a cross-validation variance (CVV) and new samples are chosen based on the maximum value predicted by the CV or CVV metamodel. Approaches based on CV error include those by Jin et al. (2002), Busby et al. (2007) and the Accumulative Error (ACE) approach Li and Azarm (2006) and Li (2007), which use LOO errors.

The method by Busby et al. (2007) uses an adaptive gridding algorithm which divides the input space into a non-uniform grid cells. For each of these grid cells, a CVE is calculated based on the points that already exist in the design. In the cells with maximum CVE, a locally optimal point is sought using the MED method. The grid cells that do not have any points are assigned an arbitrarily large value of CVE, which can result in false predictions in subsequent stages. The performance of this

method was compared against response surface based metamodeling techniques and was shown to be superior. Further numerical experiments and comparisons using more sophisticated metamodels are required to evaluate the method's applicability.

The methods by Jin et al.(2002) and Li and Azarm (2006) use a relatively simple approach; first to predict the cross-validation errors at different points in the design space and then new points are chosen based on maximum value of the predicted CV error. In general CV error based approaches tend to allocate points close to each other resulting in clustering. The methods by Jin et al. (2002) and Li and Azarm (2006) can be summarized in two steps as follows:

- (a) Develop a simplified metamodel for the LOO prediction errors and scale the resulting LOO errors with the distance of the unobserved points from existing samples.
- (b) Choose new sample as the one with the maximum value of the LOO error calculated in Step-a.

Jin et al. (2002) use an averaging of LOO prediction errors while Li and Azarm (2006) use a weighted combination. The approach by Li and Azarm (2006) is described in more detail in Chapter 2 (see Section 2.5.6). Methods that use CVV include those by Kleijnen and van Beers (2004) and Romero (2006). Kleijnen and van Beers (2004) uses a supplementary metamodel of CVV and new samples are selected based on the maximum value of the predicted CVV. They concluded that their approach outperforms the LHC design and the MSE method when applied to a single response test problem. Romero et al. (2006) extend the approach proposed by Kleijnen (2004) method to multiple responses.

Another method from the literature is the mean squared error (MSE) method (Jones, 2001; Jin et al., 2002) which chooses the next sample based on the maximum value of the estimated mean squared error in the response predicted by an existing Kriging metamodel. Mathematically,

$$x_{i+1} = \arg \max s^2(x) \quad (3.1)$$

where s^2 is given by Equation 2.13.

Hendrickx et al. (2006) propose a distributed computing approach for adaptive DOE and metamodeling, in which multiple metamodels are evaluated at each stage simultaneously and the best model is chosen for the next step.

Overall, the shortcomings of the above mentioned approaches can be summarized as follows: (a) the methods use estimated optima and/or the estimation errors in the response, which can be misleading especially when the number of initial samples is small, (b) clustering of samples, (c) isotropic models fail to capture the response space and (d) scalability of the approaches to higher dimensions and a wide range of applications is not demonstrated (e) comprehensive comparison with other relevant approaches from literature. In order to address these shortcomings an adaptive DOE approach for single response deterministic simulations is proposed in this chapter. A test suite of 24 numerical and engineering problems from the literature is also compiled so that the applicability and scalability of the proposed approach and the previous DOE approaches (i.e., MED by Shewry and Wynn, 1987, MSD by Jin et al., 2002, and ACE by Li and Azarm, 2006) can be evaluated over a range of input dimensions and response behaviors. The objective of the proposed approach is to

obtain a good estimate of the entire response space. There are many applications where a metamodel with reasonable accuracy in the entire design space is desired, such as the two cases in the following:

- (a) Multiobjective optimization: In multiobjective optimization problems, the designer is not trying to maximize or minimize one particular objective function, but instead trying to find out a tradeoff between the multiple objectives. Such a tradeoff generally does not occur at the extreme values of the objective functions.
- (b) Multi-level design: Consider a multi-level design problem as shown in Figure 3.1. The system level objective f is a function of sub-system objectives f_1 and f_2 and also additional design variables. Approximation is used at the subsystem levels to predict the responses f_1 and f_2 . In these types of design problems, the designer is not interested in the extreme points of the function being approximated (i.e., f_1 and f_2); instead the designer is interested in finding an estimate to a different objective function (i.e., f in this case). The functions being approximated may not contribute to the designer's objective function in a monotonic manner (i.e., F may be highly non-linear) and thus the extreme point of the designer's objective function f may not correspond to the extreme points of the functions f_1 and f_2 which are being approximated. A design problem of such nature is studied in Chapter 5.

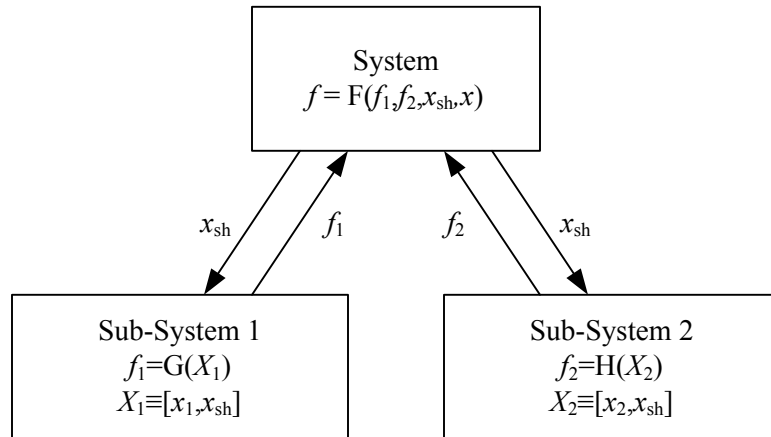


Figure 3.1 Multi-level design problem

3.3 Terminology

This section introduces the specific terminology used in the proposed approach.

3.3.1 Response Characteristics

The response or the output of an engineering simulation can have a Continuous And Multi-Modal (CAMM) characteristic. Figure 3.2 shows examples of a CAMM and a non-CAMM region in the response space for a single-input single-output simulation. The response function used to generate Figure 3.2 is adapted from Li (2007).

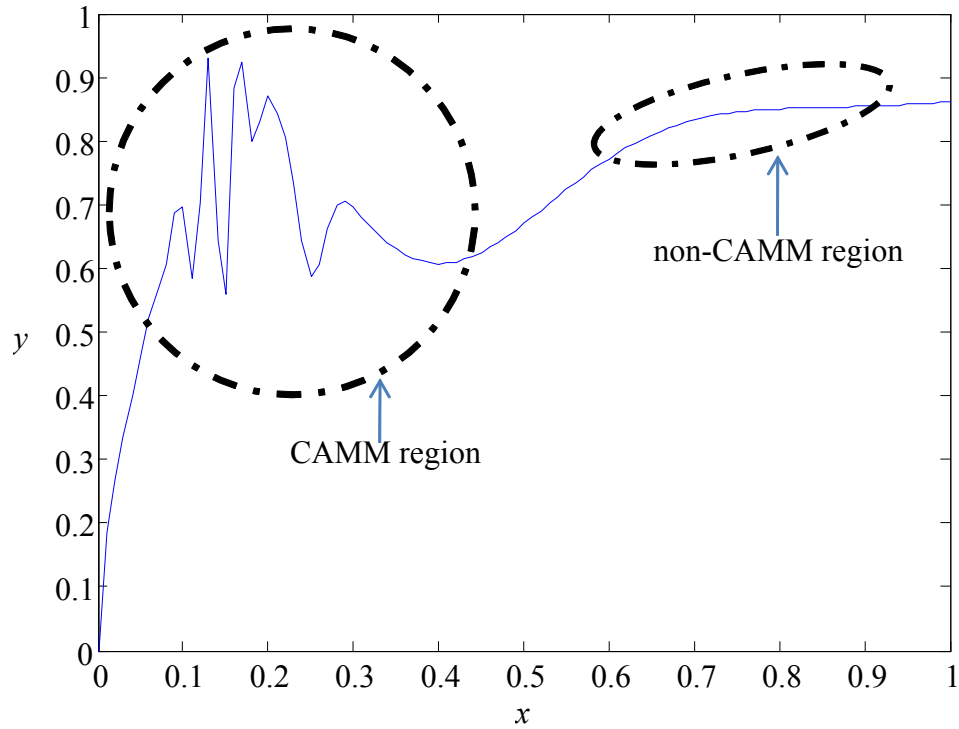


Figure 3.2 Regions of sensitive response

An example of response which is highly multi-modal is shown in Figure 3.3. This plot corresponds to the Schwefel's function (Hedar, 2005). Any adaptive DOE approach should be able to identify such CAMM regions in the response space. Intuitively, we would expect the approach to sample more points in the CAMM region.

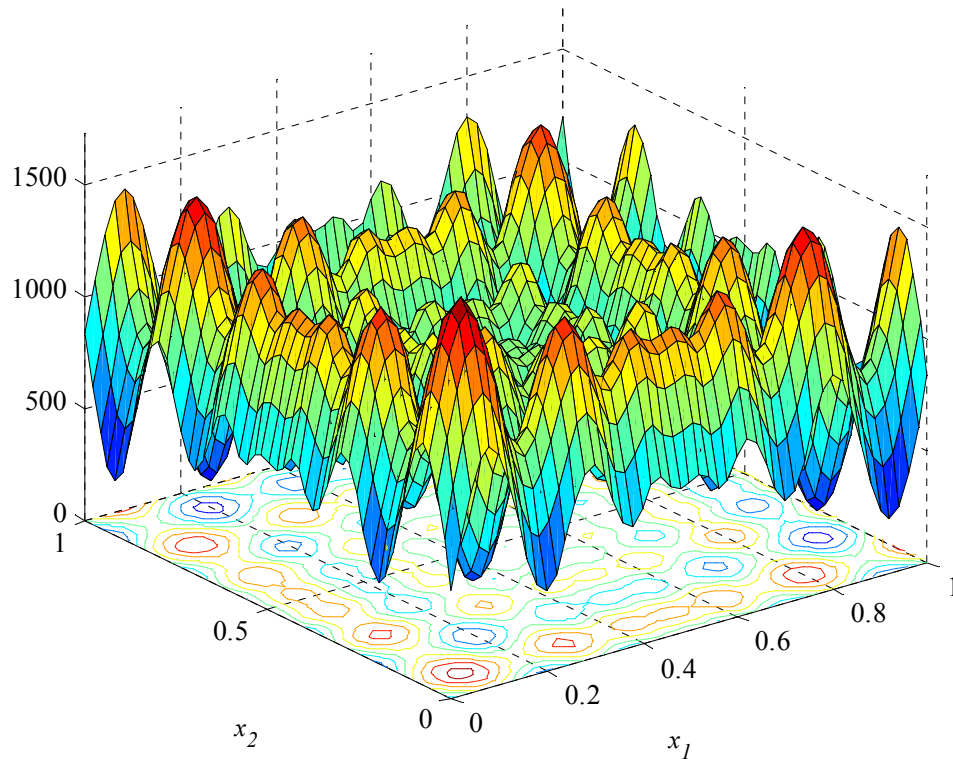


Figure 3.3 Highly multimodal response function

3.3.2 Leave-One-Out Cross-validation Error

The method of cross-validation (Cressie, 1993; Meckesheimer et al., 2002) has been studied extensively. The advantage of this method is that no additional function evaluations, i.e., simulations calls are required. The method of cross-validation is used to assess metamodel accuracy given a current or existing design. At each step, one point is omitted from the current design and the remaining points are used to build a metamodel. The resulting metamodel is then used to evaluate the response for the omitted point and an error measure (e.g., actual error or absolute error) is calculated. This cross validation error is termed as the Leave-One-Out (LOO) error. Let there be n experiments in a design. Then the LOO error for a point x_i in the design can be represented as:

$$e_{LOO}(x_i) = |y_i - \hat{y}_i| \quad (3.2)$$

It is important to point out that the LOO error is not a sufficient measure of the metamodel accuracy. It is actually a measure of the sensitivity or insensitivity of the metamodel to the lost information (Cressie, 1993). Thus an insensitive metamodel is not necessarily accurate. But the LOO error calculation does allow us to probe the response space for CAMM regions.

An example of the LOO error calculation and the resulting metamodel response is shown in Figure 3.4 (adapted from Li, 2007). The true response for the function is also shown in the figure. The metamodel was developed with 10 sample points. Then the LOO error (e_{LOO}) was calculated by omitting the point $x=0.25$. The resulting metamodel and the LOO error is shown in the figure. It is important to note how sensitive the metamodel is to the ‘lost information’ due to omission of the point $x=0.25$.

Eq. (3.2) is the generally used form of the LOO error calculation in the literature. While it does allow us to probe the response space for CAMM regions of the response, the LOO error quantity is sensitive to the magnitude of the response surface. This issue can be addressed by using a proper normalization of the response values and by using these normalized values in the DOE and metamodel development phases. But the information required for normalization, i.e., lower and upper bounds on the response is not generally known a priori. To alleviate this problem, it is proposed to use the following definition of LOO error (i.e., relative LOO error):

$$e_{LOO}(x_i) = \frac{|y_i - \hat{y}_i|}{y_i} \quad (3.3)$$

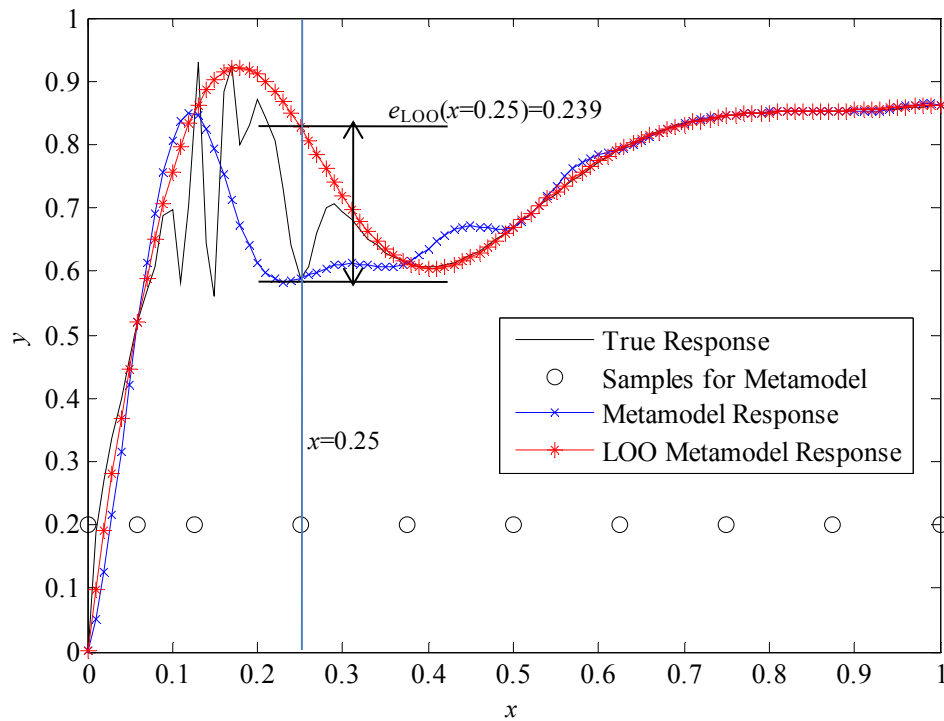


Figure 3.4 LOO error calculation

This relative LOO error can be intuitively much more practical, since in engineering design problems, a globally accurate metamodel is expected to predict the response as close as possible, generally with a certain error bound (e.g., with 10% of true value). The difference between the actual LOO and the relative LOO is shown in Figure 3.5 for a test problem P8 from Appendix-A. The design comprised of 20 points and the LOO errors were calculated for these points using Equations (3.2) and (3.3). Note that relative LOO error is highest for a point close to (0.5, 0.5) where as the actual LOO error value is higher for several points, away from point (0.5, 0.5), especially on the boundary. Similar trends are observed for other test problems from Appendix-A.

Thus, the conventional (absolute) LOO error can be misleading and its use as a criterion for selecting new samples can lead to inefficient designs. In this dissertation the proposed relative LOO error is used and henceforth the LOO error refers to the relative LOO error given by Eq. (3.3).

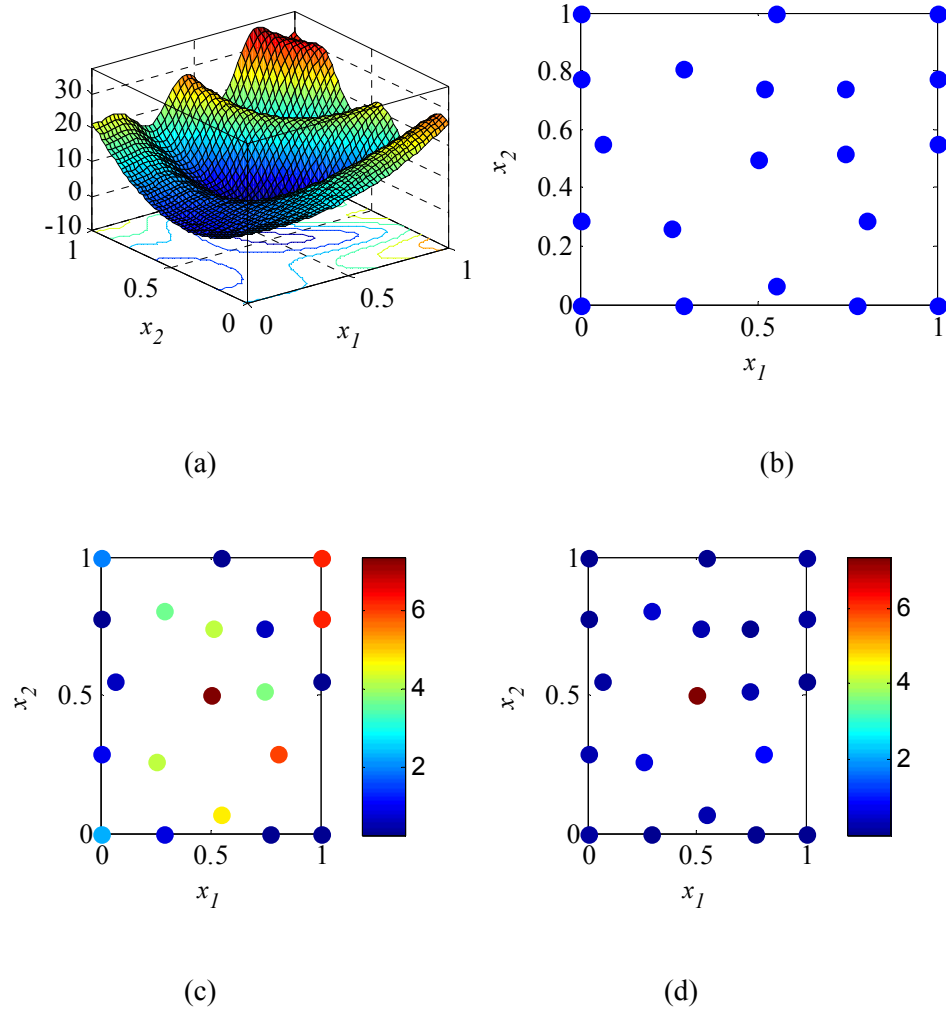


Figure 3.5 LOO Error (a) Response surface for P8, (b) initial design, (c) Actual LOO error and (d) relative LOO error

3.3.3 Level of Dominance

As mentioned in Chapter 2, all the solutions in a Pareto set are non-dominated with respect to each other. This notion of non-domination does not consider the magnitude of different objective values. In the context of multi-criteria decision making, Koppen et al. (2005) introduce the concept of fuzzy dominance using the metric termed as degree of dominance. The degree of dominance (DoD) first introduced in Koppen et al. (2005), is defined as follows: Let $f^{(1)}$ and $f^{(2)}$ be two objective values of two solutions in the context of a multi-objective optimization problem with M objectives. Then the degree of dominance of solution $f^{(1)}$ over solution $f^{(2)}$ is a constrained norm in the objective space and is defined as:

$$\mu_{12} = \frac{\prod_{i=1}^M \min(f_i^{(1)}, f_i^{(2)})}{\prod_{i=1}^M f_i^{(1)}} \quad (3.4)$$

μ_{12} is the amount by which solution (1) dominates solution (2). Eq.(3.4) is a constrained division, i.e., if any of the f_i^k is zero, then the corresponding indices are ignored from the calculation. μ_{21} can be defined in a similar manner. The above definition has the following interesting properties:

- (a) The degree of dominance is not symmetric between two solutions.
- (b) It is defined in the context of a set of solutions.
- (c) It is not affected by the scales of the different objectives since the same objectives from different solutions occur in the numerator and the denominator.

We use this concept in the context of a set of non-dominated solutions. For each solution in a set of n non-dominated solutions, it is proposed to define the Level of Dominance (LoD) ρ_i for a solution i as follows:

$$\rho_i = \sum_{k=1}^n \mu_{ki} \quad (3.5)$$

Thus ρ_i gives the sum total of the degrees of domination for a given solution and thus a solution with the lowest value of ρ_i is the least dominated solution in the set. This would allow us to choose a single solution from a set of Pareto solutions. There are many techniques in the literature for design selection amongst Pareto solutions, but most of them require additional information about the designs or some kind of preference articulation about the different objectives. The method proposed above does not require any such information and can be used to choose designs based solely on the relative magnitudes of the objective function values. Other similar methods can be used as well (Deb, 2001).

This method is used in subsequent sections when it is required to choose a single solution from a set of Pareto solutions obtained from solving intermediate optimization problems while selecting new samples.

3.4 Proposed Cross-Validation Based Approach for Adaptive DOE

This section describes the new proposed approach for single response adaptive DOE. The approach is termed as Space-Filling Cross-Validation Tradeoff (SFCVT) method. This approach was inspired by the work of Li and Azarm (2006) and Li (2007). The work reported in the literature (Jin et al., 2006; Li and Azarm, 2006; Li,

2007) on adaptive design of experiments focuses on prediction error and distance based criteria. For instance, the cross validation error criterion allocates new points in the region(s) with high nonlinearity in the response space and can result in some areas of the design space with insufficient points while clustering in regions with nonlinearity. The model used for prediction of cross-validation errors should be reasonably robust and accurate otherwise the model may predict false CAMM regions thereby wasting precious function calls. On the other hand any approach solely based on the distance criterion, such as the maximin scaled distance method (Jin et al., 2002) will most likely distribute available points across the entire design space, when intuitively one would expect more sample points to be allocated in regions with high nonlinearity or high cross validation errors. Thus, the DOE approach should continuously make a tradeoff between a cross-validation and a space filling (or distance based) criterion to sample a next point. This leads us to devise a two objective optimization problem where the objectives (cross-validation and space filling) are conflicting since they compete for the same resource (i.e., available functions calls). The presumption here is that the end-user of the metamodel is interested in the prediction capability of the metamodel over the entire design space and not just local or global extreme (minimum and maximum) points.

3.4.1 Overview of Proposed Approach

We present two different problem formulations based on the space-filling vs. cross validation tradeoff. The first formulation termed as the SO formulation, is a single-objective formulation, in which the space-filling criterion is treated as a constraint and the optimization objective is to find a point in the input space with the

highest estimated value of the LOO error. In the second formulation, termed as MO formulation, the space-filling criterion is treated as an objective along with cross validation error. Results are presented for both formulations, but only the SO formulation is used when comparing the SFCVT method with other DOE methods from literature.

The approach starts out with an initial design. Based on this initial design, the LOO errors are calculated for each point in the design and a Kriging metamodel is developed for the LOO errors. The metamodel is then used to predict LOO errors for unobserved points. An additional criterion termed as “Space-filling metric” is introduced as well. The space filling criterion insures judicious allocation of samples across the entire design space with emphasis on CAMM regions. The SO or the MO formulation is then solved to choose the next experiment. A step-by-step description of the approach along with a flow chart is given in Section 3.4.8.

3.4.2 Choice of Initial Design

The proposed approach starts with an initial design. The purpose of having an initial design is to get a good representation of the CAMM regions in the response space. The initial design is chosen to be a space-filling design with a specified number of points. An implicit assumption in our approach is that the initial design provides a reasonable representation of the response space. Here, a space filling design approach such as the maximum entropy design is used; however any other space filling design method such as those mentioned in Chapter 2 can be used as well.

An important factor influencing the success of an adaptive DOE approach is the number of points in the initial design. The number of points in the initial design

should be a function of the problem dimension and as such is very much problem dependent. It is proposed that the number of points in the initial design should be half of the total number of available function calls. This proposition was used as a starting point for initial studies and will be investigated further. There is a possibility that some problems may require fewer number of points in the initial design (and thus more adaptively sampled points) and vice-versa.

3.4.3 LOO Error Prediction

The relative LOO cross-validation error is used in the proposed approach to explore the design space and sample new points. The LOO error, by definition, can be easily calculated for the current points in the design. But there is no way to calculate it for points not in the current design, i.e., unobserved points. It is proposed to develop a metamodel for the LOO errors based on the current design. This metamodel can then be used to predict the LOO error for other unobserved points.

The metamodeling method used here is Kriging. As described in Chapter 2, using a Gaussian correlation, the LOO error (e_{LOO}) can be correlated in space using the following equation:

$$\hat{e}_{LOO}(x_0) = \mu(x) + r^T R^{-1}(y - I\mu)$$

$$\text{where, } y = \begin{bmatrix} e_{LOO}(x_1) \\ \cdot \\ \cdot \\ \cdot \\ e_{LOO}(x_n) \end{bmatrix} \quad (3.6)$$

where $\hat{e}_{LOO}(x_0)$ is the predicted LOO error for an unobserved points x_0 , $\mu(x)$ is the mean of LOO errors for points in the current design, r^T is the correlation vector explained in Chapter 2 and R is the correlation matrix with each term of R given by:

$$R(i, j) = \exp\left(-\sum_{l=1}^d \theta_l |x_{il} - x_{jl}|^{p_l}\right) \quad (3.7)$$

In Eq. (3.7), d is the dimension of the input space, and θ_l is the correlation parameter along each dimension of the input space. Based on studies in the literature (Jones, 2001) a value of 2 is chosen for p .

3.4.4 Space-filling Criterion

As mentioned earlier, a purely cross-validation based approach can result in clustered samples in the design space. In order to avoid this clustering the use of a space filling criterion is proposed. This space filling metric can be based on Euclidean distance or the scaled distance (Jin et al., 2002) in the design space.

The first space filling metric is the maximin distance in the design space. For each experiment in an existing design D , we compute the minimum non-zero distance of this point from all other points in D . Thus for n points, we have n non-zero distances. We compute the maximum of these distances and set the space filling metric to be equal to one-half of this maximum value. This will ensure that the new sample point will not be placed close to existing points in the design. This space filling metric S is independent of the metamodeling technique used. Mathematically, S can be represented as:

$$\begin{aligned}
ds(x_i) &= \min(\|x_i - x_j\|_2), \forall x_i \in D \wedge (i \neq j) \\
S &= 0.5 \times \max(ds(x_i)), \forall x_i \in D
\end{aligned}
\tag{3.8}$$

Earlier in this dissertation we proposed to use Kriging as the metamodeling technique.

The space filling criterion from Eq. (3.8) is used in the SO formulation. An alternative space filling criterion can also be used which is dependent upon the use of Kriging as the metamodeling technique. This alternative space filling criterion is simply the mean square prediction error obtained using the Kriging predictor. The SO and the MO formulations for choosing the new sample are described next.

3.4.5 Choosing Next Sample

Once a model for e_{LOO} and the space-filling metric have been selected, the next sample is chosen such that it has the maximum value of e_{LOO} and is sufficiently far away from all existing points in the current design. Mathematically this can be represented as:

$$\begin{aligned}
x_{n+1} &= \arg \max_x \hat{e}_{LOO} \\
&\text{s.t. } \|x - x_k\|_2 \geq S \quad \forall x_k \in D
\end{aligned}
\tag{3.9}$$

The problem in Eq. (3.9) tries to find out the next sample as the one with the maximum value of the predicted LOO error, \hat{e}_{LOO} , and which is sufficiently away from all points in the current design. S is defined in Eq. (3.8). Due to implementation issues, if the problem depicted in Eq. (3.9) fails and cannot be solved, then the next point is chosen using the MSE method. The optimization problem may fail because

there are no feasible solutions remaining implying that the design space is saturated. The problem may also fail to solve due to implementation issues such as numerical rounding and ill-conditioned matrices. Note that all the candidate points in the design space that satisfy the constraint are treated equally with respect to e_{LOO} . There is no spatial correlation taken into account.

An alternative formulation using the mean squared error as the space-filling criterion is proposed as follows:

$$x_{i+1} = \arg \max_x (\hat{e}_{LOO}, s^2) \quad (3.10)$$

This formulation uses the MSE (s^2) as a second optimization objective. MSE allows us to account for the spatial correlation amongst different designs in different dimensions. Moreover, the use of s^2 can be thought of as an adaptive space-filling design. The problem in Eq. (3.10) tries to find the next point such that it has the maximum value of the predicted LOO error and also has the maximum MSE.

The formulation presented in Eq. (3.10) is an unconstrained multiobjective optimization problem and as such will yield a set of Pareto solutions because there is an inherent tradeoff between the LOO errors and MSE criteria. All the Pareto points can be chosen as the next set of samples (instead of one point at a time). But this may not result in the best design. The challenge is to select one single design at each stage. A single solution can be chosen based on one of the following procedures:

- (a) Amongst the Pareto solutions, choose the one with maximum value of e_{LOO} or s^2 , i.e., one of the extreme Pareto solutions. The decision can be made based on the relative magnitudes of each quantity in the set.

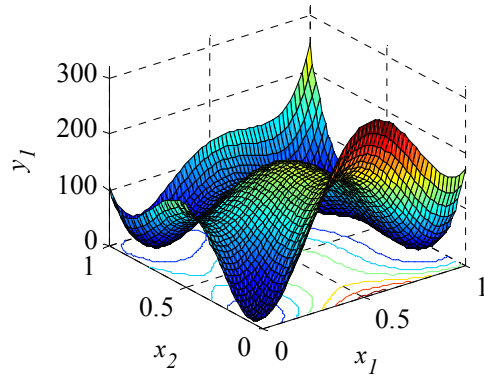
- (b) Choose the solution with the minimum value of level of dominance, which is described in Section 3.3.3 or first k solutions with lowest values.
- (c) Choose all the Pareto solutions.

Options (b) and (c) above are useful in the context of distributed computing when more than one simulation can be invoked simultaneously thereby reducing the overall execution time. Choosing one point per stage should be most effective, but it can be very slow since only one simulation is invoked per iteration.

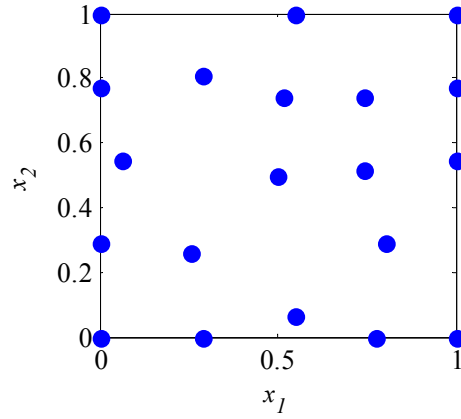
An example of the trade off between the two objective functions, i.e., the e_{LOO} and the MSE is shown in Figure 3.6 for Himmelblau's function (Floudas et al., 1999). Figure 3.6a shows the actual response for the function, 3.6b shows the initial design. Figures 3.6c and 3.6d show the estimated e_{LOO} and the MSE surface. Figure 3.6e shows the Pareto set obtained by maximizing the MSE and the LOO errors and Figure 3.6f shows the new designs corresponding to the MSE vs. LOO error tradeoff. It can be clearly seen that there is a certain amount of tradeoff between the two objectives.

In both cases, the space filling metric ensures that the new samples are sufficiently away from the existing design. Note that the MSE is theoretically zero for points in the current design. Thus this will prevent existing points from being sampled again.

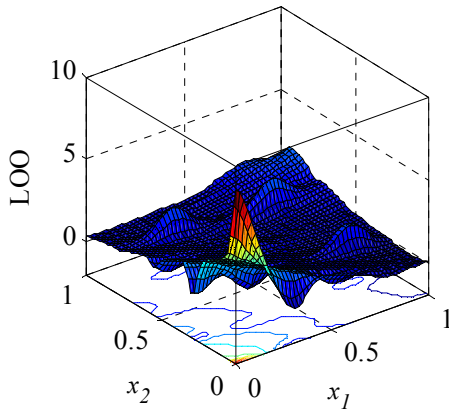
The above optimization problems can be solved using a direct or exhaustive search technique or using a genetic algorithm and need not be solved exactly. In this dissertation, the exhaustive search was used for problems with two dimensions while a MOGA (Deb, 2001) was used for problems with more than two dimensions.



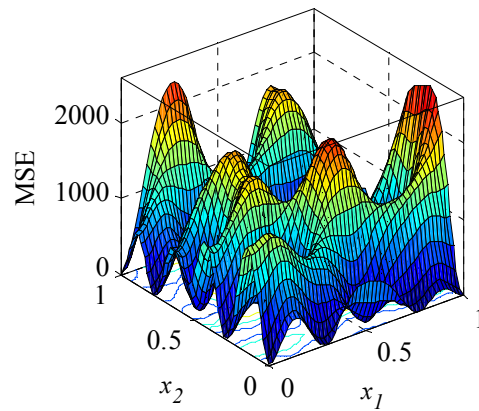
(a)



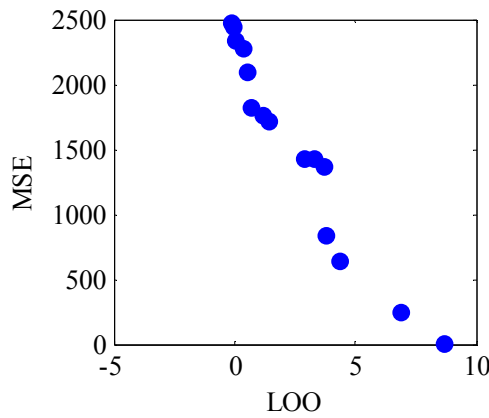
(b)



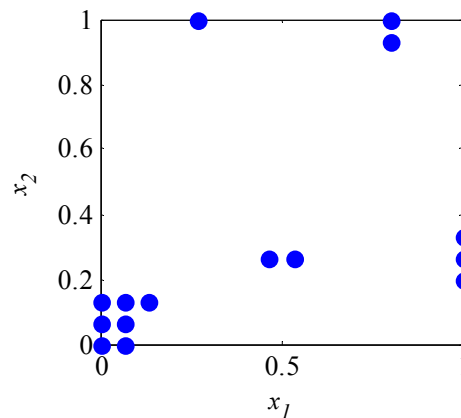
(c)



(d)



(e)



(f)

Figure 3.6 (a) Response for Himmelblau's function, (b) initial design, (c) LOO error surface, (d) MSE response surface, (e) MSE vs. LOO Pareto and (f) new designs based on MSE vs. LOO Pareto

The end-result of adaptive sampling should result in a acceptable metamodel. Figures 3.7, 3.8 and 3.9 show the effect of using the above two formulations on the performance of the resulting metamodels. In this example we choose the test problem P3. The single objective (SO) SFCVT formulation is compared against the multiobjective formulation. For the multiobjective formulation, we choose samples based on the level of dominance (MO-LoD), the point closest to the origin based on L2 norm (MO-L2) and the two extreme (maximum MSE value, MO-Max-MSE, and maximum LOO error value, MO-Max-LOO) points. The initial number of samples for each case was 20. Additional 10 samples were added using the SFCVT method. Metamodels were developed and evaluated using a random sample after every two additional points. The metamodel based on only initial design was also evaluated, thus giving a total of six sample steps as shown in the figures.

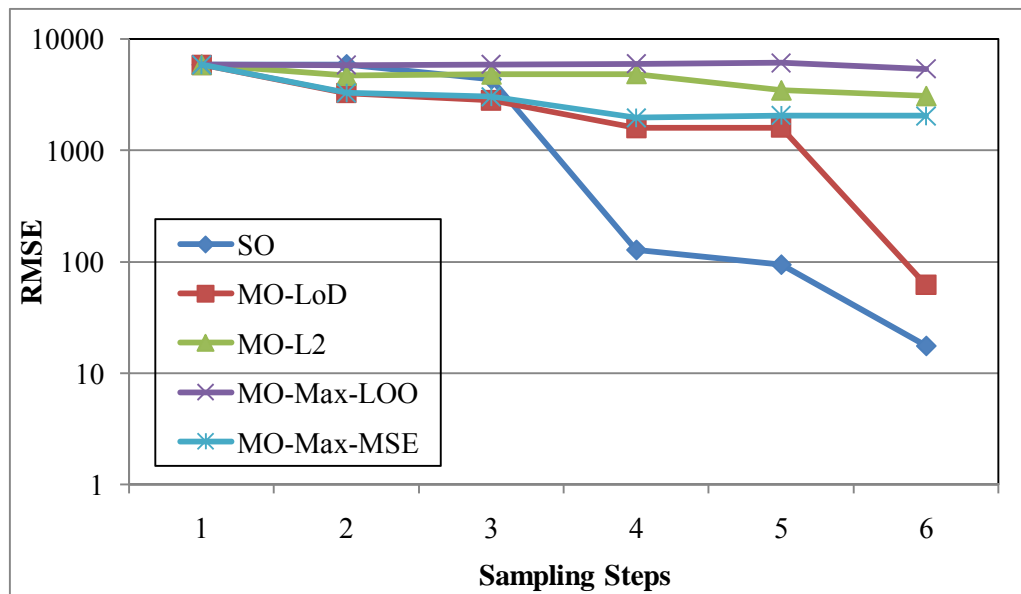


Figure 3.7 RMSE for problem P3

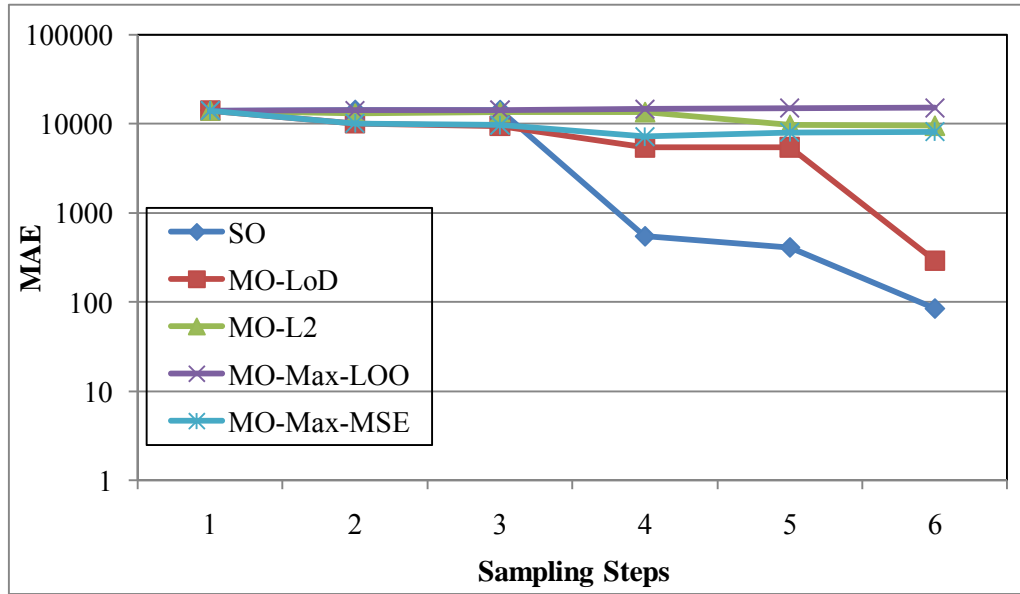


Figure 3.8 MAE for problem P3

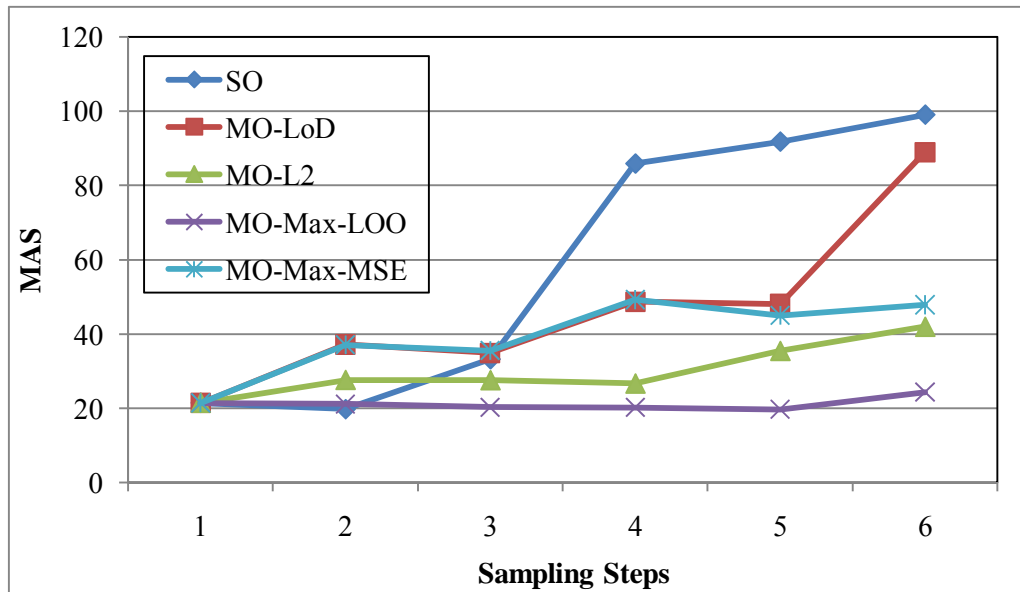


Figure 3.9 MAS for problem P3

Based on Figures 3.7-3.9, it is observed that the single objective formulation and the multi-objective formulation with the LoD selection provide consistently better

RMSE, MAE and MAS values. It is also seen that selecting any of the extreme points does not result in a good metamodel. While this behavior is strongly exhibited for test problem P3, this study was repeated for all other test problems (P1-P20) and it was found that for majority of the test problems the selection of the extreme points did not result in a good metamodel. For test problem P3, we also observed that selecting the next sample based on the L2 distance does not necessarily yield a good metamodel. This is because the L2 distance calculation is affected by the magnitudes and the distribution of the resulting Pareto solutions (MSE vs. LOO) in the MO formulation.

3.4.6 Design Update

The simulation is invoked for the sample obtained in the previous step and then this experiment is added to the current design D . In this way, the approach can sample as many points as desired by the end-user.

3.4.7 Stopping Criteria

In real world engineering design problems, resources are limited and generally a limit is placed on the available number of function calls or simulation calls. This limit is used as the stopping criterion for the proposed approach. When computational resources are readily available, but still limited, an elaborate stopping criterion such as the steps below should be used:

Step-1: Sample sufficient number of random points and evaluate their true response. These random points will be used to evaluate the metamodel performance.

Step-2: During each stage of the proposed approach or during intermediate stages (e.g., once every 5 new samples), develop a metamodel using the current design and evaluate its performance against the random sampled points in Step-1.

Step-3: If the RMSE, MAE, RRMSE, RMAE and MAS values obtained after predicting the response for the random samples using the metamodel are acceptable, stop sampling new points.

3.4.8 Step-by-Step Description of Proposed Approach

Figure 3.10 shows a flow chart for the proposed approach. This flow chart assumes that the stopping criterion used is the maximum number of available function calls.

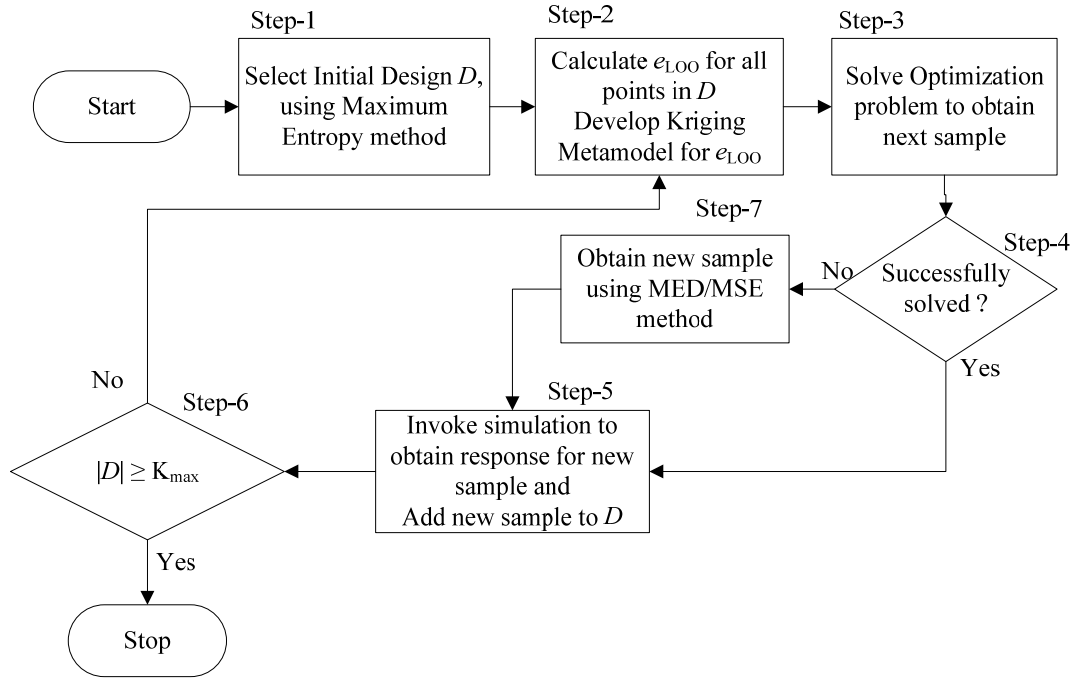


Figure 3.10 Flow chart for the proposed single response adaptive DOE method

Let K_{\max} be the maximum number of available function calls. The different steps are as follows:

Step-1: Generate an initial design D using the MED method and the chosen number of initial samples.

Step-2: Calculate LOO error for all the points in the initial design and build a Kriging based metamodel for the LOO errors.

Step-3: Solve the optimization problem discussed earlier in Eq. (3.9) or (3.10) to obtain the next sample point. In this dissertation, both formulations are used.

Step-4: If the optimization fails or if there are no feasible solutions, then go to Step-7; else go to Step-5.

Step-5: Evaluate the true response for the new point and add it to D .

Step-6: If the number of points in D is equal to the available number of function calls, then Stop, otherwise continue to Step-2.

Step-7: Compute the next sample using either the MED or the MSE method and proceed to Step-5.

The computational complexity of this approach is discussed in Section 3.5.6 along with actual CPU times obtained from numerical experiments.

3.5 Application Examples

In this section, the proposed approach is applied to several numerical test problems from a test suite developed as a part of this dissertation. The problems in the test suite have been carefully chosen to evaluate the different aspects of simulation responses such as being highly nonlinear and multimodal in nature and to demonstrate the scalability of the proposed approach. The details (Sasena et al., 2000; Jin et al., 2002; Busby et al., 2007) of the test problems are described in Appendix-A. All of the test problems are of multi-input single-output type with the number of inputs ranging from two to eight. The test problems are designated as P1 through P24 for brevity. The prefix ‘P’ is omitted in certain plots due to space restrictions. The Kriging implementation available in the MATLAB (Matlab, 2007) DACE Toolbox (Lophaven et al., 2002) was used.

The proposed approach using the SO formulation is compared to other single response DOE approaches from the literature. The non-adaptive approach used for comparison is the MED (Shewry and Wynn, 1987; Koehler and Owen, 1996) method

and two adaptive DOE methods used for comparison are the MSD method (Jin et al., 2002) and the ACE method (Li and Azarm, 2006; Li, 2007) described earlier in Chapter 2. The comparison is performed on the basis of metamodel predictions for a random test sample using a fixed number of samples (i.e., fixed number of function evaluations). Since random samples are used for evaluating the performance of resulting metamodels, the numerical experiments are repeated 10 times each to obtain descriptive statistics for the results. The repeat count of 10 was chosen based on available computational resources. The descriptive statistics are presented in the form of a box plot (McGill et al., 1978), also known as a box and whisker plot.

The test matrix used for conducting numerical experiments is shown in Table 3.1. The table shows the test problem numbers, the problem size i.e., input dimension or number of inputs, the number of points in the initial design, the number of new sampled points, number of random test points used and the number of runs conducted for repeatability. The initial design was generated using the MED method. The SO formulation from Eq. (3.9) and the MO formulation Eq. (3.10) were used to obtain new sample points and the performance of resulting metamodels were compared. When comparing the proposed approach with those from the literature, only the SO formulation was used. The metamodel acceptability threshold ε_{MAS} was set to 0.1 (i.e., 10%) for the lower as well as upper bound.

Table 3.1 Test Matrix for Comparison

Test Problems	Problem Input Dimension	Initial Design	New Samples	Random Test Samples	Repeat Runs
P1-P16	2	20	20	2000	10
P17-P20	4	40	40	4000	10
P21-P24	8	80	80	8000	10

A Factor of Improvement metric is introduced to compare metamodel performance and to visualize the comparison results as described next.

3.5.1 Metamodel Comparison: Factor of Improvement

The accuracy of two metamodels can be compared by calculating the relative reduction in RMSE or MAE between the two models as follows: The Factor of Improvement (FoI) for metamodel RMSE of the proposed approach over another baseline approach is defined as:

$$\text{RMSE FoI} = (\text{RMSE}_{\text{Baseline}} - \text{RMSE}_{\text{Proposed}}) \times 100 / \text{RMSE}_{\text{Baseline}} \quad (3.11)$$

Thus, a positive FoI indicates that the ‘Proposed’ metamodel is superior to the ‘Baseline’ metamodel. Similarly, FoI for MAE, RRMSE and RMAE can be defined. Clarke et al. (2005) propose a similar metric based on using the standard deviation of the RMSE instead of the actual values.

3.5.2 Results for the Proposed Approach

The MAS of the proposed approach using the SO formulation are shown for the different test problems in Figures 3.11 and 3.12. Figure 3.11 shows the MAS values for all the test problems for one single numerical experiment. Figure 3.12 shows the

descriptive statistics for MAS, obtained after conducting the numerical experiments 10 times.

We observe from Figure 3.11 that 16 out of 24 test problems have a score of less than 50. One reason for this is that a fixed correlation was used for Kriging metamodels. The type of test problem is not known a priori and thus there is no way to choose a best suited correlation except by trial and error.

The plot shown in Figure 3.12 needs some explanation. The plot is termed as a box plot and shows the following five parameters in order: minimum value, 1st quartile, median, 3rd quartile and the maximum value. Thus from Figure 3.12, the vertical line in the box is the median value. Outliers are represented by the “+” signs on either end of the minimum or the maximum values.

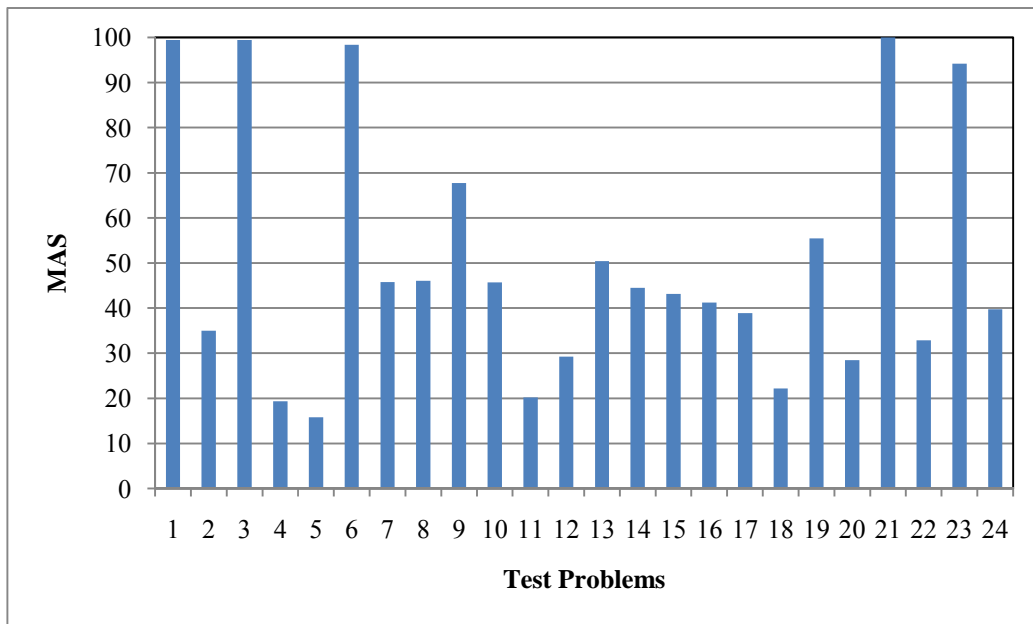


Figure 3.11 MAS for designs from the proposed SFCVT approach

Figure 3.13 shows the comparison of the MAS values obtained using the two different formulations, i.e., the SO and the MO formulations. The level of dominance

criteria was used to select one point at a time for the MO formulation. It can be seen that the two formulations yield comparable results (MAS within ± 5) for 17 out of 24 test problems. Figure 3.14 shows MAS comparison for the two formulations, when extreme points are selected at each stage. Again, 17 out of 24 test problems show comparable results. The corresponding RRMSE and RMAE values (not shown here) for the two formulation are also comparable. The MO formulation can be used when multiple sample points are desired per stage, which can then be evaluated simultaneously taking advantage of parallel computing.

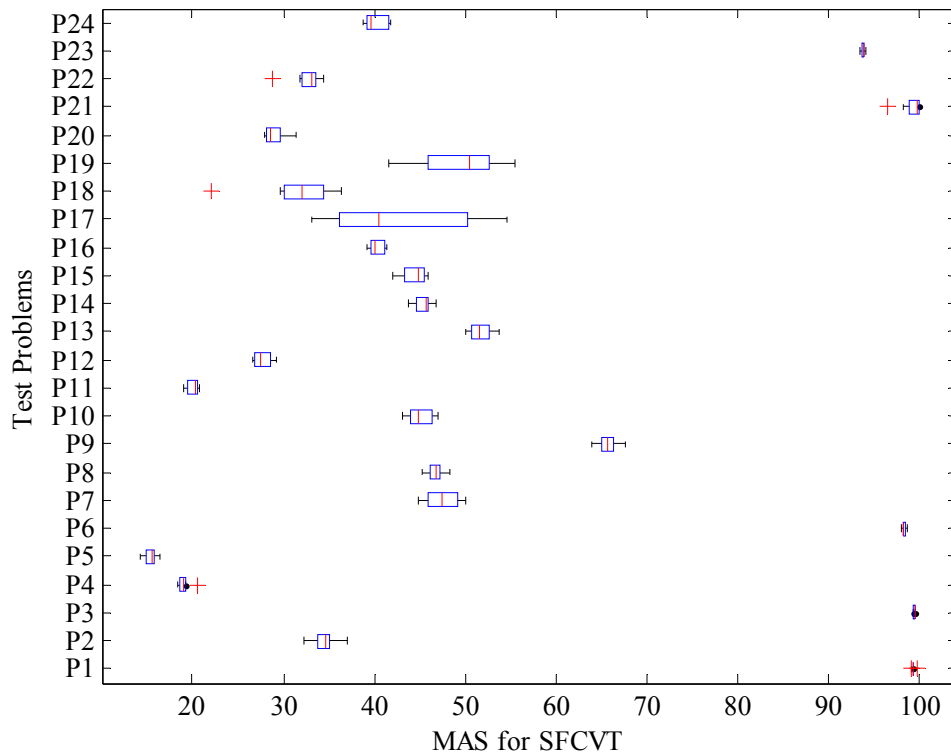


Figure 3.12 MAS for the proposed SFCVT approach

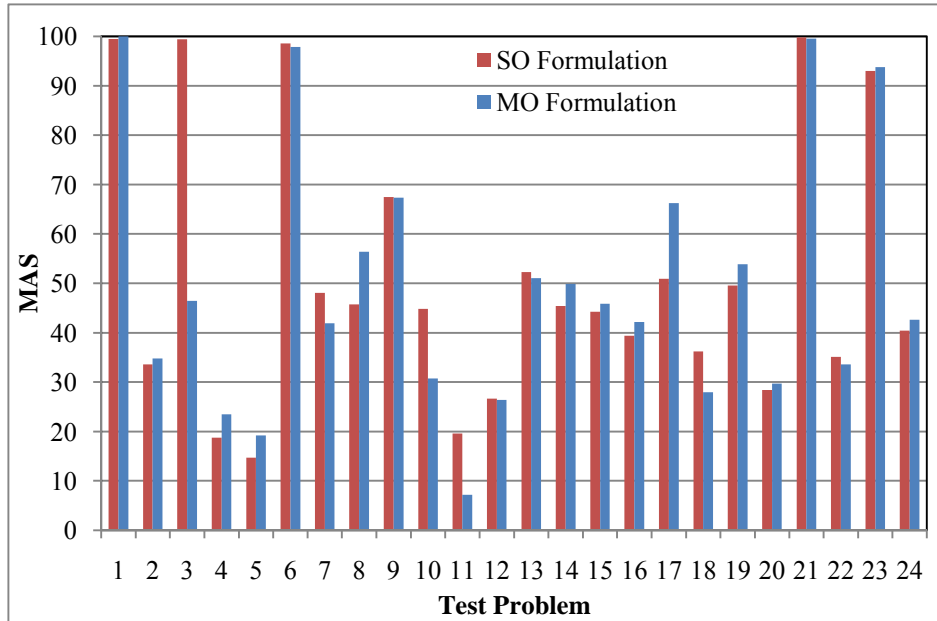


Figure 3.13 MAS of the SO and MO formulations, using LoD as selection criterion in MO formulation

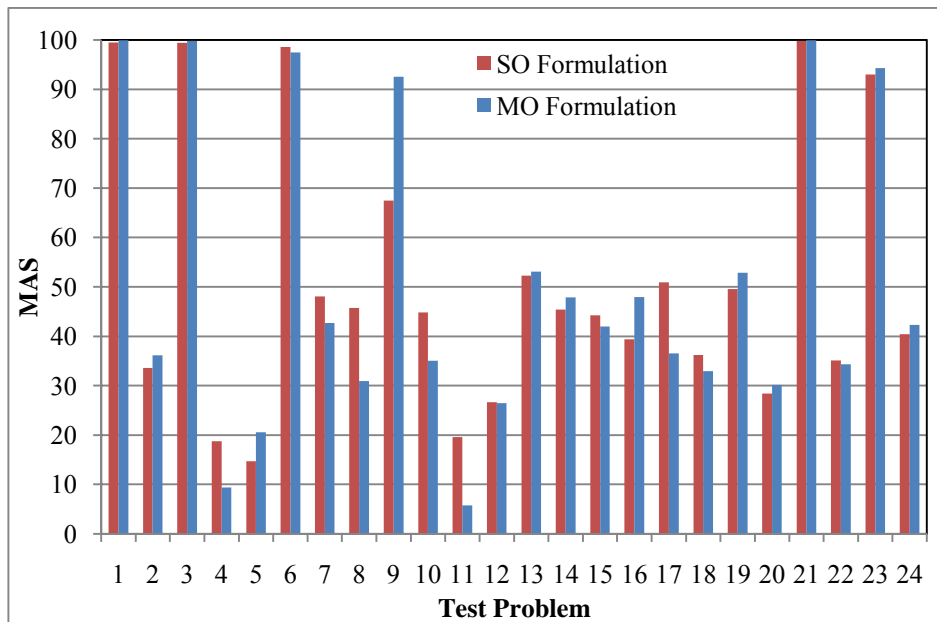


Figure 3.14 MAS comparison of the SO and MO formulation, using Extreme points criteria in MO formulation

The RMSE, MAE, RRMSE and RMAE plots results for the proposed approach are shown in the following sections where the SFCVT method is compared with three methods from the literature. The SO formulation was used for this comparison. In cases where results are presented in the form of box plots, conclusions are drawn based on the median values shown in the box plot. In some cases, when all values in a box plot are very close, the entire plot appears as only one horizontal or vertical (based on plot orientation) line.

3.5.3 Comparison with MED Method

In this section, the proposed approach is compared with the MED approach (Shewry and Wynn, 1987). In order to ensure a fair comparison, the number of initial designs and the total number of designs was fixed. Numerical experiments were carried out as per the test matrix presented in Table 3.1. The results for MAS for the MED method and the proposed SFCVT method are shown in Figure 3.15. In this comparison it can be observed that the proposed approach outperforms (i.e., yields higher MAS) the MED method in terms of MAS in 11 of 24 test problems. Figure 3.13 shows the box plot for MAS values for the MED method. The horizontal length of the boxes is small, indicating a consistent performance of the MED method on the random sample points used for verification. Upon further investigation it was found that the default correlation function used in the SFCVT method for the LOO error prediction was not suitable i.e., it did not give a good prediction of the LOO errors. Changing the correlation to an exponential function (see Chapter 2) improved the results dramatically for test problem P4, P5, P9 and P14-P16.

Figures 3.17, 3.18, 3.18 and 3.20 show the RMSE FoI, MAE FoI, RRMSE FoI and RMAE FoI of the proposed SFCVT method over the MED method. The proposed approach was better in terms of RMSE for 15, in terms of MAE for 16, in terms of RRMSE for 16 and in terms of RMAE for 18 out of 24 test problems. These numbers were obtained based on the median values from Figures 3.17-3.20. We can define the term “strictly better” for FoI, when all the values represented by the box plot are greater than 0. Thus, the proposed approach performed strictly better than the MED method in terms of RMSE for 10, in terms of MAE for 12, in terms of RRMSE for 11 and in terms of RMAE for 13 out of 24 test problems. The proposed approach faired the worst on problem P10. Upon further investigation, it was found that the metamodel for the LOO errors was not sufficiently accurate and as a result only the space-filling methods (i.e., MED and MSD) showed an acceptable metamodel. Moreover, it was observed that for problem P10, the LOO error metamodel was sensitive to the initial maximum entropy design sample and as such never yielded a good model for the LOO errors in intermediate stages, ultimately resulting in an inferior design. Further studies on initial design were conducted for problem P10. It was found that if LHC design is used as the initial design or even if the prior variance and correlation parameters were changed for the MED method to generate initial design, the resulting metamodel has a better performance than that obtained using the MED method.

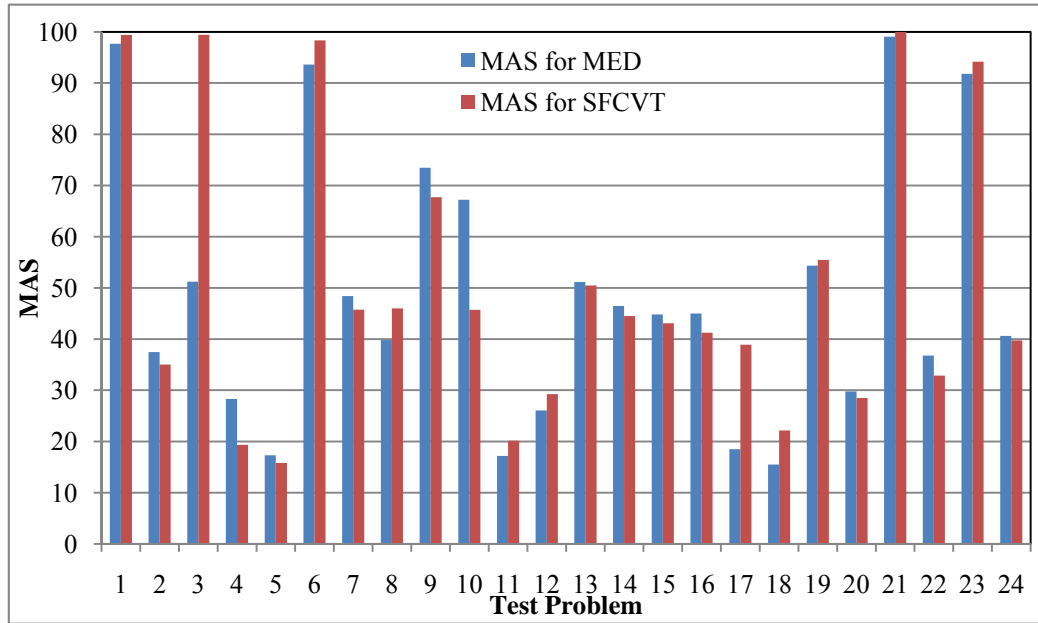


Figure 3.15 MAS comparison for MED vs. SFCVT

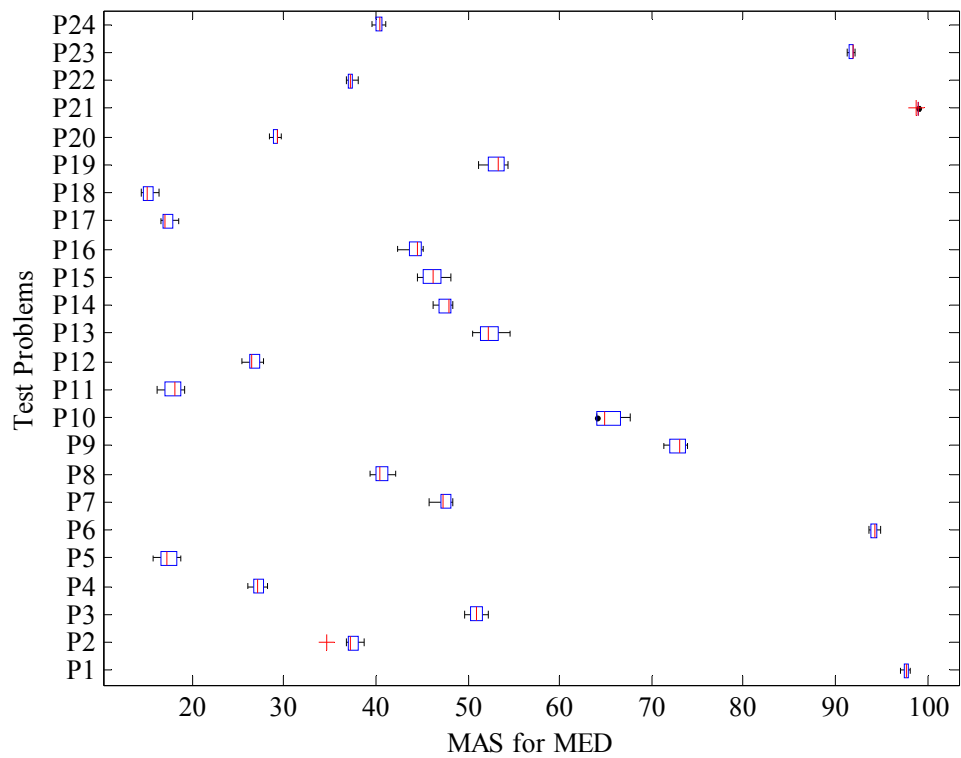


Figure 3.16 MAS for MED approach

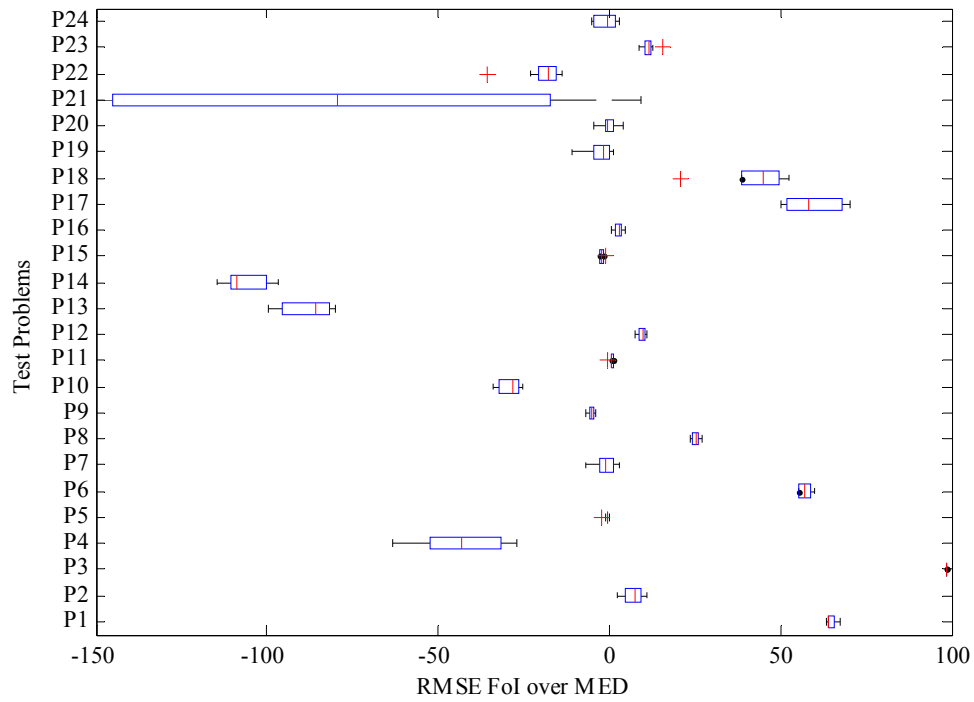


Figure 3.17 RMSE FoI of proposed approach over MED method

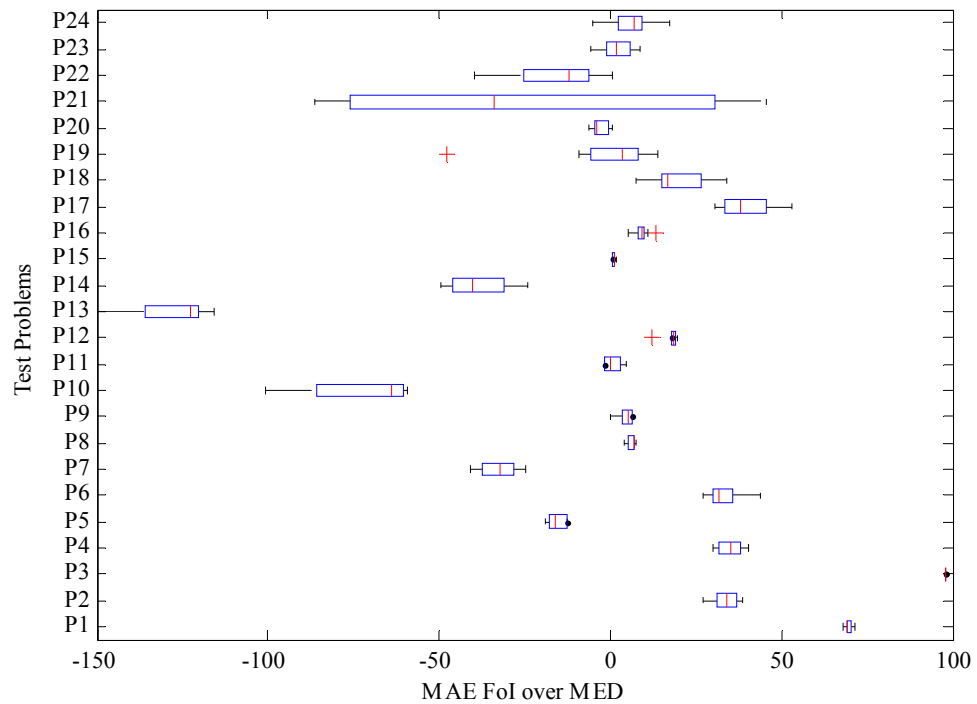


Figure 3.18 MAE FoI of proposed approach over MED method

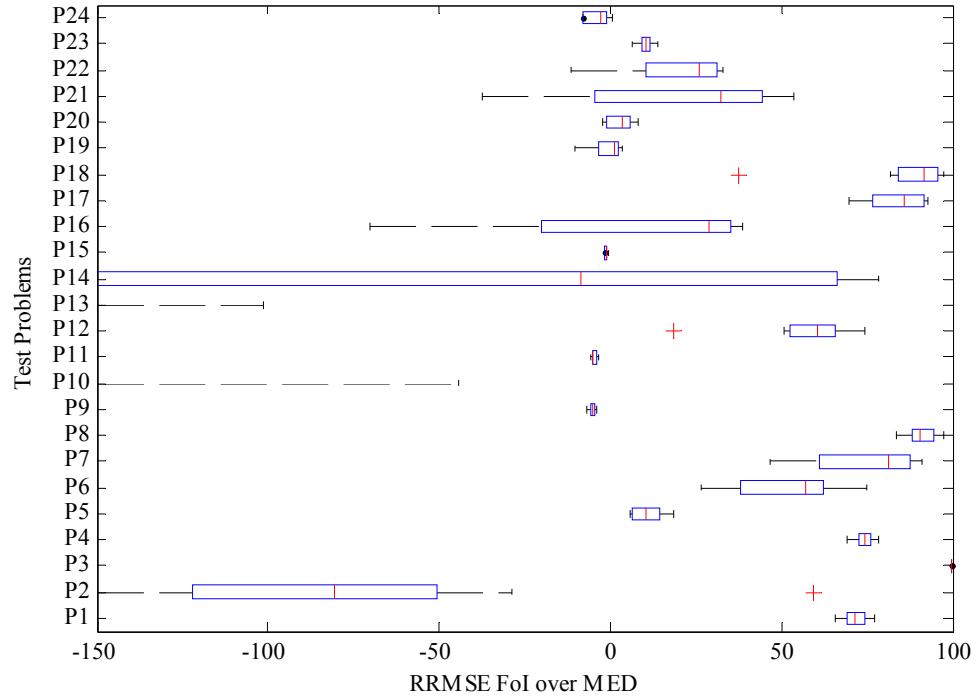


Figure 3.19 RRMSE FoI of proposed approach over MED method

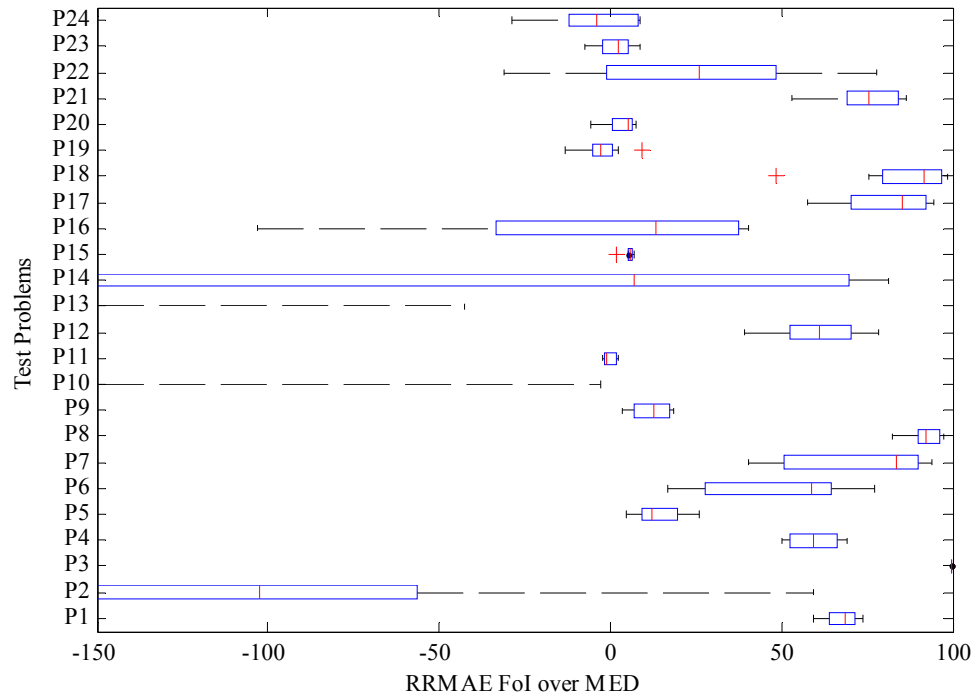


Figure 3.20 RRMAE FoI of proposed approach over MED method

In Figures 3.17-3.20, the width of the box plots for some of the test problems is very long, e.g., P21 in Figure 3.17. This indicates that the number of repeat runs was not sufficient and more numerical experiments need to be conducted.

The problem P10 is further analyzed here. Figure 3.21a and 3.21b show the design generated using the MED and the SFCVT methods, respectively. The corresponding verification error (i.e., absolute value of the difference between actual and predicted response) plots are shown in Figures 3.21c and 3.21d for MED and SFCVT respectively. For this case, the MAS for SFCVT is much lower than that for MED. We now tweak the correlation parameter θ used in the MED method. The new designs are shown in Figure 3.22a and 3.22b. The corresponding error scatters are shown in Figures 3.22c and 3.22d for MED and SFCVT respectively. Note that even though the overall MED design hasn't changed significantly, the design generated using the SFCVT method is drastically different and its performance is now comparable to that of the MED method. This shows that for certain problems, the SFCVT approach is sensitive to the initial design.

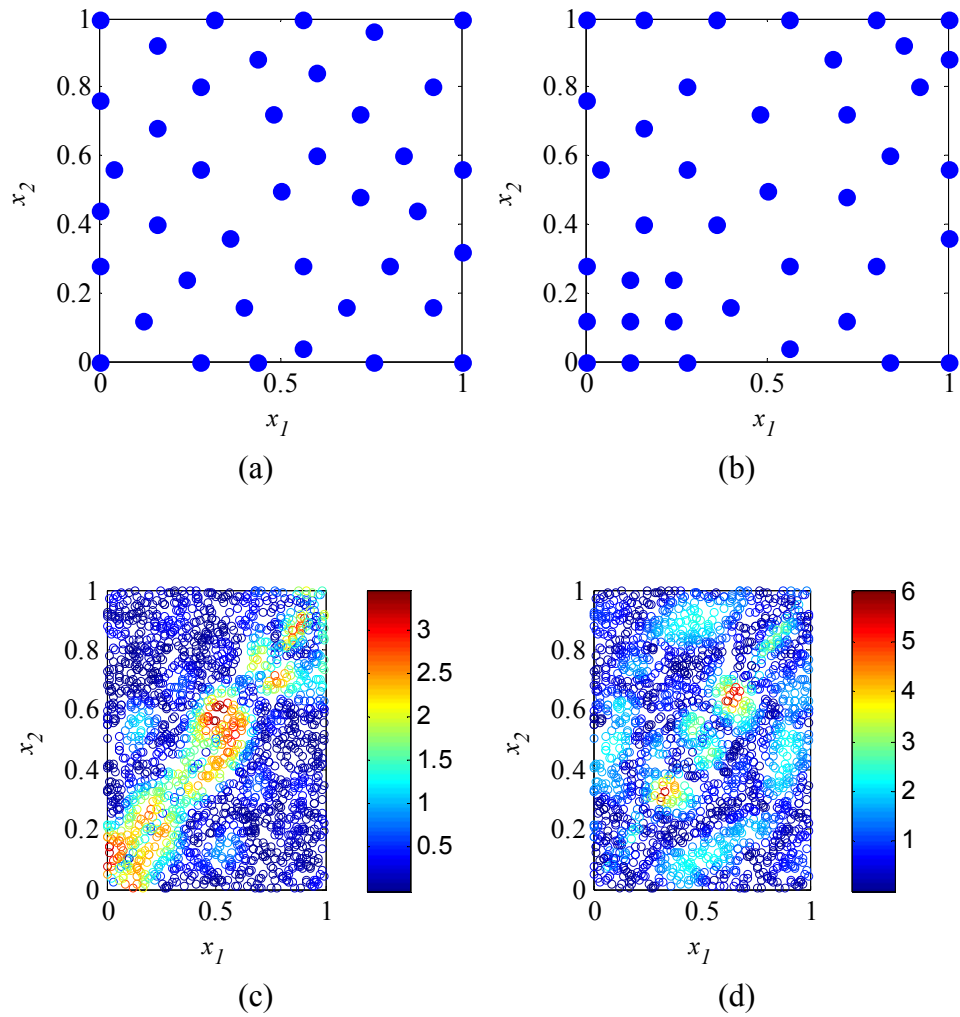


Figure 3.21 Problem P10, (a) MED design, (b) SFCVT design, (c) absolute error using MED and (d) absolute errors using SFCVT

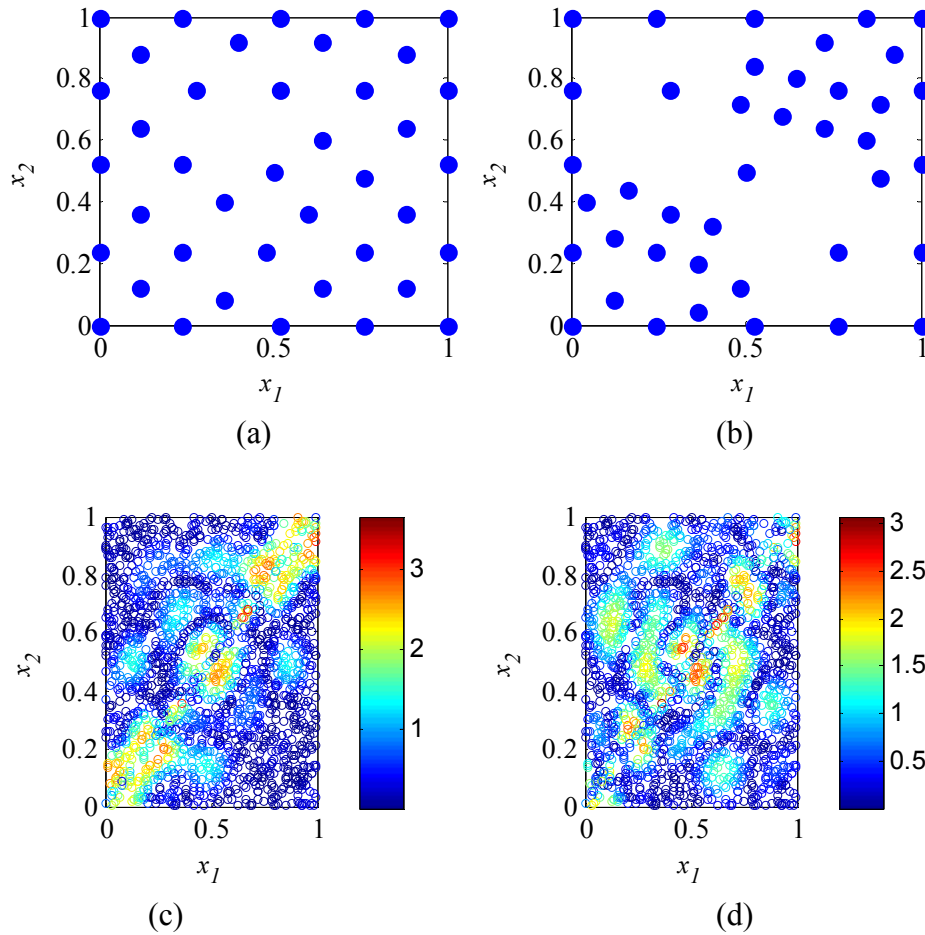


Figure 3.22 Problem P10 with modified initial design, (a) MED design, (b) SFCVT design, (c) absolute error using MED and (d) absolute errors using SFCVT

3.5.4 Comparison with MSD Method

In this section, the proposed approach is compared with the MSD method (Jin et al., 2002). Again, the number of initial designs and the total number of designs was fixed. The results are shown in Figures 3.23-3.28.

From Figure 3.23, we see that the proposed approach outperforms the MSD method in only 6 out of 24 test problems. The performance improvement of the MSD method over the proposed SFCVT method in terms of MAS is small, except for problems P7, P9 and P10. Figure 3.23 shows the box plots for MAS values obtained

from the MSD method. Figures 3.25, 3.26, 3.27 and 3.28 show the RMSE FoI, MAE FoI, RRMSE FoI and RMAE FoI of the SFCVT approach over MSD method. Based on the median values, the SFCVT method performs better than MSD method in 12 out of 24 problems for RMSE, 11 out of 24 for MAE, 13 out of 24 for RRMSE and 13 out of 24 for RMAE.

The LOO error model issue for problem P10, described in previous section is present in this case as well. Only the MSD and the MED methods work well on problem P10.

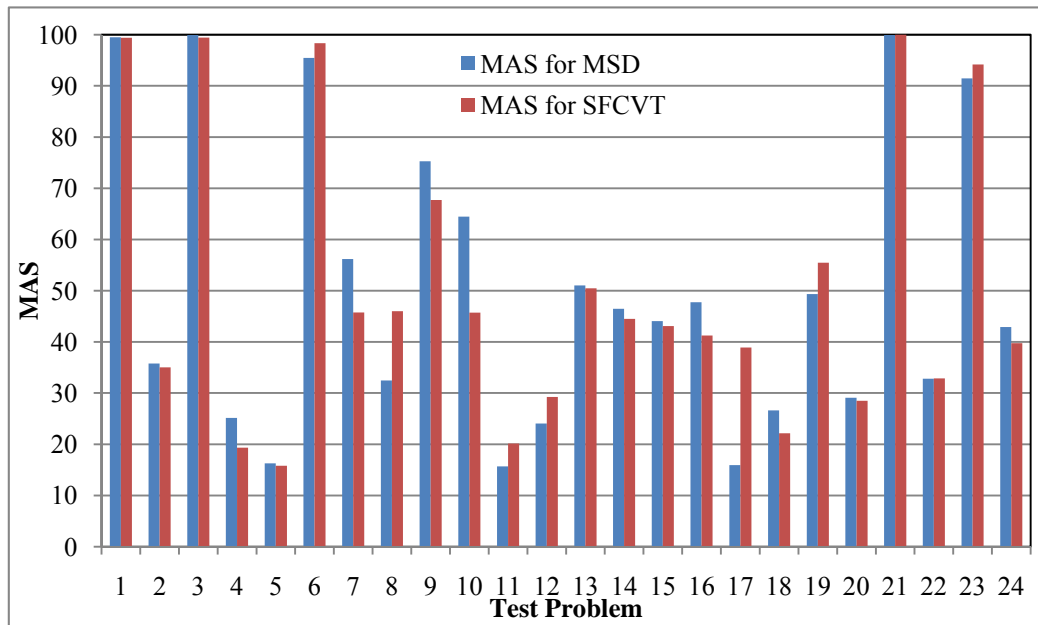


Figure 3.23 MAS comparison for MSD vs. SFCVT

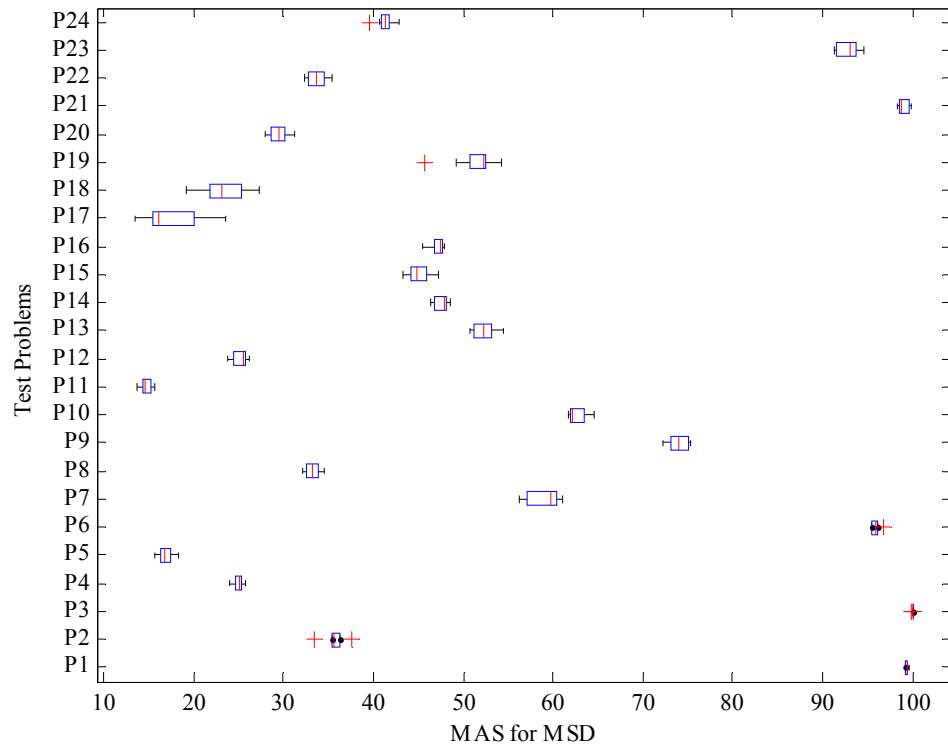


Figure 3.24 MAS for MSD method

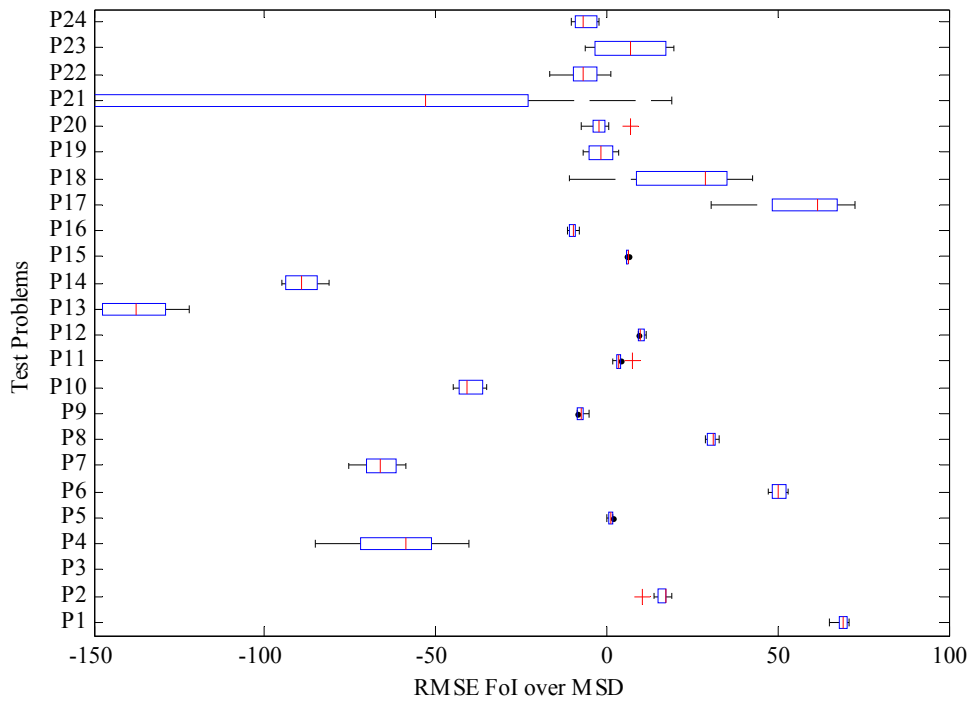


Figure 3.25 RMSE FoI of proposed approach over MSD method

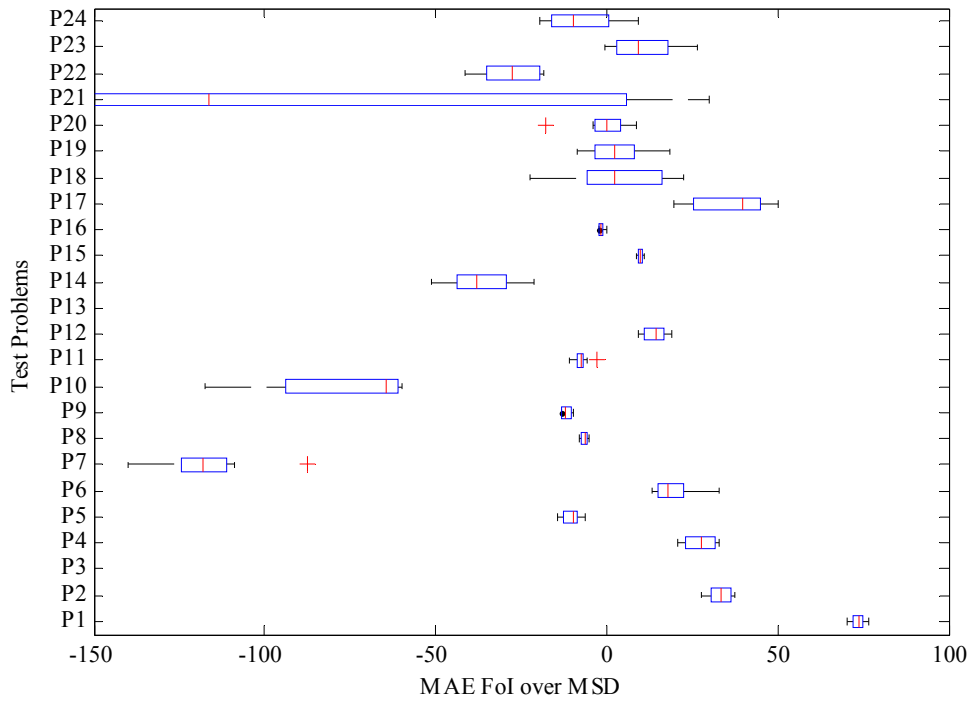


Figure 3.26 MAE FoI of proposed approach over MSD method

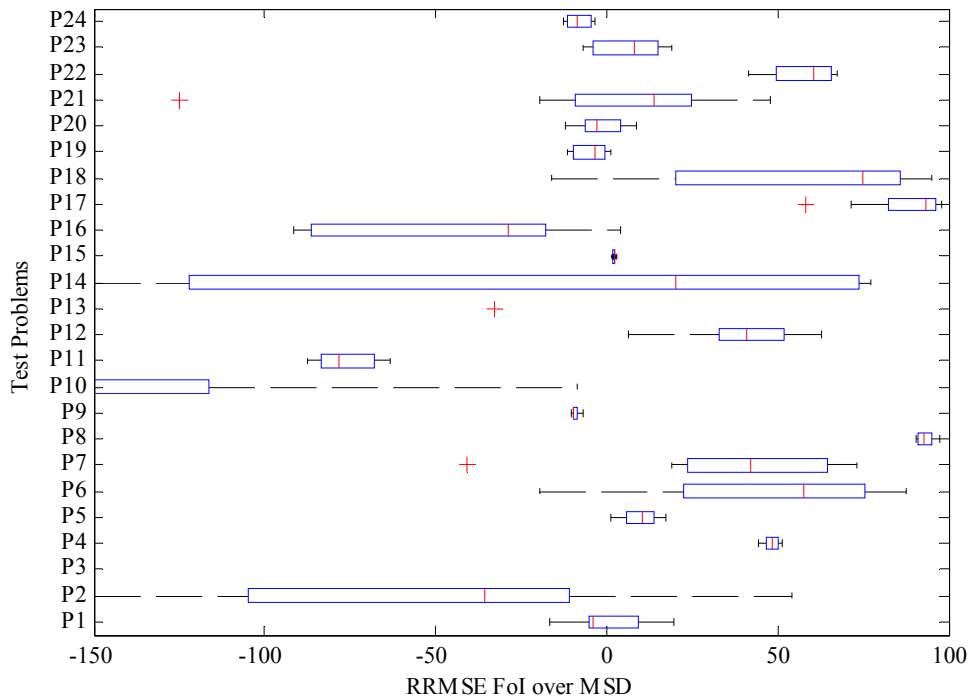


Figure 3.27 RRMSE FoI of proposed approach over MSD method

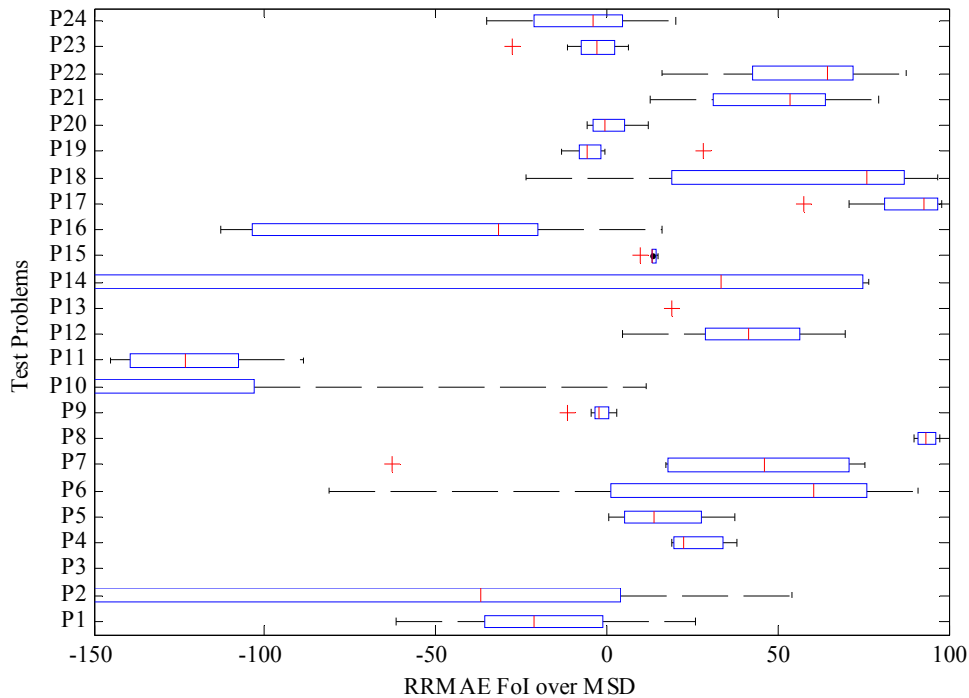


Figure 3.28 RMAE FoI of proposed approach over MSD method

3.5.5 Comparison with ACE Method

The proposed approach is also compared with the ACE method (Li and Azarm, 2006; Li, 2007). Due to programming issues with the available ACE implementation, the comparison could only be carried out for problems with two input variables. Figure 3.29 shows the comparison of MAS for the SFCVT and the ACE method. It can be observed from Figure 3.29 that the proposed SFCVT approach has better MAS than that of ACE method for 11 out of 16 test problems. The other FoI plots are shown in Figures 3.30 – 3.33. Again, based on median values, the SFCVT method performs better than the ACE method in 11 out of 16 problems in terms of RMSE, 11 in terms of MAE, 10 in terms of RRMSE and 11 in terms of RMAE.

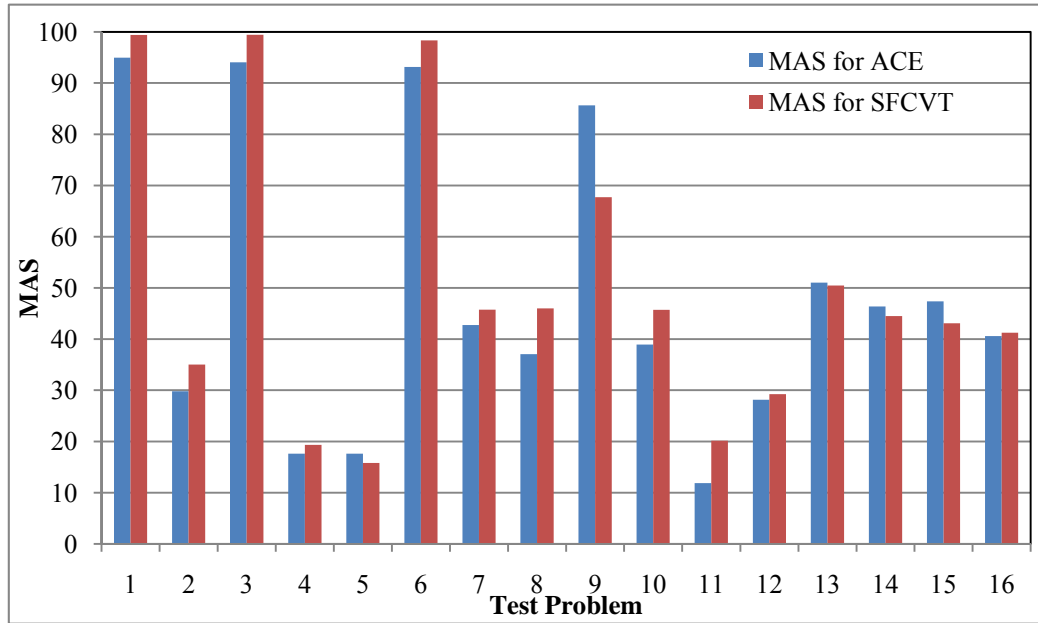


Figure 3.29 MAS comparison for ACE vs. SFCVT

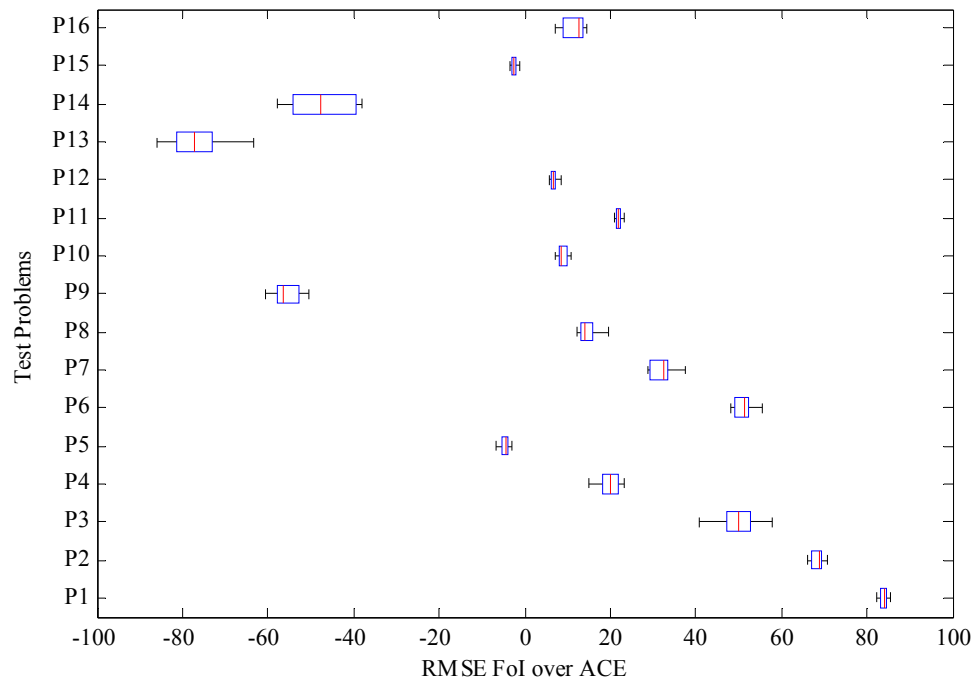


Figure 3.30 RMSE FoI of proposed approach over ACE method

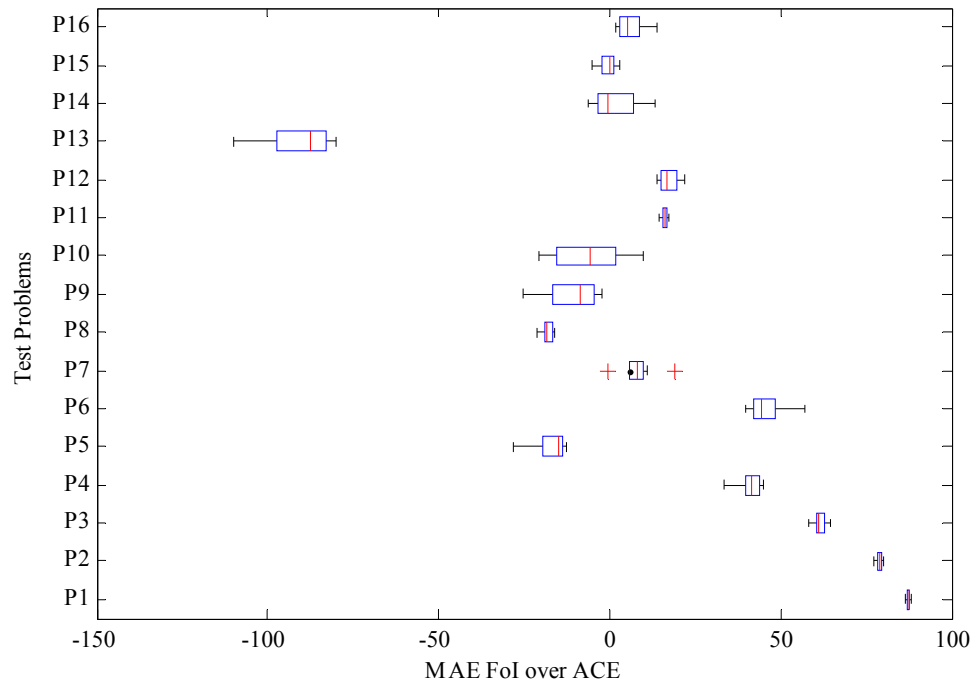


Figure 3.31 MAE FoI of proposed approach over ACE method

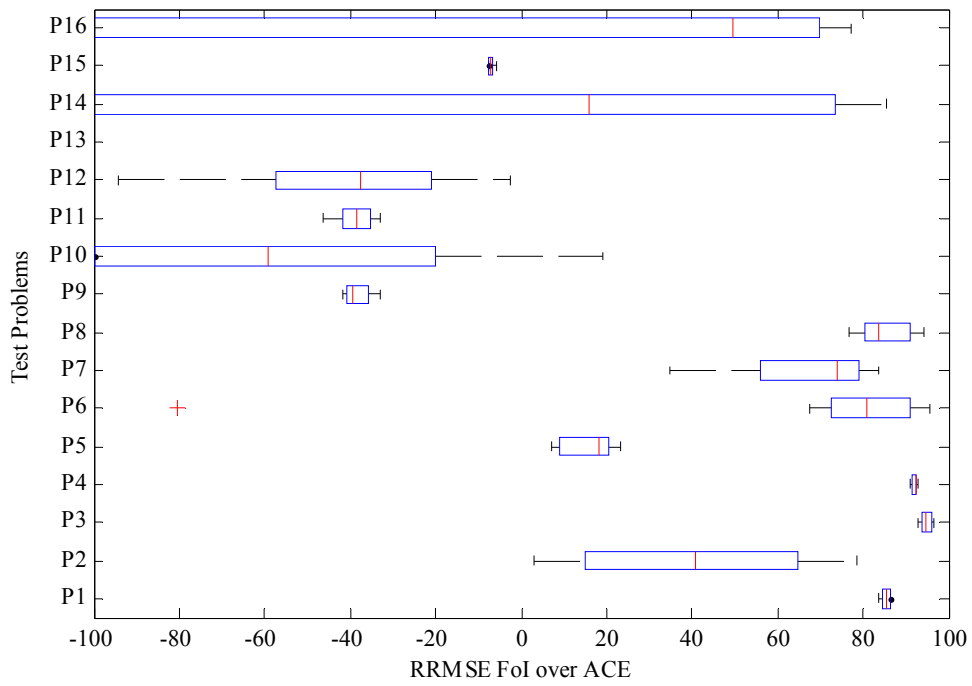


Figure 3.32 RRMSE FoI of proposed approach over ACE method

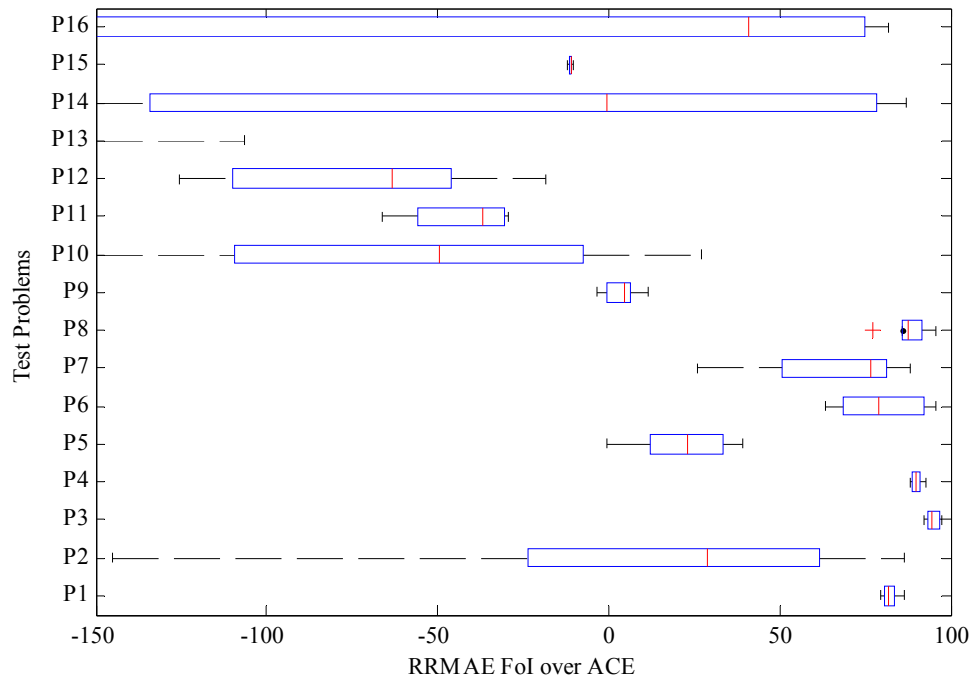


Figure 3.33 RMAE FoI of proposed approach over ACE method

The proposed approach is also applied to a real-world engineering design problem which focuses on the research and development of the next generation of air-cooled heat exchangers. The details and the results for this engineering example are discussed in Chapter 5.

3.5.6 Effect of Initial Design

In this section we briefly study the effect of the number of points in the initial design. For any given problem, there are an optimal number of points that should be present in the initial design. While this number cannot be arrived apriori for black box functions, in this section we study the effect of the number of points in the initial design for a fixed number of total available function calls. The effect of the choice of the initial design can also be studied.

The MED method is used to generate initial samples. The total number of sample points is fixed at $(20 \times d)$, where d is the problem dimension. Numerical experiments are conducted starting with $5d$ and $10d$ as the number of samples in the initial design. The verification of the resulting metamodels, expressed using MAS, RRMSE and RMAE are shown in Figures 3.34-3.36 below.

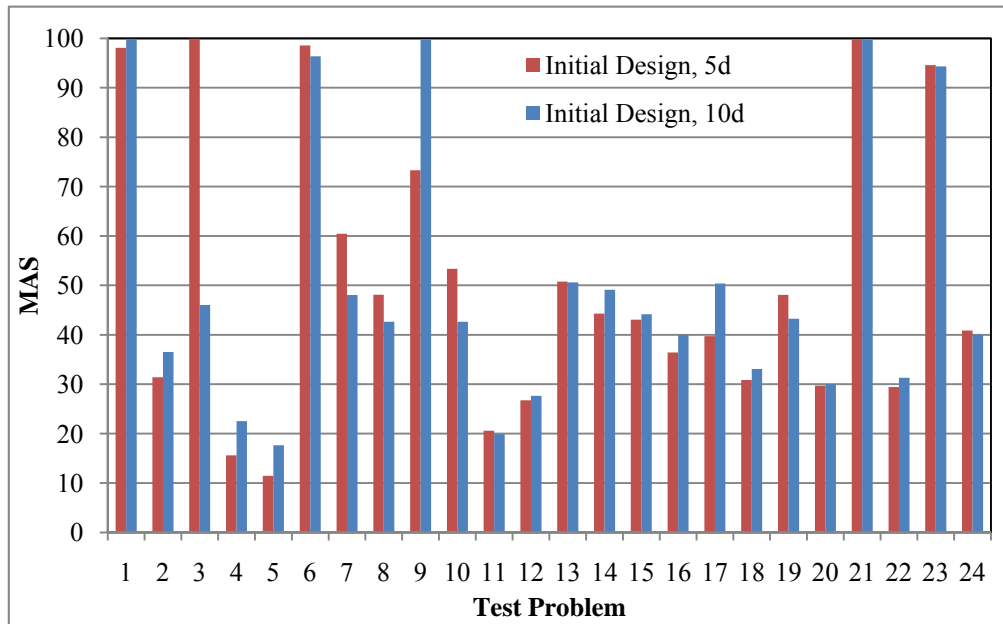


Figure 3.34 MAS comparison for $5d$ and $10d$ points in initial design

Figure 3.34 shows that for certain problems (e.g., problems 5, 7 and 10) the fewer number of points in the initial design results in a better metamodel, thus pointing out that more adaptive samples are necessary to capture function behavior in the CAMM regions. The metamodels for other problems (e.g., 4, 5, 9 and 17) perform better with a higher number of samples in the initial design. This is because a lower number of initial samples are not sufficient to capture all the CAMM regions in the response space. Similar behavior is observed for RRMSE and RMAE as shown in Figures 3.35 and 3.36 respectively.

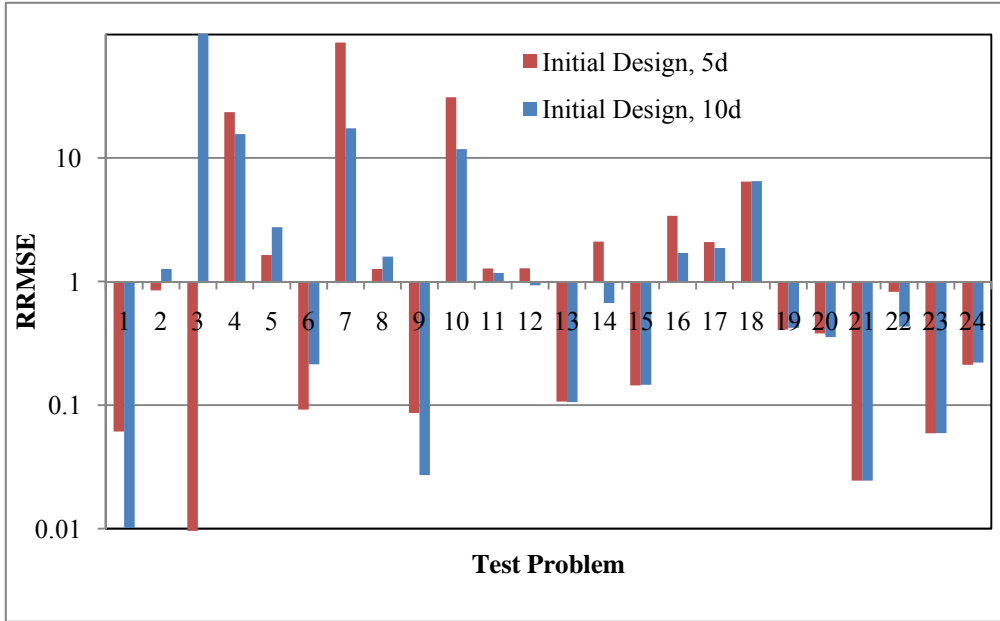


Figure 3.35 Metamodel RRMSE for 5d and 10d points in initial design

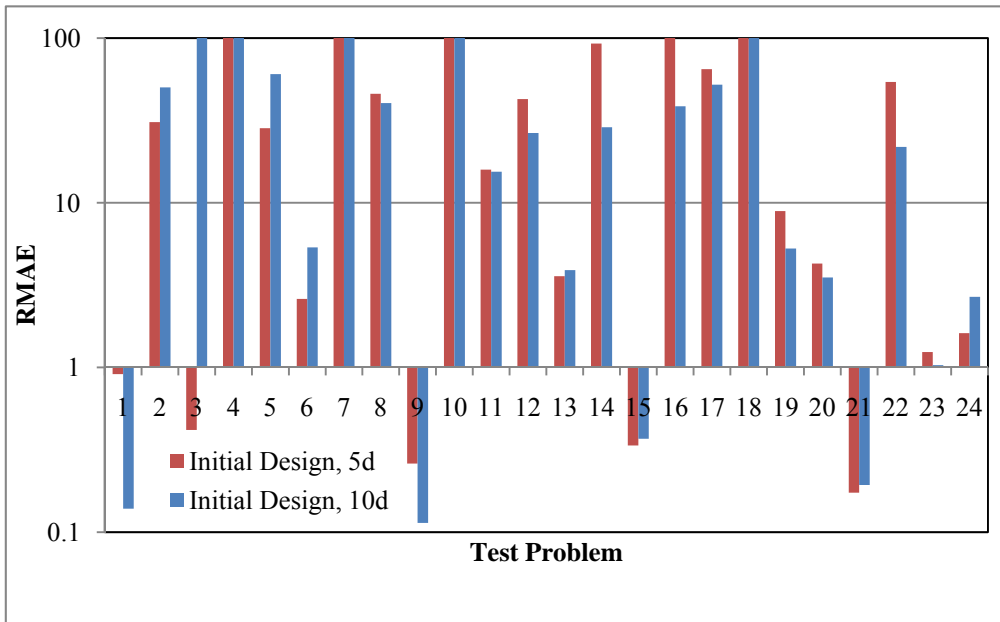


Figure 3.36 Metamodel RMAE for 5d and 10d points in initial design

3.5.7 Scalability to Higher Dimensions

The SFCVT method was also applied to test problems with higher dimensions. Four test problems with scalable closed form expressions were chosen. The single objective formulation was used. The 16 and 24 dimensional versions of test problems P3 (Dixon-Price function) and P5 (Griewank function) were used. The test problems are described in Appendix-A. The MAS values were compared with those obtained using the MED method and the MSD method. The comparison is shown in Figure 3.37. The MAS values are very comparable for test problem P3 for 16 dimensions, but for other test problems, the SFCVT method performs worse than the MED and the MSD method. This can be explained by the fact that the test problems are highly multi-modal as such the method gets trapped into a subset of the CAMM regions. For such functions (e.g., Griewank function), a space-filling approach is better suited. It should be pointed out that the function behavior is assumed to be unknown.

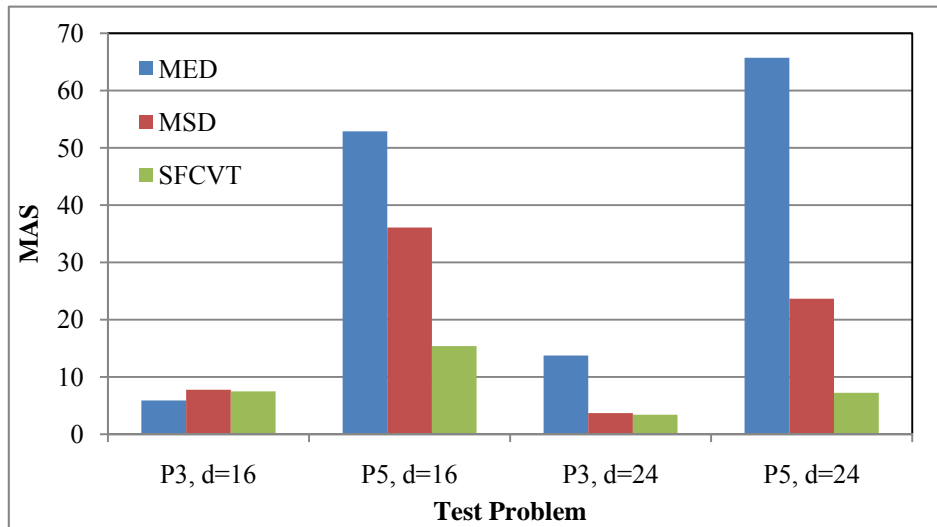


Figure 3.37 MAS comparison when SFCVT method is applied to higher dimension problems

3.5.8 Comments on Computational Effort

The computation time for the proposed SFCVT approach is dominated by the LOO error calculation and the optimization problem which is solved to arrive at the next sample. Note that in the LOO error calculation, the correlation parameters are re-estimated for every point in the current design.

In general, for the same number of function calls, any adaptive DOE approach will require more computation time than a non-adaptive approach. In order to generate the same number of new samples, the SFCVT method requires on average twice as much time as the MED, MSD or the ACE method. While, for the test case considered, the comparison is made for the same number of function calls, but at the end of the sampling process the resulting metamodels have differing accuracies. For example, it is observed that the SFCVT method performs better (in terms of its accuracy for the same number of function calls) on test problems with non-symmetric CAMM regions (e.g., test problems P1, P3, P6, P8), where as for test problems with multiple distributed and symmetric CAMM regions (e.g., test problems P4, P7, P10) a space filling (i.e., non-adaptive approach) is better suited. As such, for test problems with non-symmetric CAMM regions, SFCVT method will require less computational effort to arrive at a globally accurate metamodel.

3.6 Empirical Procedure for Function Call Allocation

In this section we propose an empirical procedure for resource allocation for single response adaptive DOE method. The resource refers to the available number of function calls.

3.6.1 Problem Statement

In practical applications, the number of available function calls is limited. These function calls need to be used for DOE phase and metamodel verification. Thus a systematic method is required for the allocation of function calls, either for metamodel development (i.e., adaptive sampling) or for random verification.

This problem can be greatly simplified if some information about the behavior of the function is known before hand. As with the assumptions earlier, we assume that no information about the function is available a priori.

3.6.2 Proposed Empirical Procedure

The proposed empirical procedure is based on the notion that as more and more samples are added to a design, the performance of the metamodel does not improve proportionately. In other words, the metamodel is already at its best (i.e., no improvement in MAS, RMSE, MAE etc.) and new samples do not add any new information to it.

The procedure starts out with a set of inputs from the designer. The inputs required are the maximum available function calls (K_{\max}), minimum number of points to be used for verification (N_v) and the minimum required MAS (MAS_{crit}). It is implicit that the procedure has access to the simulation tool to carry out the required

function evaluations. Let d be the problem dimension, i.e., the number of inputs variables, D be the current design. Note that D is initially empty.

The different steps are explained below.

Step-1: Accept the inputs F_{\max} and N_v . Set counter $k = 0$.

Step-2: Generate random test points and evaluate their true response. Update counter k .

Step-3: Generate initial design using MED or other suitable method and evaluate the true responses. The number of points in the initial design is set to

$$N_{init} = 2 + (d + 1) \times (d + 2) / 2 \quad (3.12)$$

The reason for using Eq. (3.12) is as follows: the second term in Eq. (3.12) is the number of points required in a second order polynomial regression equation which is used in the response mean calculation in Kriging. The first term (i.e., 2) ensures that during LOO error calculation, the resulting regression is a valid least-squares system.

Step-4: Use the adaptive DOE method proposed earlier to generate d additional points.

Step-5: Develop a metamodel using the current design and then evaluate its performance using the random points generated in Step-2. Compare its performance with metamodel in previous iteration. If $(k+d) > K_{\max}$, then STOP. If this is the first iteration, then go to Step-9. If the current MAS is greater than the previous MAS and if the current MAS is greater than MAS_{crit} , then go to Step-6 else go to Step-7.

Step-6: If $(k + d) > K_{\max}$, then STOP, else Sample d new points randomly and add them to the verification design. Go to Step-10.

Step-7: Calculate the LOO errors and the standardized residual for the current design. If the number of points with a standardized residual greater than 3, is more than two, go to Step-8, else go to Step-9. The standardized residual is just the ratio of the cross-validation error and the mean error predicted by Kriging.

Step-8: Sample d new points using the MED or other suitable space-filling method and compute the corresponding responses. Update D with the newly generated d points. Go to Step-10.

Step-9: Sample d new points using the adaptive DOE method and compute their response. Update D with the newly generated d points.

Step-10: Update counter k , $k = k + d$. If $(k < K_{\max})$, go to Step-5 else STOP.

3.6.3 Numerical Experiments

The procedure is applied to the test problems P1 through P16. The numerical experiments are conducted 20 times, using the following parameters, $K_{\max} = 60$, $N_v = 20$, $MAS_{\text{crit}} = 50$. The MED method was used to generate the initial design and the adaptive DOE method proposed in section 3.4 is used to adaptive sample new points. The results are shown in the form of a box plot. Figure 3.38 shows the distribution of the number of points used in developing the metamodel. In 10 out of 16 test problems, all available points were used for adaptively sampling new points. This is because, the criteria for acceptance of the metamodel was too strict ($MAS_{\text{crit}} = 50$).

Figure 3.41 shows the number of points used in verification. The sum of points in Figures 3.40 and 3.41 for each case must be equal to K_{max} .

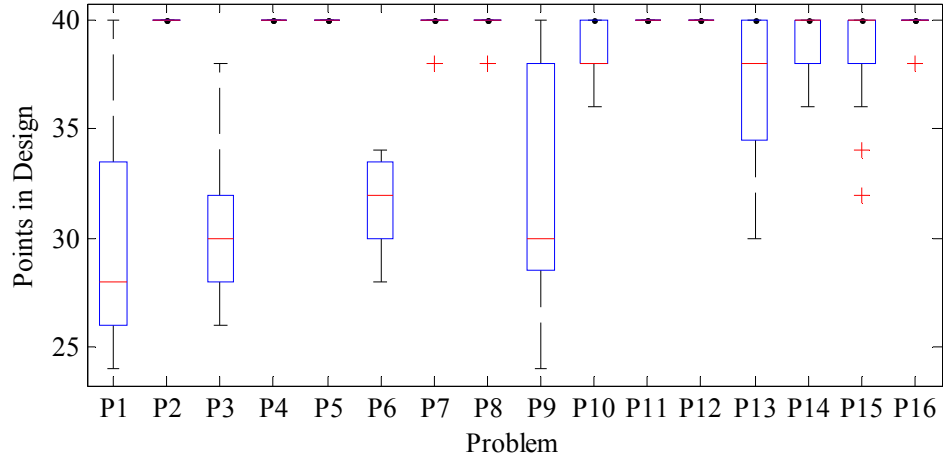


Figure 3.38 Points used for developing metamodel

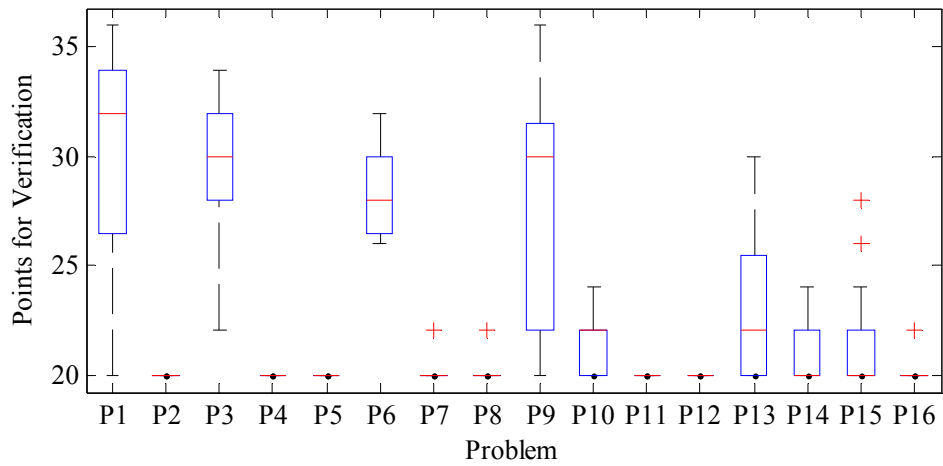


Figure 3.39 Points used for verification

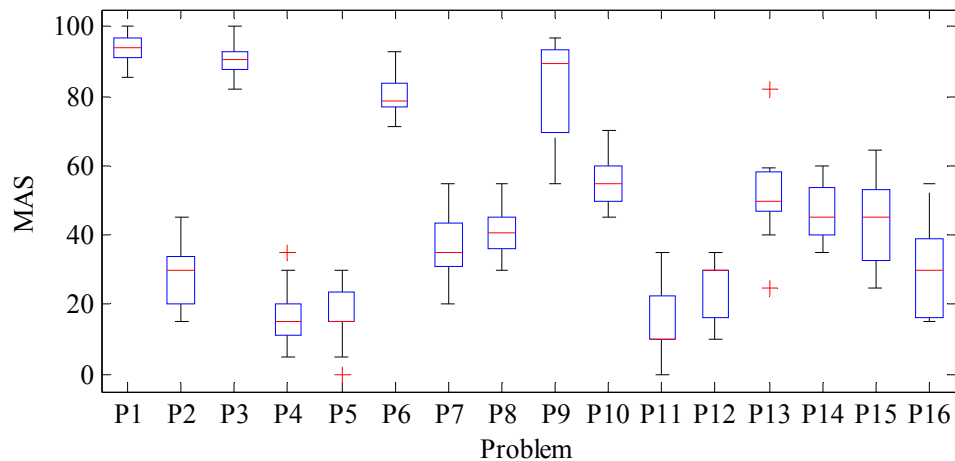


Figure 3.40 Resulting MAS for test problems

Figure 3.40 shows the MAS for the resulting metamodels. Again, it is observed that the resulting metamodels fall short of the prescribed MAS criteria on several test problems. As a result, the procedure never samples additional points for verification.

3.7 Summary

An adaptive DOE approach for single response deterministic simulations is developed based on the tradeoff between cross-validation errors and space-filling criterion. The proposed approach is based on the premise that at each stage during an adaptive DOE procedure, a tradeoff has to be made between allocating new sample in a region of the design space that is sparsely sampled and allocating a new sample in a region where the response is estimated to be multi-modal, non-smooth or noisy. The proposed approach uses the concept of cross-validation error, specifically leave-one-out error to probe the response space for sensitive regions. It also uses a space filling metric to identify the sparsely populated regions of the design space. Two different space filling metrics are used. First, the concept of maximin distance is used; wherein

all the dimensions of the input space are treated equally and only a Euclidean distance is used as a criterion. This gives us the SO formulation for the DOE problem. Second, the MSE is used as a space filling metric resulting in a multiobjective optimization problem, termed as the MO formulation. The advantage of MSE is that the distances in each dimension are weighted and the use of this metric is suitable when Kriging is used as the metamodeling approach. The maximum distance metric can be used with or without the Kriging metamodeling approach. The MO formulation of the proposed approach can provide one or more samples at each stage. This has the advantage of being able to sample more points, hence more information from the design and response space, in the same amount of clock-time. This is especially useful when the approach is used along with a parallel computing framework.

The proposed approach is applied to a suite of numerical and engineering test problems comprising of 24 single response functions from the literature. When comparing the results obtained using the SO and the MO formulation, it was found that they both yield comparable results. The SO formulation is then compared with three methods from the literature. The results show that the proposed approach outperforms the maximum entropy design (MED) method and two additional adaptive DOE methods, the MSD and the ACE method from the literature, in most of the test problems with regards to MAS, RMSE and MAE. Numerical experiments are conducted several times to gather statistical results.

The proposed approach relies on a good set of starting designs that represent the design space reasonably well. Based on the numerical experiments it is observed that starting with an excessive number of initial designs (thereby less adaptive designs for

fixed number of function calls) actually results in an inferior metamodel. It is also observed that in certain cases, the starting design may never yield a good metamodel for the LOO errors, causing the approach to fail.

In the next chapter an adaptive DOE method for multiresponse deterministic simulations is presented.

Chapter 4 Multiresponse Adaptive Design of Experiments

4.1 Introduction

This chapter proposes a new adaptive DOE method for multiresponse deterministic computer simulations.

Many real world engineering simulations are characterized by multiple inputs and multiple outputs. The simulation models are complex, generally iterative in nature and yield all output values in a single execution, i.e., when a simulation is executed with a set of inputs, all the outputs are calculated simultaneously. These outputs or responses, in the context of design optimization, may be objective values, constraint values, design attributes or simply other outputs of interest from the simulation. Naive application of approximation-assisted optimization to such a simulation would involve developing a metamodel for each response separately. In other words, for each output an adaptive DOE approach is used to create a set of samples. These samples may not be the same for each output, thus wasting a large number of function calls. In order to alleviate this problem, multiresponse approximation models (Li et al., 2006; Li, 2007; Romero et al., 2006) have been proposed in the literature. As opposed to single response approximation methods, multiresponse approximation methods, as the name implies, try to simultaneously achieve metamodels for multiple outputs using a minimum number of function calls. In this chapter, the problem of adaptive DOE for multiple responses is posed as a multiobjective optimization problem, where there is a tradeoff between allocating samples for improving the metamodel performance for one response vs. another. The proposed approach is

termed as Multiresponse Space-filling Cross-Validation Tradeoff (MSFCVT) method. It is shown that the proposed approach performs better than the previous methods presented in the literature when applied to the same test problems.

The remainder of this chapter is organized as follows: Section 4.2 provides a detailed literature review on existing techniques for multiresponse approximation, Section 4.3 describes the proposed approach. Section 4.4 demonstrates the applicability and scalability of the proposed approach by applying it to a range of test problems from the literature and comparing its performance against previous DOE methods.

4.2 Literature Review

There are two aspects in multiresponse approximation. First is the simultaneous DOE for multiple responses. The DOE method must sample new points such that they improve the performance of the metamodels for all responses at the same time. Second is the metamodel development, in which we can develop one metamodel for each response or we can develop a multiresponse metamodel for all responses simultaneously. In this section brief overview of metamodeling techniques for multiresponse approximation is presented followed by a review of adaptive DOE techniques. Even though the DOE is the first step in approximation, we first present the metamodeling techniques and then the DOE, since DOE is the focus of this chapter.

As discussed in Chapter 3, numerous approximation techniques have been introduced in the literature for single response approximation. The underlying

assumption of these metamodeling techniques is that the engineering design simulation generates a single response i.e., scalar output. Many complex engineering simulations yield multiple responses in a single execution, i.e., for a single set of inputs a single set of outputs (or responses) is generated. One can treat each of these responses as being an output of a single simulation and then construct a DOE and a metamodel for each of the responses, which is a fairly common approach.

Some research has been conducted to handle multiple responses in a computationally efficient manner, though the literature on multiresponse adaptive design of experiments is sparse. The problem of simultaneously handling multiple responses has been addressed for regression methods by combining the multiple-responses into a “value” function (Chiao and Hamada, 2001; Derringer and Suich, 1980). An extension of Kriging, termed as Cokriging (Ver Hoef and Cressie, 1993) has been proposed to handle multiple responses. Romero et al. (2006) propose a multiresponse meta-modeling approach based on the use of covariance matrix of the responses. This is very similar to the Kriging method, where the predicted output is now a vector with more than one element. They also propose an extension to the MED method, termed as the modified MED (MMED) method, to handle multiple responses. The covariance matrix in the MMED method is based on the multiresponse covariance function (Romero et al., 2006) of the underlying metamodel. A dependent metamodeling (DMM) approach (Li et al., 2006) was also proposed, wherein instead of developing a metamodel in which each response is a function of the input design variables, the response is assumed to be a function of the input designs variables as well as other responses. This results in a system of

nonlinear equations (metamodels) that needs to be solved to evaluate the multiple responses. The DMM technique implies that the DOE for each response should be constructed such that it includes the input design variables as well as the other responses. Based on these inferences, Li et al. (2006) also include an extension of the maximum entropy design method to include the response space. We term this approach as the MED for dependent metamodel. Li et al. (2006) applied their approach to examples with two input variables and two responses. Further testing of the method by Li et al. (2006) is necessary to evaluate the general applicability of their approach.

Romero et al. (2006) proposed an adaptive DOE approach for multiresponse approximation. Their approach is similar to the Kriging approach, but the covariance function is a multivariate Gaussian function which accounts for the multiple responses. The resulting covariance matrix includes contributions from the multiple responses as well. To complement this metamodeling technique, they proposed two adaptive sampling schemes. The first technique is an extension of the maximum entropy sampling method (i.e., MMED), wherein the augmented covariance matrix is replaced by the new covariance matrix from Romero et al.'s (2006) method. Second, the Kleijnen and van Beers (2004) approach of maximum cross-validation variance (MCVV) is extended to include multiple responses. In single response case, the Kleijnen and van Beers (2004) approach finds the next sample as the one that maximizes the cross-validation variance while in the multiple response case, Romero et al. (2006) propose to use the trace of the cross-validation covariance matrix for the multiple responses. The trace calculation and hence the approach requires that the

responses be scaled properly in order to be effective. Romero et al. (2006) applied their approaches to 3 test problems (with 2 inputs – 1 response) and for multiresponse case; they selected two single response test problems to mimic multiple responses. Their studies found that the modified MED method outperformed the MCVV method. They used 3 test problems in their numerical experiments and the conclusion was that optimal Latin-hypercube (LHC) as initial sampling technique along with their proposed adaptive MED method results in metamodels that are more robust and accurate or better than other sampling approaches. The MCVV method needs to be applied to additional test problems with multiple inputs and outputs to evaluate its general applicability.

Based on the literature so far, the existing approaches for multiresponse adaptive DOE suffer from the following drawbacks: (a) scaling and/or normalization of inputs and responses, which is not very intuitive especially when the design problem is not known before hand, (b) the approaches have used multiresponse metamodels and no comparison has been made to single response metamodels with multiresponse DOE (c) general applicability is not known, i.e., the approaches have not been applied to a broader set of numerical or engineering design problems with more than two inputs and responses. In this chapter a new adaptive DOE method for multiple responses is proposed which extends the LOO error and the space filling criteria defined in Chapter 3 to multiple responses. The proposed multiresponse approach is applied to a total of 10 test problems from the literature. Two of these test problems are from Li et al. (2006) and Romero et al. (2006) and are used for comparison against published literature.

4.3 Multiresponse Adaptive DOE Approach

In this section we provide the details of the proposed approach. As mentioned in Chapter 3, an adaptive DOE approach has to make a tradeoff between allocating experiments in sparsely sampled areas versus allocating experiments in regions corresponding to the CAMM regions of the response space. In Chapter 3, these two aspects were handled using a LOO error metric and a space-filling criterion. In the proposed approach for this chapter the same concept is extended to multiple responses. In a multiresponse case, the tradeoff is not only between the LOO error and the space-filling criteria, but also between the LOO errors for the individual responses.

The different steps in the proposed approach are described in the following sections. A detailed flow chart of the entire procedure is explained in Section 4.3.8.

4.3.1 Overview of the Proposed Approach

The proposed approach starts with an initial design. The purpose of this initial design is to provide preliminary information about the response space. Based on the initial design, LOO errors are calculated for each response and a metamodel built for LOO errors corresponding to each response. As mentioned in Chapter 3, the LOO error calculation used in this dissertation is the relative LOO error defined in Chapter 3. A constrained multiobjective optimization problem is then formulated which aims at finding points in the design space that simultaneously have the maximum value of the LOO error for each response and are at the same time sufficiently away from existing points in the current design, D . The solution to this multiobjective optimization problem is a set of Pareto points from which a single point is chosen as

the next sample. The single point is chosen based on the criterion described in Section 4.3.5. The newly chosen point is then evaluated for its true response and is added to the current design D . The procedure is repeated, starting with the LOO error calculation followed by choosing the next sample, until a stopping criteria is reached (e.g., such as the maximum number of function calls is reached). The details of individual steps are described in the following sections.

4.3.2 Choice of Initial Design

As mentioned in Chapter 3, the initial design is crucial to the success of an adaptive DOE strategy and the resulting metamodel. In the proposed approach, it is recommended to use the MED method to generate an initial design. Again, the reason for using the MED method is to have a good representation of the entire input space. The number of points in the initial design is influenced by the size of the problem as well as the response behavior. Since the response behavior is not known a priori, we use $(10 \times d)$ as the number of points in the initial design, where d is the problem dimension (i.e., number of input variables).

4.3.3 LOO Error Calculation

In Chapter 3 it was proposed to use a Kriging based LOO error prediction model for the response. In case of multiple responses, we extend our earlier single-response approach to include a LOO error model for multiple responses. The metamodeling technique for this LOO error model is Kriging. We can use multiple single response Kriging models, a multiresponse Kriging model or the Cokriging method (see Section 4.2). We use multiple single-response Kriging metamodels as opposed to a multiresponse Kriging model. In other words, the LOO errors for each response are

calculated separately and one metamodel for LOO errors corresponding to each response is developed. The difference is that when individual metamodels are used, the correlation parameters are calculated for each response separately. In multiresponse Kriging, there is only one set of correlation parameters for all the responses, resulting in less accurate metamodels. The Gaussian correlation discussed in Chapter 2 is used for Kriging, but other correlations can be used and in some cases may be required due to the nature of the responses.

4.3.4 Space-filling Criterion

The space filling criterion is similar to the one proposed in Chapter 3. The metric S is defined as follows:

$$\begin{aligned} ds(x_i) &= \min(\|x_i - x_j\|_2), \forall x_i \in D \wedge (i \neq j) \\ S &= 0.5 \times \max(ds(x_i)), \forall x_i \in D \end{aligned} \quad (4.1)$$

4.3.5 Choosing Next Sample

As mentioned in Chapter 3, the problem of choosing the next sample point is a tradeoff between allocating of the experiment in a CAMM region (with higher LOO error values than other regions) or allocating the sample in a sparsely sampled region of the space (indicated by the space filling metric). In order to extend this to multiple responses, we choose the LOO errors for different responses as the tradeoff values subject to the space filling metric constraint. This is mathematically represented as follows:

$$\begin{aligned} x_{n+1} &= \arg \max_x \hat{e}_{LOO}^j \quad j = 1, \dots, m \\ \text{s.t. } &\|x - x_k\|_2 > S \quad \forall x_k \in D \end{aligned} \quad (4.2)$$

Note that the above optimization problem is an MOOP and thus will generally yield a set of Pareto optimal solutions. The challenge then is to select one or more points to conduct experiments. There are different methods that can be used to choose the next samples as follows:

- (a) Choose all the Pareto points. This would involve sampling a large number of points in each stage.
- (b) Choose points from the Pareto set that have the highest value of the LOO error for a given response, implying a preference or affinity towards one particular response.
- (c) An extension of (b) is to choose all points from the Pareto set that have the highest predicted LOO error values for each of the responses, resulting in (at most) m points being sampled per stage, where m is the number of responses.
- (d) Use a more elaborate technique such as level of dominance approach described in Section 3.3.3.

An example of the above mentioned tradeoff between the LOO errors for different responses is shown in Figure 4.1. Figures 4.1a and 4.1b show the response surfaces for a 2-input 2-output numerical example. The initial design is shown in Figure 4.1c. The LOO errors are calculated for all points in the design space and using a non-dominated sorting algorithm, a Pareto set is found as shown in Figure 4.1d. As seen from Figure 4.1d, clearly there is a tradeoff between the LOO errors for the two responses. The corresponding LOO error surfaces for the two responses are shown in

Figures 4.1e and 4.1f. We observe that the LOO error surfaces are nonlinear and multimodal in nature.

The problem in Eq. (4.2) can also be formulated as an unconstrained optimization problem as shown in Eq. (4.3).

$$x_{n+1} = \arg \max_x [\hat{e}_{LOO}^j, s_j^2] \quad j = 1, \dots, m \quad (4.3)$$

The above formulation essentially tries to maximize $2m$ objectives, where m is the number of responses. The formulation presented in Eq. (4.2) is helpful when Kriging is used as the metamodeling technique and when individual metamodels are built for each response, because the Kriging predictor also calculates the value of s along with the predicted response.

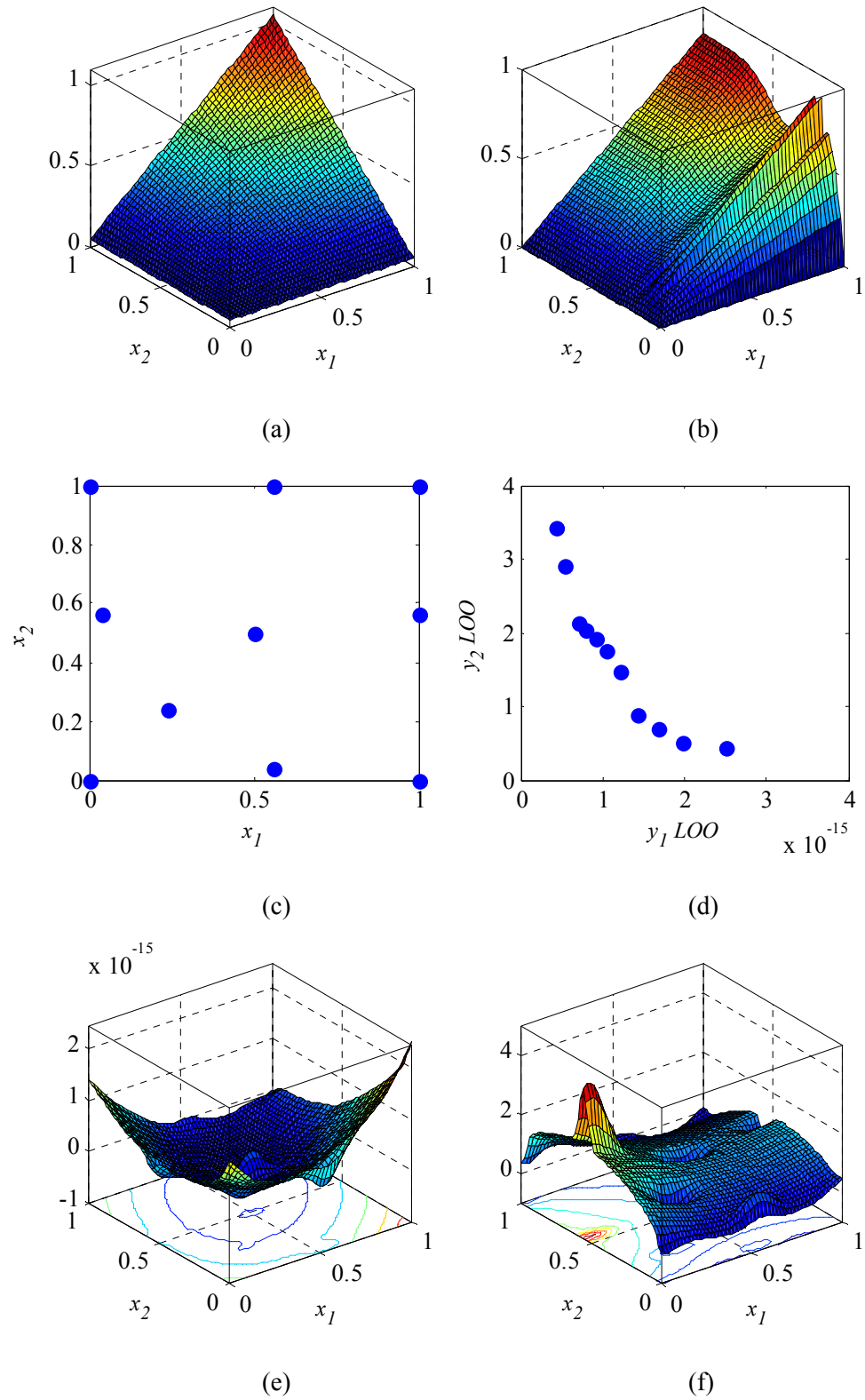


Figure 4.1 LOO error tradeoff, (a) Response surface for y_1 , (b) response surface for y_2 , (c) initial design, (d) y_1 vs. y_2 LOO error tradeoff, (e) LOO error surface for y_1 , and (f) LOO error surface for y_2

4.3.6 Design Update

The new point or points selected in Section 4.3.5 are evaluated for their true responses and added to the current design D .

4.3.7 Stopping Criteria

The stopping criteria in this case can be one or more of the following:

- (a) Maximum number of function calls
- (b) Acceptable error measure (i.e., RMSE, MAE) or performance criteria such as MAS (described in Chapter 2), for one or more responses based on an existing test sample of randomly generated points.
- (c) Acceptable value for the norm of an error measure, e.g., the maximum value of MAE amongst all responses, based on a test sample.

Generally in practical applications, the maximum number of available function calls is used as the stopping criterion and the same is used in this dissertation.

4.3.8 Step-by-Step Description of the MSFCVT Approach

Let K_{\max} be the maximum number of available function calls. The different steps are as follows:

Step-1: Generate an initial design D with predefined number of samples using the MED method.

Step-2: Calculate LOO errors for all responses for all the points in the initial design and build the Kriging based metamodel for the LOO errors.

Step-3: Solve the optimization problem discussed in Eq. (4.2) or (4.3) to obtain the next sample(s).

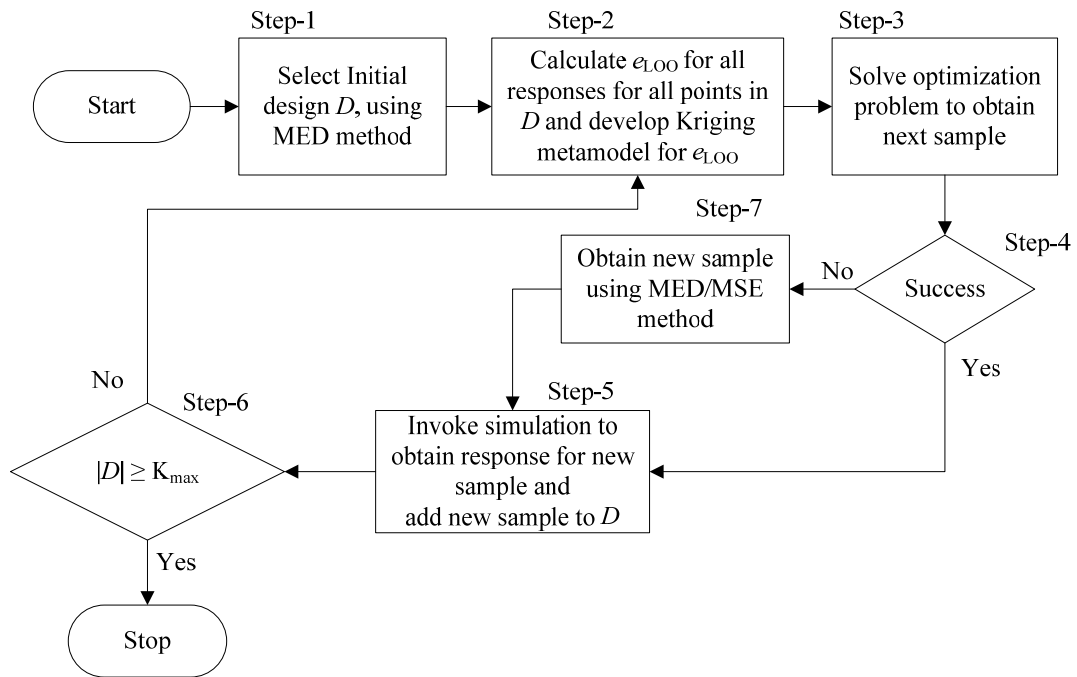


Figure 4.2 Step-by-Step flow chart for MSFCVT approach

Step-4: Check if the optimization problem in Step-3 is solved. If the optimization fails, or if there are no feasible solutions go to Step-7, else go to Step-5.

Step-5: Evaluate the true response for the new point(s) and add it to D .

Step-6: If the number of points in D is equal to the available number of function calls, then Stop, otherwise continue to Step-2.

Step-7: Compute the next sample using either the MED or the MSE method and proceed to Step-5.

4.4 Application Examples

In this section, we apply the proposed approach to several numerical and engineering test examples from the literature and from the test suite developed as a part of this dissertation to evaluate its applicability and scalability to a wide range of problems.

The metrics of MAS, RMSE, MAE, RRMSE, RMAE and the FoI are calculated individually for each response.

4.4.1 Numerical Example-1

The first numerical example is taken from Li et al. (2006) as a challenging test problem for multiresponse approximation. We note that the response y_2 in Eq. (4.4) is basically the product of x_1 and a highly nonlinear function (Farhang-Mehr and Azarm, 2005) which was described in Chapter 3. This makes the problem challenging. The problem is a two-input two-response test problem with a closed-form expression and is shown in Eq. (4.4).

$$\begin{aligned} y_1 &= x_1 x_2 + 0.5 \\ y_2 &= x_1 \{ (1 - e^{-2\sqrt{x_2}}) + 6x_2 e^{-7x_2} \sin(10x_2) - \\ &0.2e^{-2000(x_2-0.25)^2} + 60 \min 0, |x_2 - 0.14| - 0.08 \}^2 \\ &[\ln(x_2 + 0.2) + 1.5 \sin^2(85x_2)] \} \end{aligned} \quad (4.4)$$

The corresponding response surfaces for y_1 and y_2 are shown in Figure 4.3.

The total number of designs was fixed at 20 for a fair comparison with the DMM (Li et al., 2006; Li, 2007) design and RMSE reported in Li et al. (2006). The MSFCVT design was generated starting with an initial design of 10 points using the MED method and then adaptively sampling 10 additional points, one point at a time.

A set of 2000 randomly generated points (i.e., test sample) was used for metamodel verification. The corresponding designs and response surface for the MED and the DMM (Li et al., 2006) method are shown in Figures 4.4 and 4.5 respectively. The numerical experiments are repeated 10 times to reduce statistical bias and thus for each metamodel performance metric, we have a range of values. As in Chapter 3, a box plot (McGill et al., 1978) is used to concisely display the results.

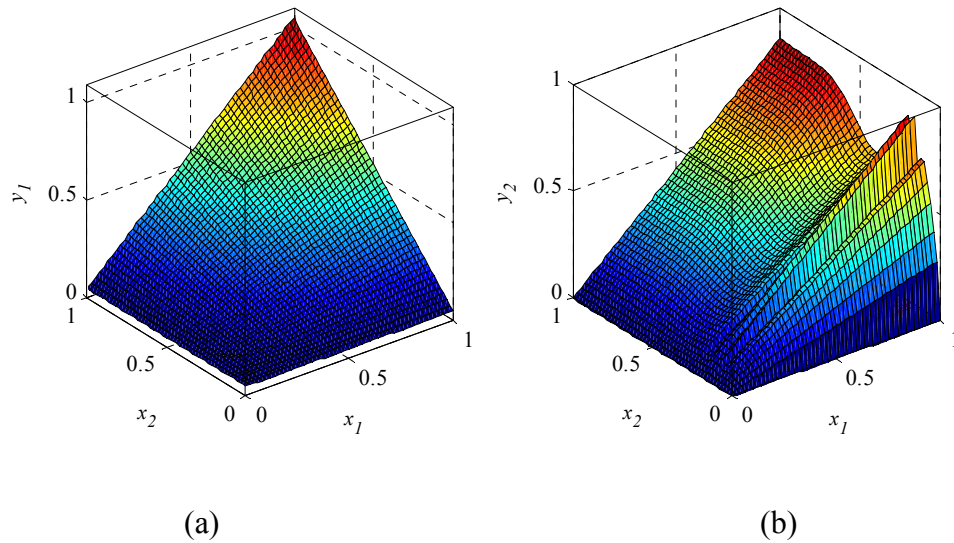


Figure 4.3 Responses for numerical example -1 from Eq. (4.4), (a) Response for y_1 , and (b) Response for y_2 .

From Figure 4.4a., we observe that the points generated using the MED method try to fill the space rather uniformly while the MSFCVT samples (Figure 4.4b) are more concentrated in the lower left of the x_1 - x_2 space. This can be explained based on the irregular behavior of the second response (y_2) shown in Figure 4.3b. The response surfaces generated using the metamodels are also shown in Figure 4.4. We observe that the response surface for y_1 closely resembles its true response surface shown in Figure 4.3a.

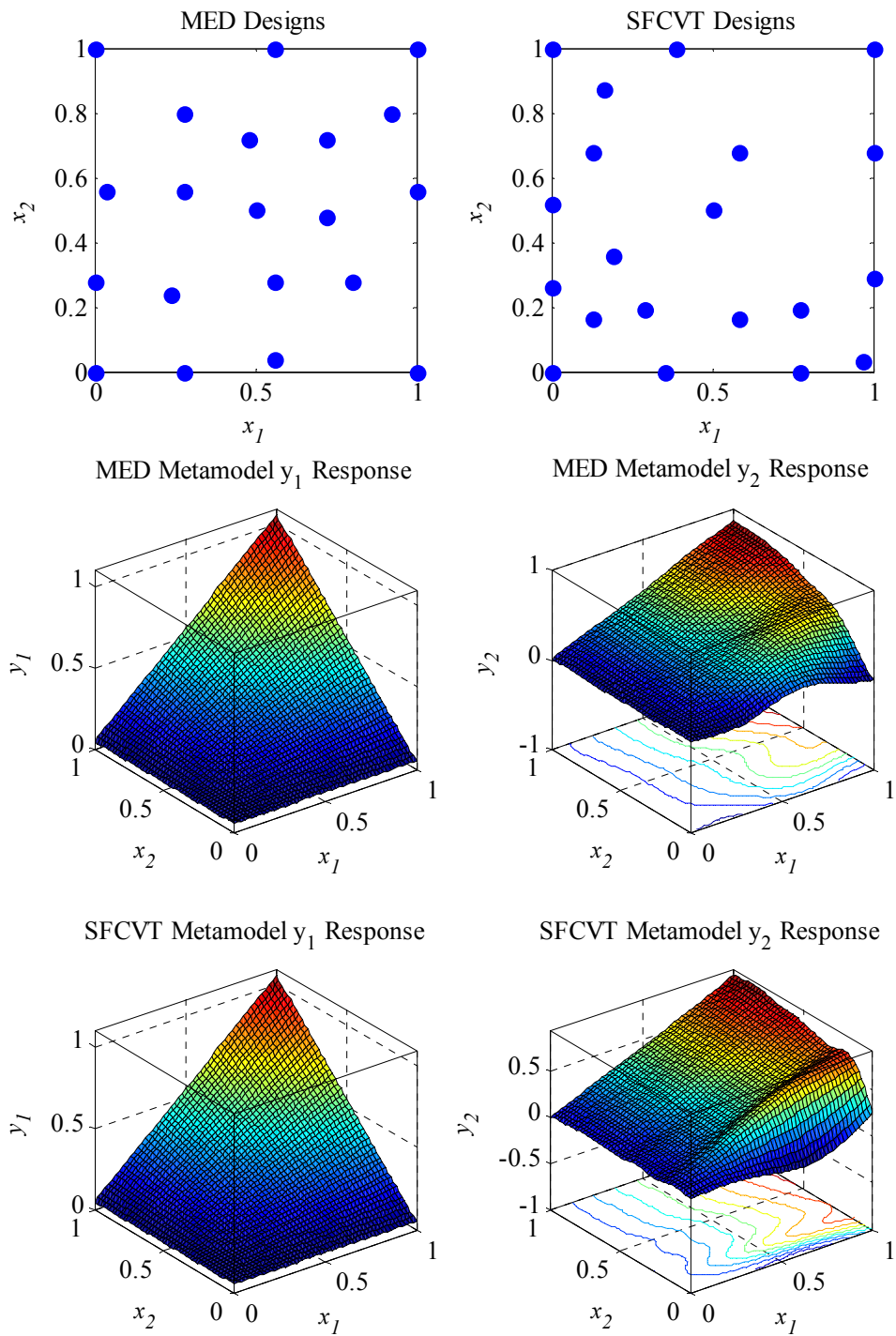


Figure 4.4 MED vs. MSFCVT approach, resulting designs and the response surfaces

In case of y_2 , the response surface generated using the MSFCVT based metamodel more closely resembled the true response surface. These observations are further supported by the metamodel performance metrics for the corresponding responses. We also note that the response y_1 is a simple function and as such after 20 samples, the metamodel performance is more than adequate for response y_1 , as the MAS values are 100 for metamodels resulting from both the MED and the MSFCVT methods.

Figure 4.5 shows the published design generated using the DMM (Li et al., 2006) method and that generated by the MSFCVT method. The design from the MSFCVT method is the same as from Figure 4.4. The DMM (Li, et al., 2006) method on the other hand appears to sample points away from the center of the design space, close towards the corners. We also observe that the metamodel for response y_1 is near perfect from both the DMM and MSFCVT methods. As for response y_2 , again it can be seen that the generated response surface from MSFCVT more closely resembles the true response surface than the one from DMM (Li et al., 2006) method.

The MAS, RRMSE and RMAE comparisons presented in Figures 4.6, 4.7 and 4.8 in the form of box plots. Figure 4.6 shows the box plots for the MAS obtained using the different methods for the two responses. The RMSE, RRMSE and RMAE obtained from the 3 methods for the two responses y_1 and y_2 are shown in Figures 4.7 and 4.8 respectively. Figure 4.9 shows the relative errors for the randomly selected test points (for 1 run) plotted as a scatter in the design space.

From Figure 4.6, it can be seen that all the three methods viz. MED, DMM and the proposed MSFCVT yield a near perfect (i.e., MAS = 100) metamodel for y_1 . But

the MSFCVT approach also provides better RMSE and MAE values for the resulting metamodels as compared to DMM and MED method as seen from Figure 4.7. For y_2 , based on the median MAS values, we see that the MSFCVT approach performs better than the MED and the DMM (Li et al., 2006) approach.

Based on median values (indicated by the vertical line within each box) from Figure 4.8, we observe that the proposed approach outperforms the DMM approach in terms of RMSE, RRMSE and RMAE, but is inferior to MED method when RRMSE and RMAE are considered. From Figure 4.5, we see that the MSFCVT method allocates more points in the lower left region of the design space. The resulting metamodel from MSFCVT has a better performance in this region which is verified by the corresponding distribution of errors as a function of test points as shown in Figure 4.9.

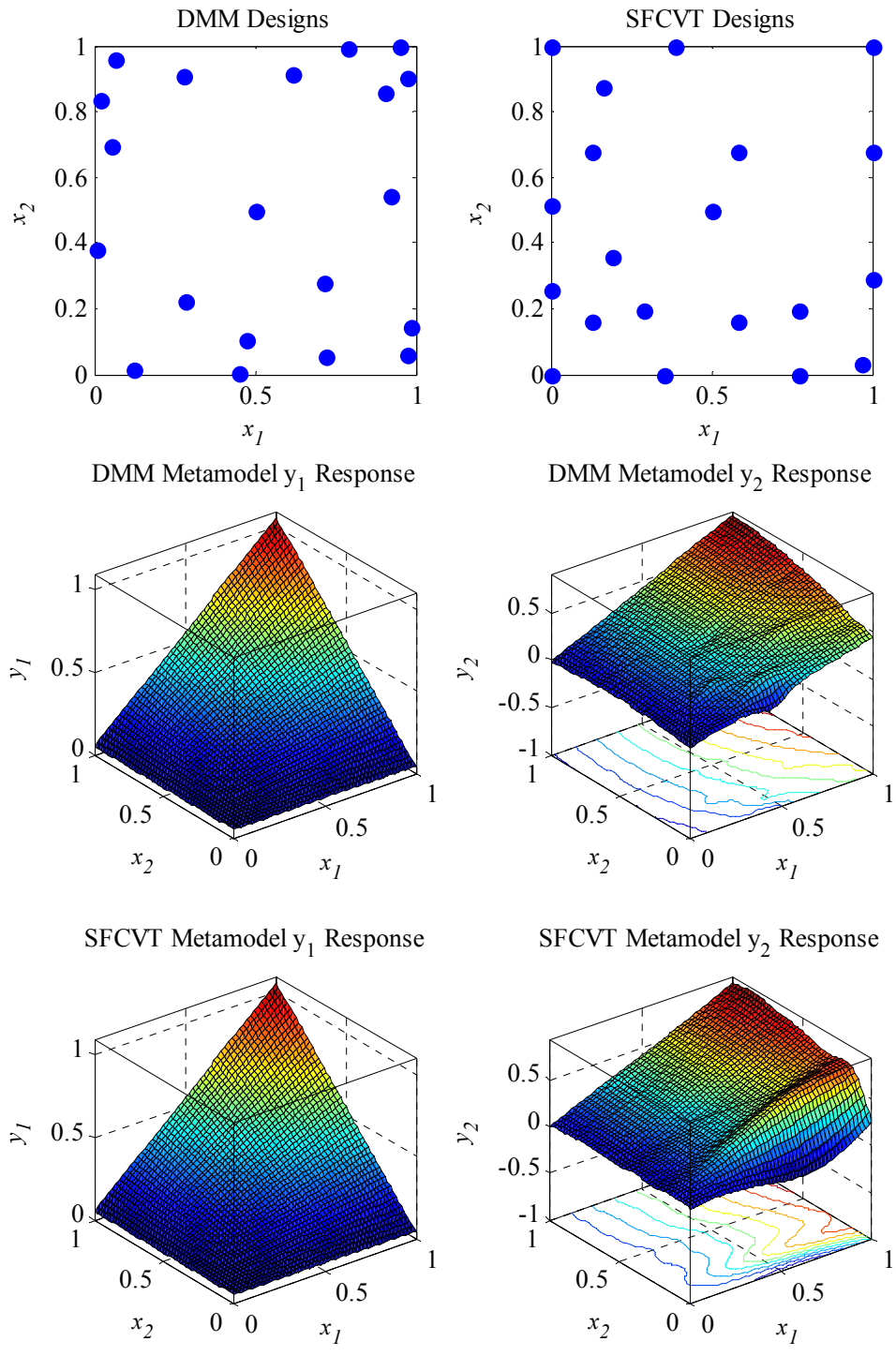


Figure 4.5 DMM vs. MSFCVT, resulting designs and metamodels

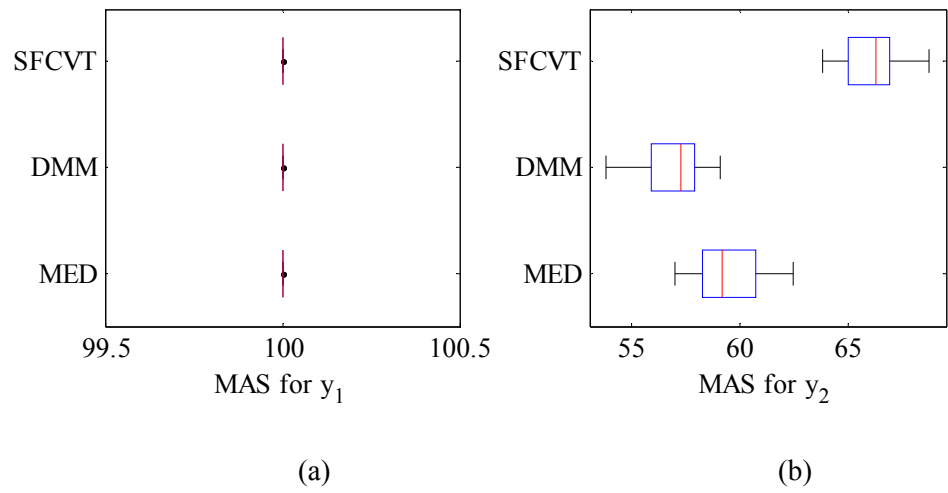


Figure 4.6 MAS Comparison, (a) Response y_1 and (b) Response y_2

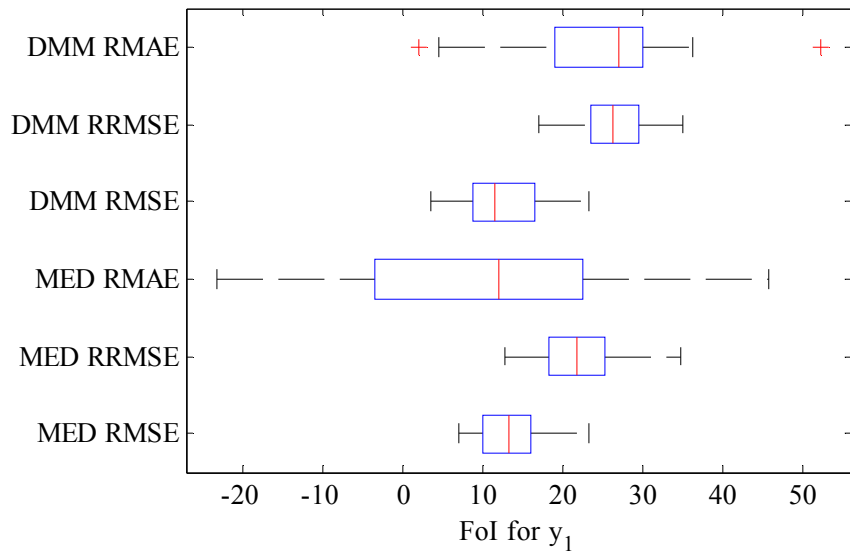


Figure 4.7 RRMSE, RMAE and RMSE FoI values for y_1 , from different methods

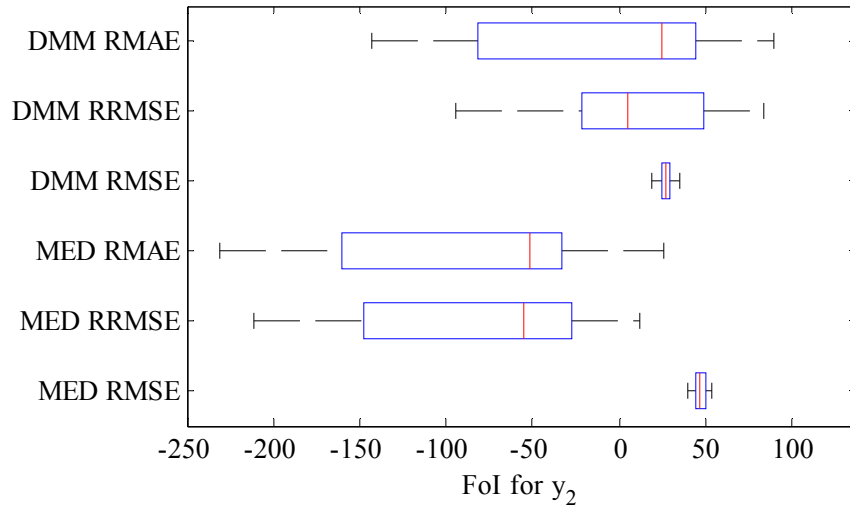


Figure 4.8 RMSE for second response y_2

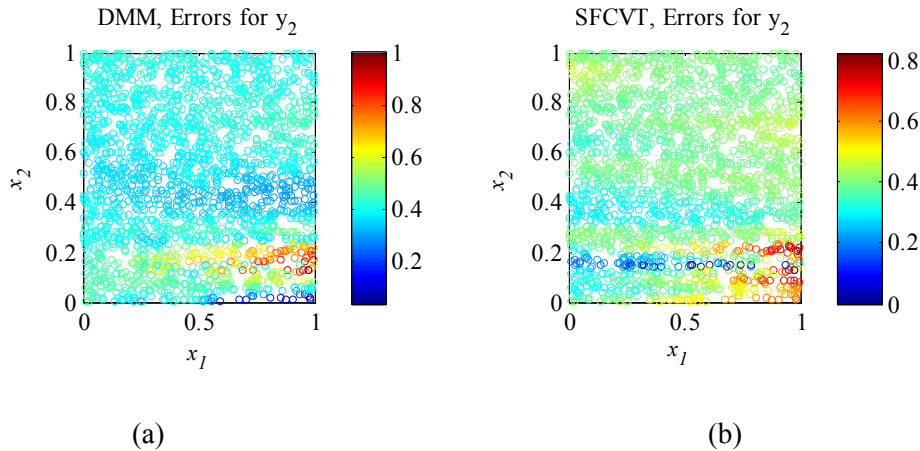


Figure 4.9 Error distribution for y_2 , (a) DMM method, and (b) MSFCVT method

The RMSE for y_2 as reported in Li et al. (2006) for the DMM method is 0.11 while the RMSE obtained from the proposed approach is 0.045, thus supporting the conclusion that the proposed approach outperforms the DMM method for this example.

4.4.2 Numerical Example – 2

This second numerical example is taken from Romero et al. (2006) to allow for a fair comparison with the results published in the literature. This test example is a

combination of two single-response test examples to represent a multiresponse simulation. It has two inputs and two outputs. The two test problems are Osio's Function and Sasena's function, designated as P9 and P8 respectively and their details are provided in Appendix-A.

Similar to the first example in the earlier section, the proposed approach is applied to this test problem. The approach starts out with 9 initial designs and a total of 19 designs. The number of design points was chosen to be 19 to allow comparison with results published in Romero et al. (2006). A set of randomly generated 2000 test points is used for metamodel verification. Changing the number of verification points to other values (i.e., 1000, 5000) resulted in a similar metamodel performance.

The true response surface for these two examples is shown in Figure 4.10a and 4.10b respectively. Figure 4.11 shows the design obtained using the MED and the MSFCVT methods and the corresponding response surfaces for the two responses. From Figures 4.11a and 4.11b, we observe that the designs generated using the MED and the MSFCVT methods appear to be space-filling in nature, but only the MED points are space-filling. The corresponding metamodel generated response surfaces are shown in Figures 4.11c and 4.11d respectively. The surface generated for y_1 using the MSFCVT method resembles more closely to the true response surface. In case of y_2 , both methods do not represent the surface very well.

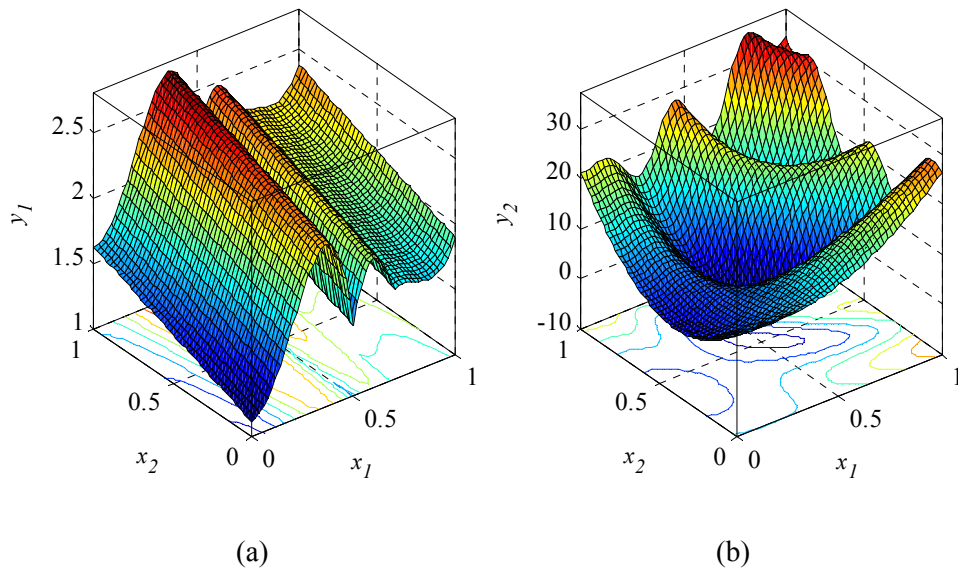
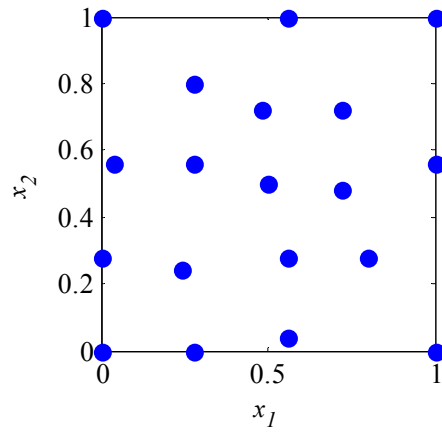


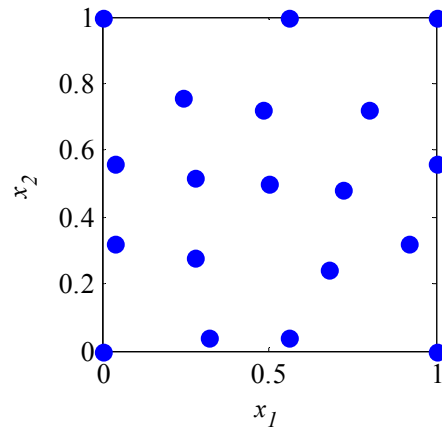
Figure 4.10 Response surfaces for Numerical Example-2, (a) response y_1 , and (b) response y_2

One reason for y_2 not being represented very well, is the initial design. If more number of points were to be added to the initial design, the predicted response surfaces would be closer to the true surfaces.

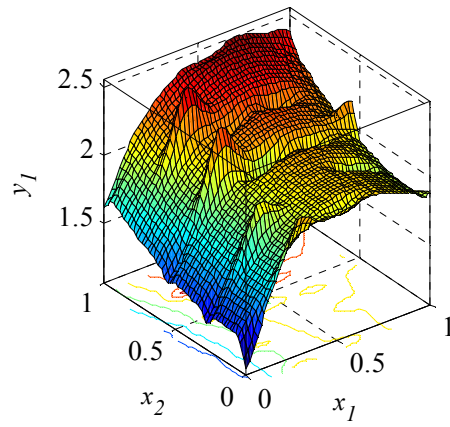
The corresponding metamodel performance metrics are shown in Figures 4.12, 4.13 and 4.14. Figures 4.12 and 4.13 show the actual RMSE and MAE for the two methods (i.e., MED and MSFCVT) for responses y_1 and y_2 respectively. Figure 4.14 shows the MAS for the two responses. Based on Figures 4.12, 4.13 and 4.14, we observe that the MSFCVT approach outperforms the MED method for response y_1 , but is marginally inferior with respect to y_2 .



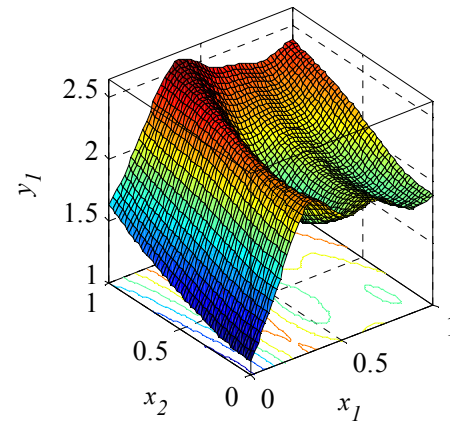
(a)



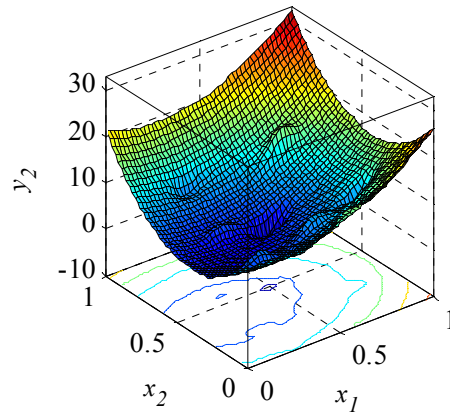
(b)



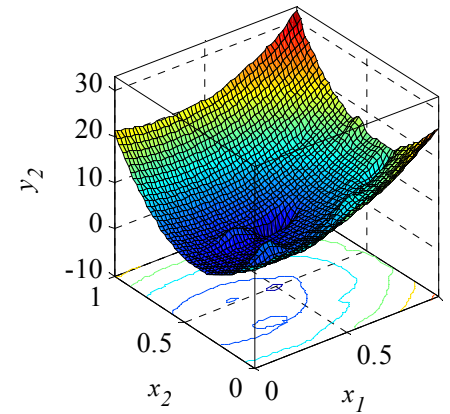
(c)



(d)



(e)



(f)

Figure 4.11 Numerical Example-2, (a) MED design, (b) MSFCVT design, (c) MED response y_1 , (d) MSFCVT response y_1 , (e) MED response y_2 , (f) MSFCVT response y_2

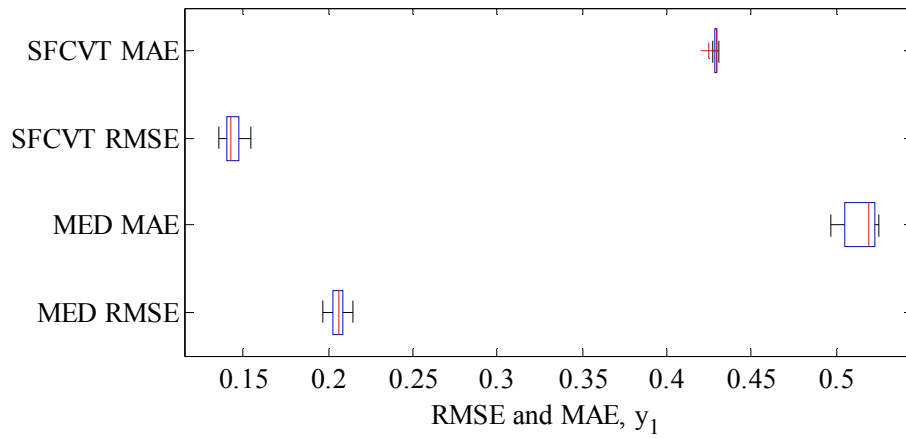


Figure 4.12 Comparison of RMSE and MAE for response y_1

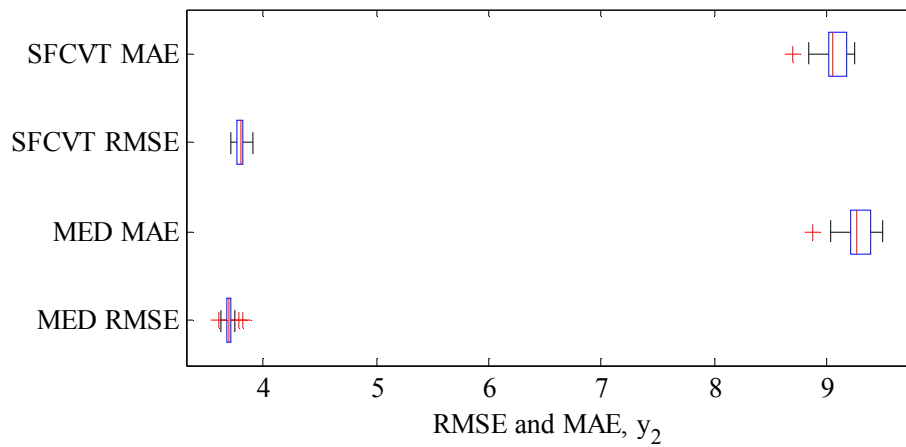


Figure 4.13 Comparison of RMSE and MAE for response y_2

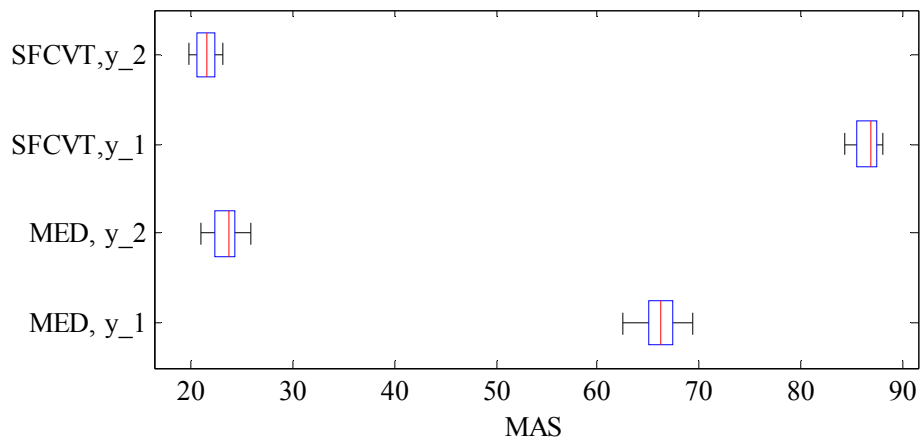


Figure 4.14 MAS Comparison for y_1 and y_2 from MED and MSFCVT approaches

Comparing the above results with those published in Romero et al. (2006), we observe that the MSFCVT approach provides a better MAE than the three approaches they proposed.

4.4.3 Application to Numerical Test Problems

In this section, a suite of 8 test problems, designated at PM1 to PM8, was compiled based on test problems from the literature. The details of this multiresponse test problem suite are given in Appendix A. In general, several single-response test problems are combined to represent a multiresponse computer simulation. A summary of the numerical experiments that were conducted is shown in the table below.

Table 4.1 Test Matrix for Multiresponse Adaptive DOE Method

Test Problem	Number of Inputs	Number of Outputs	Initial Design	New Samples	Random Test Points
PM1 – PM2	4	2	40	40	4000
PM3 – PM4	8	2	80	80	8000
PM5 – PM6	2	4	20	20	2000
PM7	4	4	40	40	4000
PM8	8	4	80	80	8000

Each of the test problems (i.e., PM1 to PM8) has multiple responses. We use the notation PM-1 to indicate the first response for test problem PM1, PM1-2 the second response for problem PM1 and so on.

The first set of results is the comparison of MAS obtained using the two different selection strategies for the MSFCVT method using Eq. (4.2). The first selection method is based on the level of dominance approach and selects one point per stage. The second selection method chooses the extreme Pareto points at each stage (i.e.

method (c) described in Section 4.3.5). The comparison is shown in Figure 4.15 for problems PM-1 to PM-4 and in Figure 4.16 for problems PM5-PM8.

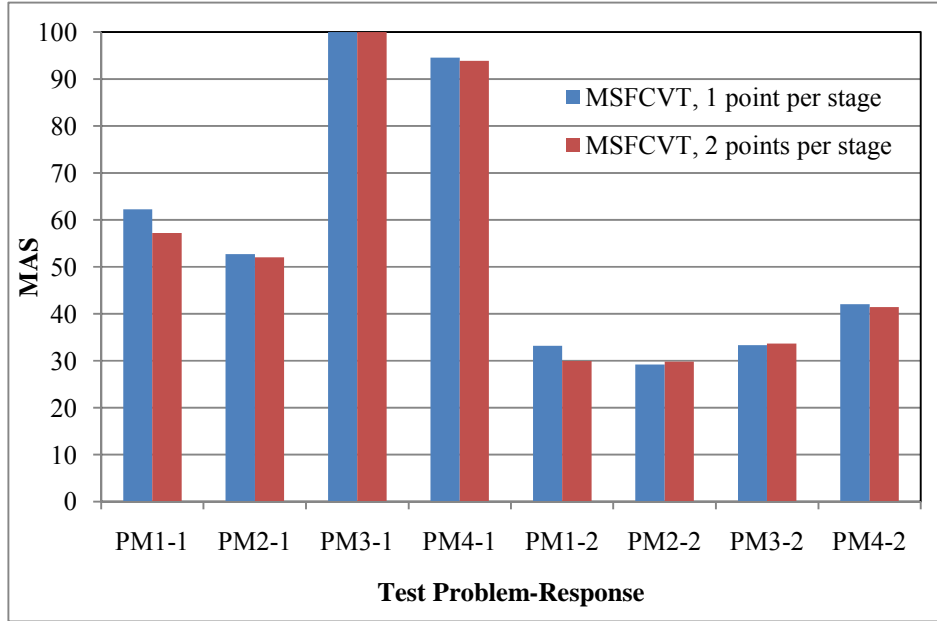


Figure 4.15 MAS comparison for MSFCVT method, choosing 1 point vs. 2 points per stage, for problems PM1 - PM4

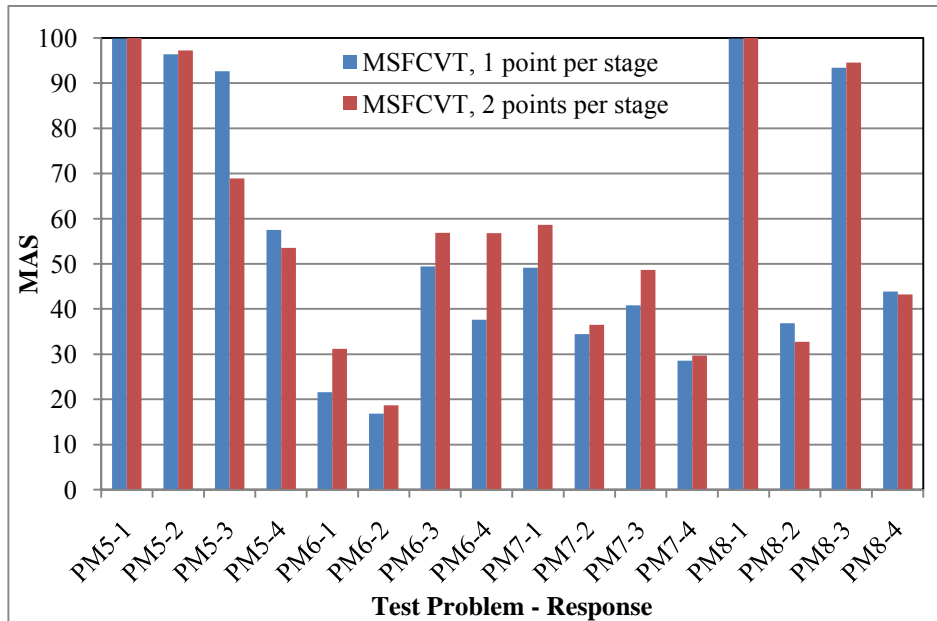


Figure 4.16 MAS comparison for MSFCVT method, 1 point vs. 2 points per stage, for problems PM5 – PM8

From Figure 4.15, for test problems PM1 to PM4, we observe that there is marginal difference between the MAS using the two methods. On the other hand, in the 4-output problems (i.e., PM5-PM8) there is significant difference in MAS for responses PM5-4, PM6-1, PM6-3, PM6-4, PM7-1 and PM7-3. Overall the 2 points per stage method works better than 1 point for problems PM6 and PM7. This is mainly because, at each stage, 4 new points are added (as opposed to one point in the 1 point per stage approach), which also increases the accuracy of the intermediate LOO error models for each of the responses. This results in a better overall metamodel even, when the total number function calls is the same. The RMSE and MAE results were comparable for the two responses and hence are not shown here.

Based on these test problems, the proposed MSFCVT method was compared with the MED method and the results are discussed next. The comparison with the MED method is based on using 1 point per stage for the MSFCVT method. The MAS for the resulting metamodels are shown in Figure 4.17. The proposed approach provides strictly better MAS for both responses for 2 out of 4 test problems. The corresponding FoI results for RMSE, MAE, RRMSE and RMAE FoI are shown in Figure 4.18. Except for the second response of problem PM3, the proposed approach performs comparably and in some cases even better (e.g., PM1) than the MED method.

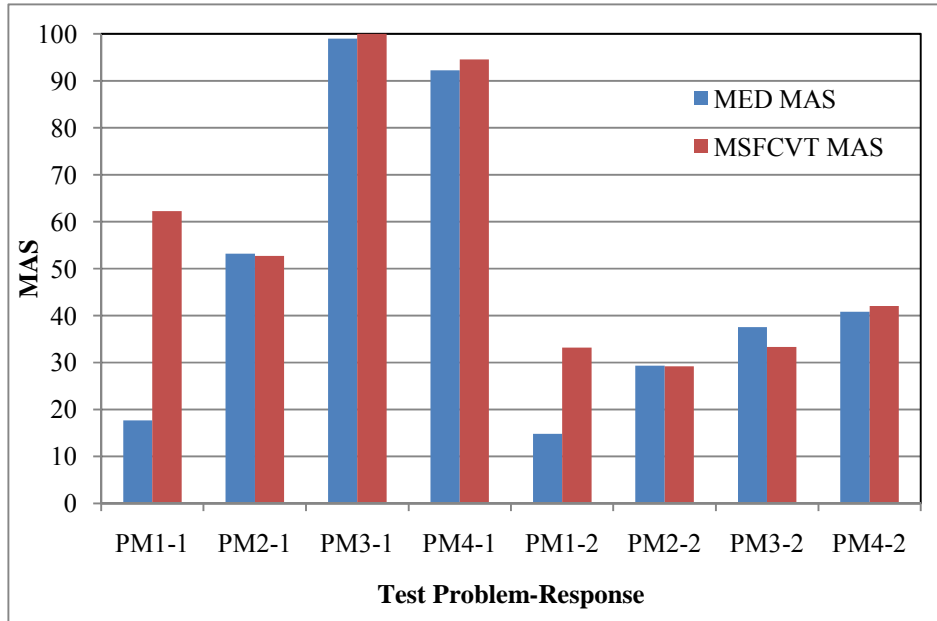


Figure 4.17 MAS for MED vs. MSFCVT method for 2 response case

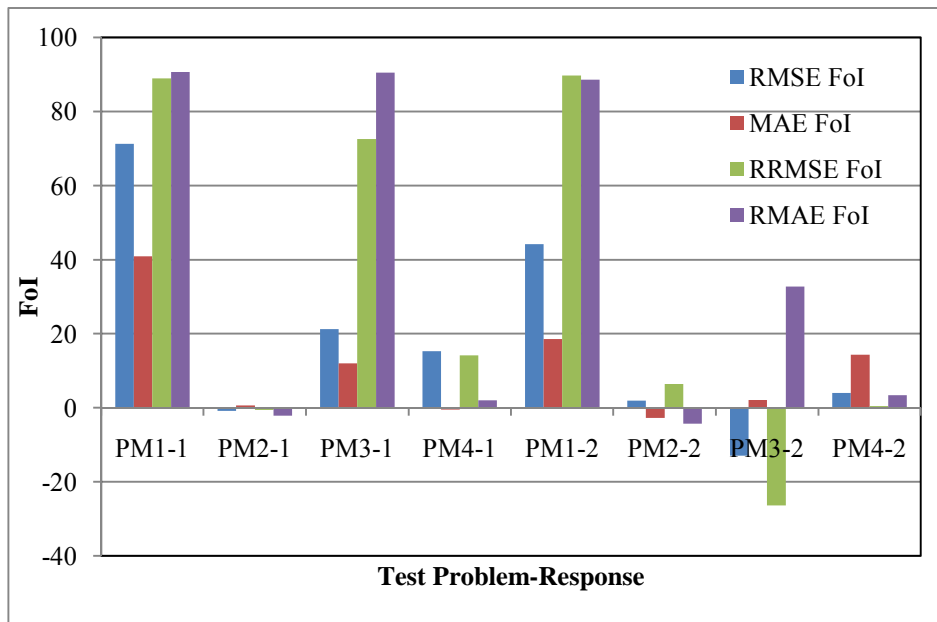


Figure 4.18 MED vs. MSFCVT, FoI values for 2 response cases

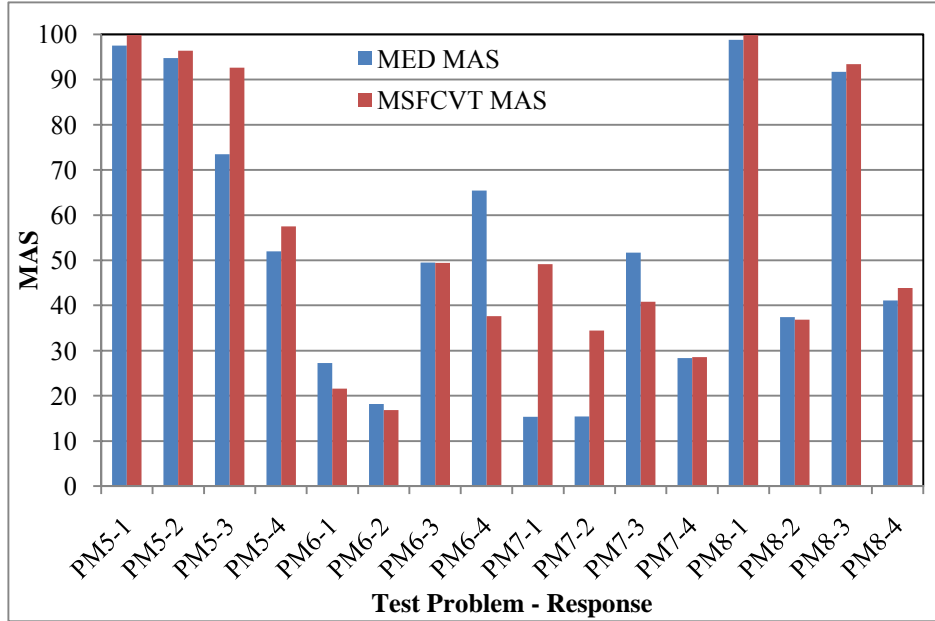


Figure 4.19 MAS, MED vs. MSFCVT method for 4 response cases

The remaining 4 test problems (PM5-PM8) are problems with 4 responses. The results for these are shown in Figures 4.19 and 4.20. From Figure 4.19, in all the test problems, except for PM6, the proposed MSFCVT approach performs comparable to or better than the MED method. Overall, based on the MAS values, the MSFCVT approach gives better metamodellers for 10 out of 16 responses. For PM6, from Appendix-A, we note that the 4th response is the Busby et al.(2007) problem (PM10) for which we concluded from Chapter 3 that the implemented SFCVT approach does not work well, because of weak metamodellers for the LOO errors in intermediate stages. Consequently, the MED method performs significantly better in terms of MAS as seen from the bars for PM6-4 in Figure 4.19.

From Figure 4.20, we observe that the MSFCVT approach gives better RMSE, MAE, RRMSE and RMAE for 7 out of 16 responses and it yields better RRMSE and RMAE in 11 out of 16 responses.

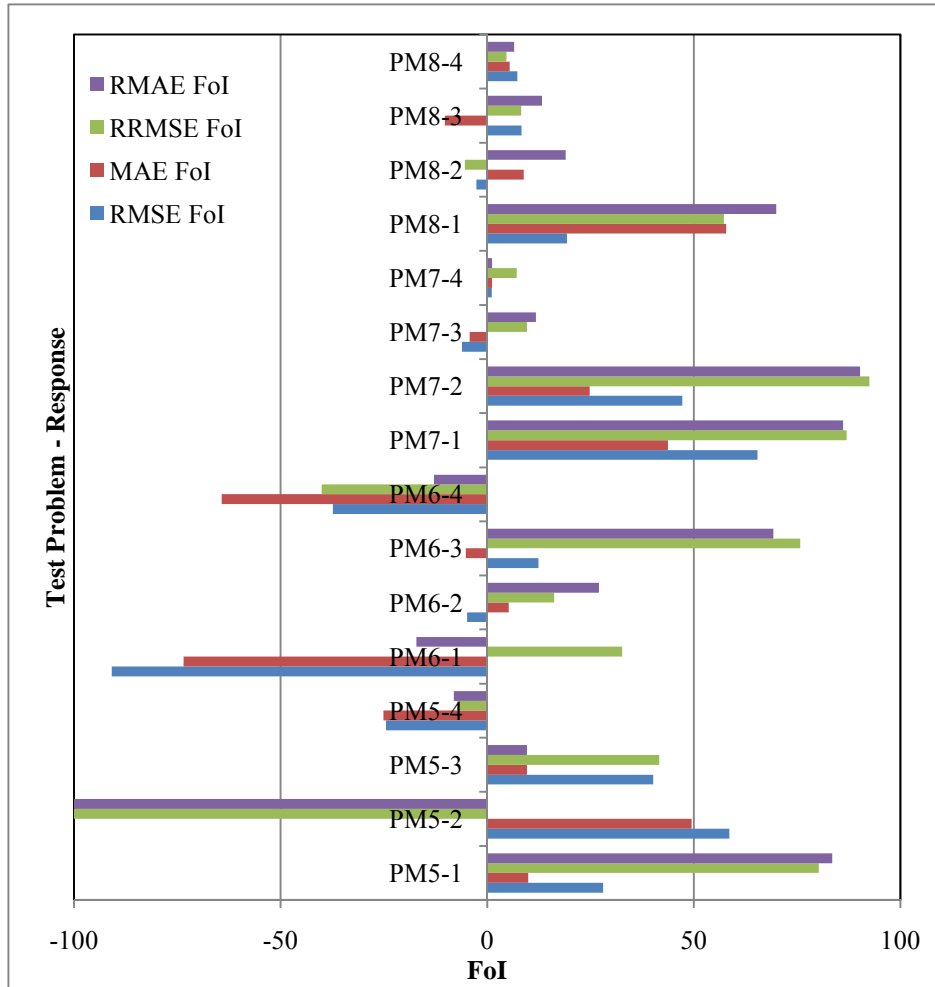


Figure 4.20 MED vs. MSFCVT, FoI for 4 response cases

It is important to point out that the test problems PM5-PM8 used the single response test problems from Chapter 3 to mimic a multiresponse simulation and the default implementation of the MSFCVT method was used. Thus, the performance of the MSFCVT method when compared with MED method will be similar to that observed for the single response cases.

4.4.4 Comparison Between Formulations

In this section we briefly present and compare the results obtained using the two different formulations given by Eq. (4.2) and (4.3). Note that there are m objectives in

the formulation presented by Eq. (4.2), where as there as $2m$ objectives in the formulation presented in Eq. (4.3), where m is the number of responses. Figure 4.21 shows the MAS obtained by applying the two formulations to test problems PM1-PM4. For both formulations, the extreme Pareto points were chosen as the next samples. For the first response, the m objective formulation seems to yield better MAS than the second formulation. Except for test problem PM-1, the two formulations yield close results for the other 3 test problems. It should be noted that even though extreme Pareto points corresponding to each objective are selected, the number of unique samples is not the same as the number of objectives. In other words, when we select extreme points for n conflicting objectives, we should have n solutions. But when some of them are not conflicting (which we don't know before hand), then the extreme points for two or more objectives coincide. Thus the number of unique samples chosen is not the same as the number of problem objectives.

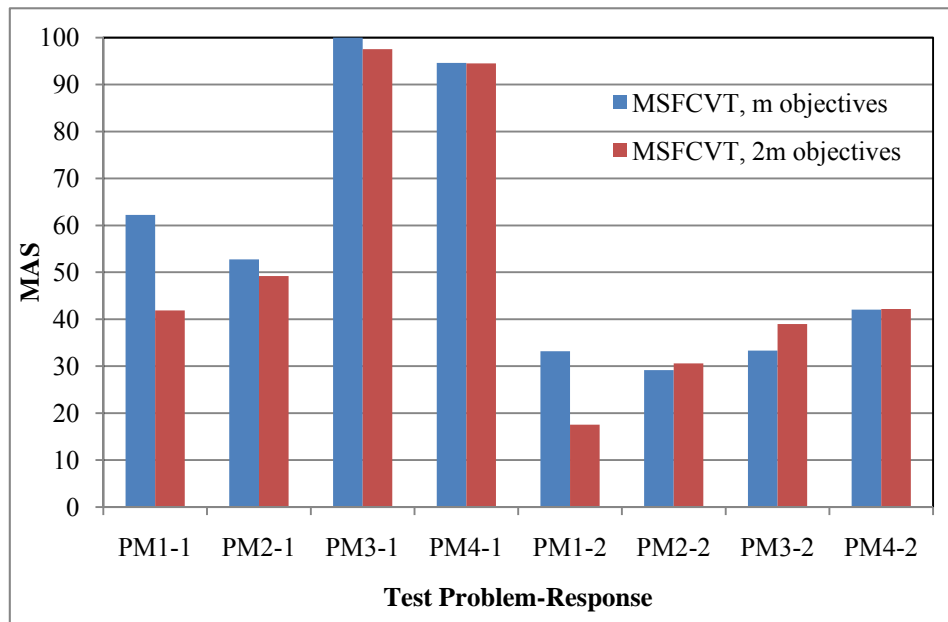


Figure 4.21 Comparison of MAS for test problems PM1-PM4, for MSFCVT formulation with m objectives vs. $2m$ objectives

The results for the test problems with four responses, i.e., test problems PM5-PM8, are shown in Figure 4.22. The MAS values are mixed (low or high for different responses) for test problems PM5-PM7, while for problem PM8 the results for all responses are comparable.

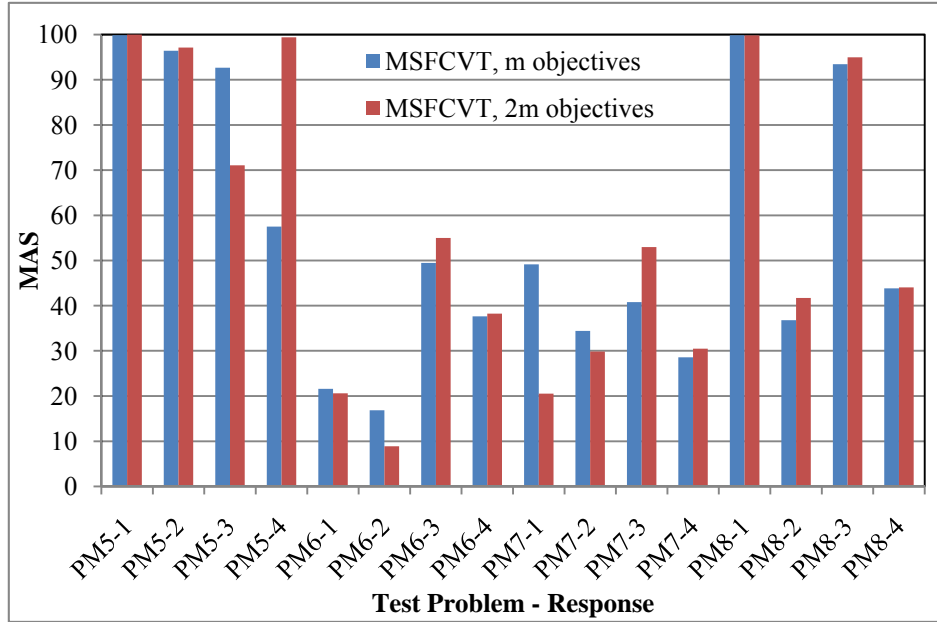


Figure 4.22 Comparison of MAS for test problems PM5-PM8 for MSFCVT formulation with m objectives vs. $2m$ objectives

Application to additional test problems is necessary to draw any generalized conclusions with regards to the two formulations.

4.5 *Summary*

In this chapter a new adaptive design of experiments approach for multiresponse computer simulations is presented. The approach extends the concept of the tradeoff between a space-filling criteria and the LOO error proposed in Chapter 3 to multiple

responses. In this case, the constrained formulation is used to choose the next sample, but now there are multiple, generally competing, objectives. One or more points can be chosen as next samples. The new sample chosen needs to strike a balance between improving the metamodels for all the different responses simultaneously vs. improving metamodels for individual responses. Alternatively, all the Pareto points could be chosen as the next samples. While this approach will utilize more function calls per stage, it will give a better representation of the response space in the early stages. The drawback of choosing all Pareto points at each stage is the possibility that the new points will be allocated much closer to existing samples. The third option to select new samples from the obtained Pareto set is simply to choose the extreme points. This will result in the selection of multiple samples per stage with the number of samples equal to the number of responses.

The proposed approach is compared with two multiresponse numerical examples from the literature. The first test problem is from Li et al. (2006) and it was found that the proposed approach outperforms the DMM method proposed by the Li et al. when applied to their particular test problem. The approach was also compared against published results for three other multiresponse adaptive DOE approaches proposed by and applied to one test example in Romero et al. (2006). Only the MAE data was available and it was found that the MSFCVT approach generates design which result in better metamodels than those published in Romero et al. (2006). The proposed approach was compared to the MED method for a suite of 8 test problems. It was found that the proposed MSFCVT method outperforms the MED method in majority of the test problem responses.

In the next chapter, we present an approximation based framework for the multi-level performance evaluation of novel heat exchangers and apply the single and the multiresponse adaptive DOE approaches to the heat exchanger design problem.

Chapter 5 Approximation Based Optimization Framework for Design of Novel Heat Exchangers

5.1 Introduction

In this chapter, a new framework for the multi-level performance evaluation and design optimization of air-cooled heat exchangers is presented. The framework uses metamodels for CFD simulations, using the adaptive DOE approach developed in Chapter 3 for design optimization of novel air-to-refrigerant heat exchangers.

Heat Exchangers (HX) are used to transfer energy from one working fluid or medium to another using a temperature gradient as the driver. The working fluids can be air, water, glycols or other refrigerants such as R134a. Air-to-refrigerant heat exchangers are widely used today in refrigeration and Air-Conditioning (AC) applications. The use of these heat exchangers include: (a) Indoor and outdoor coils for residential and commercial buildings such as houses, offices, super markets (b) the condenser, radiator and the evaporator in an automobile air cooling system (c) the coil on the back or bottom of a household refrigerator, (d) charge air coolers and intercoolers in vehicles etc. Most of the cooling equipment is based on the thermodynamic cycle termed as the vapor compression cycle or some variation of it. In general, any vapor compression cycle based equipment requires a minimum of two heat exchangers. In a basic vapor compression cycle there are four components viz. (a) compressor, (b) high-pressure heat exchanger, termed as condenser (c) an expansion device and (d) a low pressure heat exchanger termed as evaporator. Together, the two heat exchangers in an AC unit account for the more than 50% for the initial cost (manufacturing cost, also known as the first cost) and significantly

affect the performance and hence the energy consumed by the unit. In mobile applications, the weight of these heat exchangers also plays an important role in addition to the first cost, since it affects the fuel efficiency of the vehicle.

In the light of energy efficiency and energy conservation concerns, there is a growing need for more compact, high performance heat exchangers and ever present requirement to minimize cost. In the last decade a significant increase in compactness has been achieved in air-to-refrigerant heat exchangers by replacing the traditional round-tube plate fin heat exchangers with microchannel heat exchangers.

The optimization framework proposed in this chapter aims at developing a novel tool for multi-level design optimization of new heat exchangers, termed as the next generation heat exchangers (NGHX). The novel aspects of this approach are (a) to use simplified 2D CFD to evaluate performance of novel heat exchanger elements and (b) to develop and use an ε -NTU based heat exchanger model to evaluate component level performance of the novel heat exchanger elements and (c) to use the adaptive DOE approach developed in Chapter 3 to optimize the design of these novel heat exchangers. Together, these novel aspects will lead to better heat exchanger designs which are more compact than the current state of the art, as will be shown in this chapter. More explanation is needed to highlight the multi-level performance evaluation aspect of this research. In (a) above, the performance of a small heat exchanger element is evaluated using 2D CFD. These elements are then “assembled” together to form real life heat exchangers and a ε -NTU based model is used to evaluate the component level (i.e., heat exchanger as a whole) performance of these heat exchangers.

The remainder of this chapter is organized as follows: Section 5.2 provides some background information on heat exchangers and their optimization. Section 5.3 gives a summary of literature which focuses on the use of approximation assisted optimization for heat exchanger design. Section 5.4 provides details about a new heat exchanger geometry that will be analyzed in this chapter. Section 5.5 summarizes a novel approach for the multi-level performance evaluation of the new heat exchanger. Section 5.6 applies the adaptive DOE methods developed in Chapters 3 to the heat exchanger design problem. Section 5.7 provides results from the approximation assisted optimization for the NGHX. Finally Section 5.8 summarizes this chapter.

5.2 Background information

In this section, background information on conventional air-to-refrigerant heat exchangers is presented. An introduction to an ϵ -NTU based simulation tool (i.e., CoilDesigner) for performance evaluation of tube-fin and microchannel heat exchangers is also presented.

5.2.1 Tube-Fin Heat Exchangers

Tube-fin heat exchangers (ARI, 2001) generally refer to round tube bundles with fins. The fins help improve the air-side heat exchange area. A schematic of a tube-fin heat exchanger is shown in Figure 5.1.

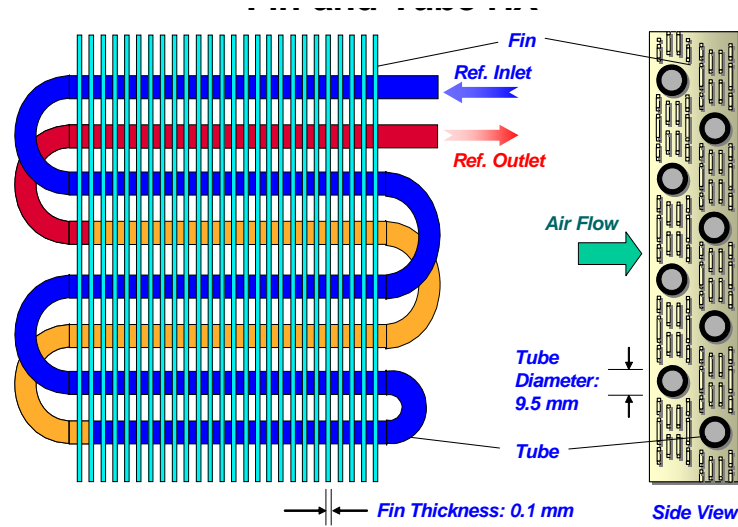


Figure 5.1 Schematic of a tube-fin heat exchanger

In tube-fin heat exchangers, tubes are arranged in a bundle across fins. The tubes are arranged from top to bottom in vertical banks, normal to the direction of the air flow. The refrigerant (e.g., water) flows through the tubes and heats or cools the air based on the application. The fins mounted on the tubes are used to extend the heat transfer area since the air side heat transfer coefficient is much less than the refrigerant side heat transfer coefficient. For simplicity, the details of fin patterns are not described here.

A general observation from Figure 5.1 is that there is a significant obstruction to the air flow due to the tubes. The nominal size of this obstruction in the air path is the same as the tube diameter. Any improvement in this air flow path should increase the performance of the heat exchanger. Using this concept as one of the foundations, the new heat exchanger technology conceived after tube-fin heat exchangers were heat exchangers with flat tubes. Flat tubes later enabled the microchannel heat exchanger which is described next.

5.2.2 Microchannel Heat Exchangers

A schematic of a microchannel heat exchanger is shown in Figure 5.2. A microchannel heat exchanger (Kays and London, 1984; Kandlikar et al., 2006) comprises of corrugated fin sheets sandwiched between flat tubes. Each tube has tiny (~ 1 mm) circular or rectangular ports through which the refrigerant flows. Microchannel heat exchangers are generally fed using an inlet and an outlet header. The division of each tube into multiple parallel flow channels greatly reduces the pressure drop on the refrigerant side. Several novel fin designs (e.g., louver fins) are available which drastically improve the air-side performance as well. The first view in Figure 5.2 is the coil face area, which is the area of the coil which ‘sees’ the air first.

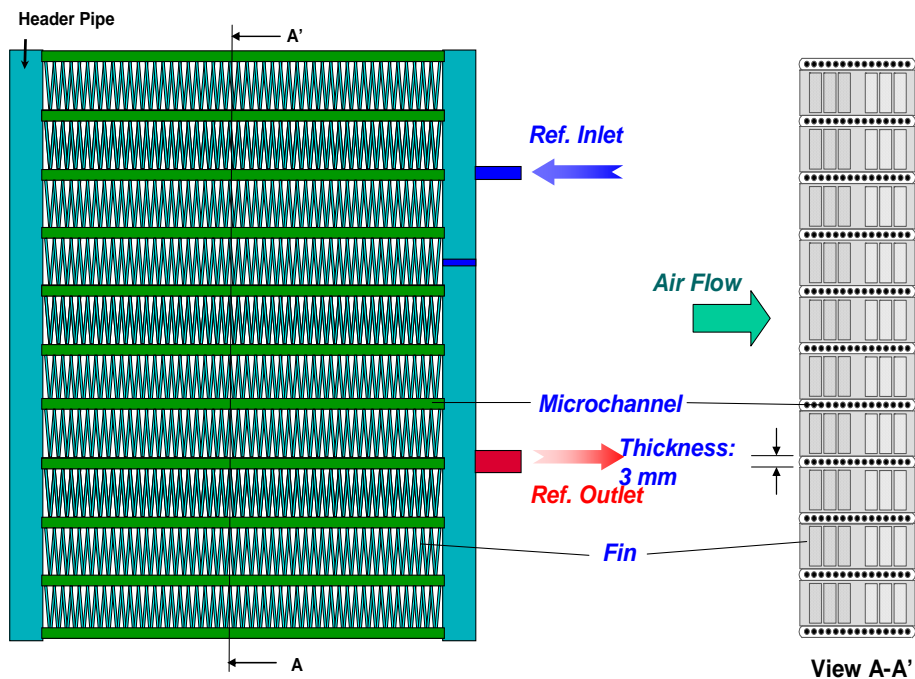


Figure 5.2 Schematic of a microchannel heat exchanger

5.2.3 CoilDesigner

CoilDesigner (Jiang et al., 2006) is a control volume based simulation tool that can simulate the performance of air-to-refrigerant and refrigerant-to-refrigerant heat exchangers. The underlying solver allows for the decomposition of individual tubes in a heat exchanger into smaller heat exchanger elements termed as ‘segments’. CoilDesigner internally uses this decomposition along with the ϵ -NTU method (Shah and Sekulic, 2003) of heat transfer calculations which helps to account for the drastic changes in transport properties (density and viscosity) during evaporation and condensation processes resulting in accurate prediction of heat exchanger performance. The methodology behind CoilDesigner is described in more details along with experimental validation in Jiang et al. (2006), Schwentker et al. (2005) and more recently in Singh et al. (2008). Optimization of tube-fin coils using MOGA with CoilDesigner has been described and demonstrated in Aute et al. (2004). It is important to note that CoilDesigner uses correlations for air and refrigerant side heat transfer and pressure drop calculations. This makes CoilDesigner very flexible, because once a correlation is available for a given tube/fin geometry, CoilDesigner can be used to simulate the coil performance using the particular tube/fin geometry. Correlations are generally based on experimental data sets, but in cases where experimental data is not available (e.g., for new heat exchangers), the heat transfer and pressure drop characteristics can be obtained using a detailed CFD simulation.

In order to evaluate performance of heat exchangers, CoilDesigner requires detailed geometrical and design information such as tube diameters, thickness, fin thickness, tube horizontal and vertical spacing, tube length, number of parallel tubes, etc. The results predicted by CoilDesigner include the overall heat load, refrigerant

side heat transfer coefficients (HTC), refrigerant side pressure drop (RDP), outlet refrigerant and air conditions, the volume of heat exchanger, material weight etc.

5.3 Literature Review

Conventional heat exchangers such as tube-fin and microchannels have been very well studied and as such there is plenty of literature which focuses on the optimization of these heat exchangers. In terms of design optimization of novel heat exchangers, the literature focuses only on the optimization of a small element or a segment of the heat exchanger. The published research can also be classified to fall in the category of shape optimization, because the research mainly focuses on the optimization of a fin or a tube shape. Heat Exchanger optimization can be carried out at the element level (i.e., small segment of heat exchanger is analyzed), at the component level (i.e., an entire heat exchanger is optimized for a given performance) and at the vapor compression system level (i.e., heat exchanger geometries are optimized as a part of system optimization). While there is ample literature available on optimization of heat exchangers based on thermal-hydraulic models, the literature review presented here is limited to the application of approximation assisted optimization with evolutionary algorithms to the design optimization of novel heat exchanger geometries.

The use of CFD based optimization is fairly common in the aerospace field. Early examples of CFD based optimization in the aerospace field include the classical aerofoil optimization (Falco, 1997; Makinen, et al., 1998) problem. CFD based optimization is yet to spread in the heating, ventilation and the air-conditioning field,

and remains an area of active research. Hilbert et al. (2006) use MOGA and CFD to optimize the shape of a tube-fin heat exchanger tube for maximum heat exchange while obtaining minimum pressure loss. The candidate shapes were represented via parameterized NURBS (Farin, 1999, 2002) and their approach used CFD coupled with optimization with no approximation involved. The resulting tube designs, similar to aerofoil shape, were highly unconventional yet intuitive.

Langer et al. (2002) propose an approach for shape optimization using parameterized CAD geometry and evolutionary algorithms. They use MATLAB as the integration platform. The optimization algorithm generates new design values for the inputs required for a parameterized geometry which is then built by a CAD program followed by FEM analysis for performance evaluation. While the integration approach is novel, there was no approximation used and actual FEM runs were carried out using a parallel cluster of computers.

Perez-Segarra et al. (2002) conducted CFD studies on conventional tube-fin heat exchangers to assess the reliability of the numerical solutions obtained from the CFD codes.

Kanaris et al. (2004) propose the use CFD for the design of novel flow channels for plate heat exchangers. In their study, the CFD results are first validated against experimental data for known channel geometries. Then, new geometries are explored in a parametric fashion in order to find better flow channels. A more recent application is presented in Park et al. (2006), in which Kriging and CFD is used for optimization of a heat sink.

Based on the available literature, it can be concluded that detailed CFD analysis and optimization is carried out only on a case-by-case basis, i.e., for fixed geometries. Moreover, the CFD analysis was carried out at the element level and no studies have been conducted to evaluate the scalability of the performance at the component (i.e., heat exchanger) level. There is no systematic method or framework for the analysis of novel heat exchangers. Moreover, approximation assisted optimization is seldom used for CFD based heat exchanger optimization.

5.4 Novel Heat Exchanger Concepts

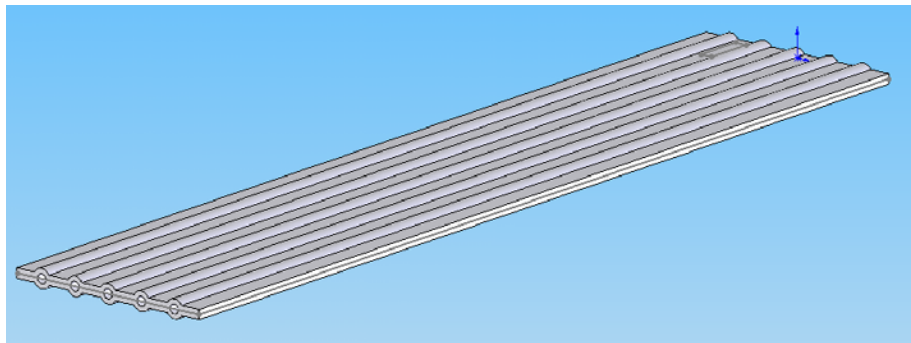
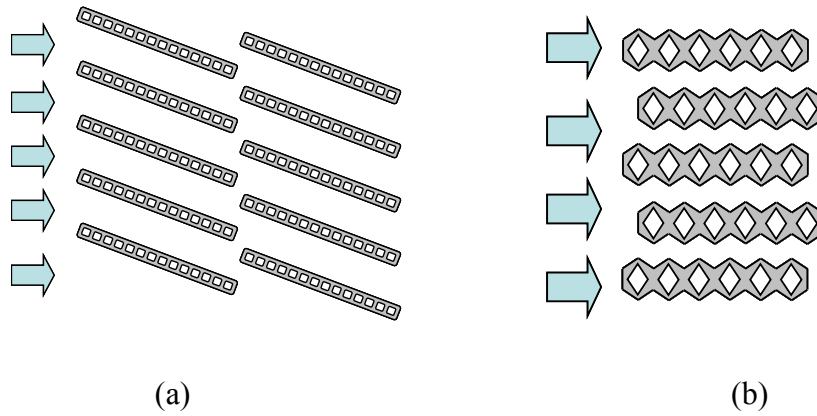
Heat exchanger design optimization is in general a very broad problem and it is important to narrow down the problem definition. As a starting point for the search of NGHX, it is important to develop new heat exchanger concepts. These concepts can then be analyzed further using CFD and approximation assisted optimization.

After a comprehensive literature review, a workshop to brainstorm for new heat exchanger configurations was conducted (Radermacher et al., 2007). The result of this workshop were a set of 25 novel heat exchanger configurations, each with its own geometry variations. Some of the sample geometries are shown in Figure 5.3 below. The arrows in Figures 5.3a and 5.3b indicate direction of the air flow.

5.4.1 Potential Geometries

In order to finalize potential geometries for further analysis, several designs were brainstormed based on creativity. Without going into the details of these designs, some basic designs were chosen for detailed analysis. These detailed designs are derived from the concept of microchannel heat exchangers and are based on the

notion of augmenting the heat transfer area per unit external volume of heat exchangers.



(c)

Figure 5.3 Concept heat exchanger geometries, Courtesy : NGHX Project (Radermacher et al., 2007), (a) and (b) multiport staggered configurations, (c) circular ports with fin sheet

5.4.2 Chosen Geometry

The heat exchanger geometry chosen for further analysis is shown in Figure 5.4. This geometry has several round tubes connected by thin sheets that act as a fin. Note that compared to traditional heat exchangers such as tube-fin (reviewed in Section 5.2.1) and microchannels (reviewed in Section 5.2.2), this geometry does not have any fins, though the metal webs connecting the individual tubes act as fins. Preliminary analysis (Radermacher and Azarm, 2007) showed that this geometry is

capable of packing more heat transfer area per unit external volume of the heat exchanger per unit material weight of the heat exchanger as compared to traditional microchannel heat exchanger, when port diameter is less than 0.4mm. The defining dimensions of the geometry are inner diameter (D_{in}), horizontal spacing (H_s), vertical spacing (V_s) and the length (L) and depth (w).

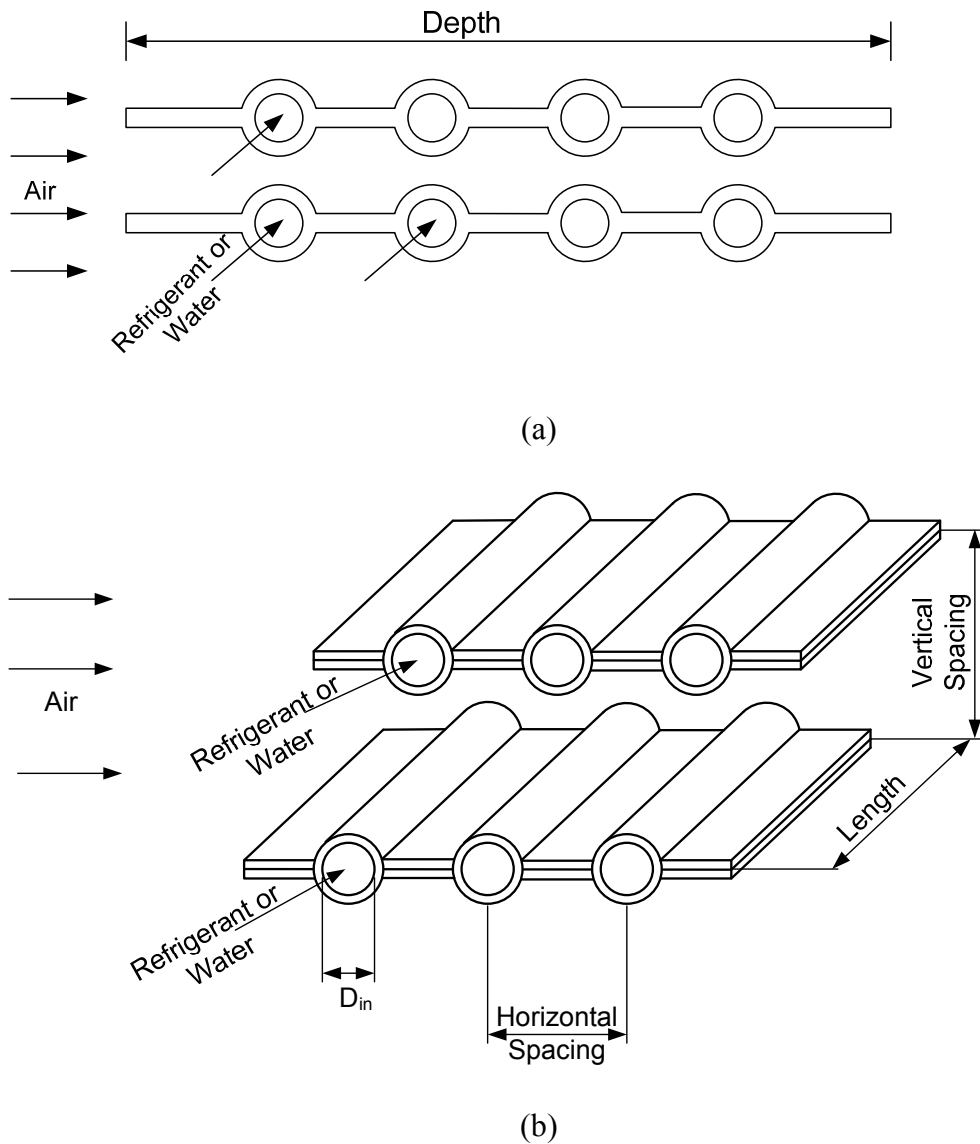


Figure 5.4 Proposed NGHX Geometry, (a) 2-D view, (b) 3-D view

Note that for simplicity we choose the geometry with circular flow channels (i.e., ports). The same geometry can be extended to include any other arbitrary port shapes.

5.4.3 Performance Evaluation Criteria

Several criteria for the comparison of heat exchangers have been discussed in the literature (Shah and Sekulic, 2003; Webb and Kim, 2005). These criteria are mainly based on thermodynamic characteristics of the heat exchanger. The particular criterion of interest is the VG criteria (Webb and Kim, 2005) in which heat exchangers are sized for a required thermal heat load with a specified flow rate. In this case study, as the title implies, we want to find the next generation of air-cooled heat exchangers and as such a more practical comparison criteria was chosen. The two criteria that were chosen were the total heat exchanger volume and the air-side pressure drop for the heat exchanger for a given heat duty. A 1 kW air-to-water microchannel heat exchanger was used as a baseline heat exchanger for comparison. The baseline microchannel was designed with CoilDesigner using the best performing tube and fin surface configurations. The inlet air and water conditions (pressure, temperature) and the flow rate are fixed.

5.5 Performance Evaluation and Design Optimization Approach

In this section, a new approach for multi-level performance evaluation of novel air-cooled heat exchangers is presented. First, the underlying assumptions are listed, followed by the details of the proposed approach.

5.5.1 Assumptions

The assumptions underlying this analysis are as follows:

- (a) The heat exchangers can be represented as cross-flow air-to-refrigerant heat exchangers as shown in Figure 5.4. A single tube can have multiple ports in the air-flow direction and a heat exchanger is comprised of multiple tubes.
- (b) The working fluids are air, on the outside, and water in the tubes. While the proposed approach is applicable for other fluids such as R134a instead of water, the corresponding analysis is much more complex and will include two-phase flow for which heat transfer and pressure drop correlations are still in development. Furthermore, the CFD simulation of two-phase flows is still an open research problem. Hence water is used to demonstrate the concept.
- (c) The performance analysis is carried out for heat exchangers comprising of single banks only, i.e. one set of tubes from top to bottom.
- (d) The performance evaluation criteria are the ones described in Section 5.4.3. Furthermore, the new designs are compared to a baseline microchannel coil that can deliver the same performance.
- (e) The header volume and header performance (i.e., flow mal-distribution) is ignored in this analysis and as such while comparing the coil face area, coil volume and material volume, the headers are ignored.

- (f) A CFD package (Fluent, 2005) will be used for any performance calculations that require CFD analysis.
- (g) In the current analysis, the tube's inner wall is assumed to have a constant temperature for the length of the segment that is being analyzed using CFD. In an actual heat exchanger, each segment of the heat exchanger will have a different tube-wall temperature. Numerical experiments were conducted and verified that this assumption does not have a significant effect on the calculated air-side heat transfer performance for the given range of input conditions.

5.5.2 Hybrid Performance Evaluation Approach

In order to evaluate the performance of a novel HX design, there are two main methods: (a) build a prototype and test it in the laboratory and (b) model the HX with a detailed simulation tool such as finite element method (FEM) or computational fluid dynamics (CFD). CFD in turn can be carried out as a two dimensional (2D) or three dimensional (3D) analysis based on the geometry. The method of building a prototype for each design is not feasible due to resource and time constraints, which leaves us the CFD approach.

The evaluation of a novel heat exchanger with the current simulation technology, i.e., with 3D CFD requires significant computational effort (e.g., several days to weeks) to evaluate a single assembled heat exchanger. 3D Analysis will also add an additional dimension i.e., tube length, to the problem.

The proposed hybrid approach aims at reducing the time required to analyze the performance of novel heat exchanger elements by an order of magnitude. This

approach uses 2D CFD for a small number of cases to evaluate the heat transfer coefficients and pressure drops.

The high level steps in the approach can be summarized as follows:

(a) Evaluate the air-side performance of a small periodic (repeating) heat exchanger element using 2D analysis. HX performance requires simultaneous analysis of fluid flow inside the tubes and the air-flow over the tubes. Here the assumption is that the tube-side performance is readily available, as is the case for most applications. If the tube-side performance is not readily available, a 3D analysis on the tube-side can be conducted to get the performance. Single phase fluid flow in microchannels has been widely investigated (Morini, 2006; Abdelaziz et al., 2008) and it was verified that the conventional correlations are still valid for heat transfer and pressure drop calculations.

(b) Use the performance evaluated in step (a) in an ϵ -NTU based tool such as CoilDesigner to assemble heat exchangers and evaluate its performance. The new heat exchanger element parameters can then be optimized based on the performance of the assembled heat exchanger.

Thus, we evaluate the performance of the novel HX element at the finite level and use the finite level performance information along with CoilDesigner to model the performance of an entire HX, i.e., macro level. This points out the multi-level aspect of the proposed approach.

The air-side performance, i.e., air heat transfer coefficient (HTC) and air pressure drop (DP), is evaluated for a small segment of a heat exchanger for a fixed tube inner-

wall temperature. It has been shown that the fixed tube inner-wall temperature assumption does not have a significant impact on the calculated air-side heat transfer coefficient values. The use of fixed tube inner wall temperature also implies that we do not need to account for the flow inside the tubes and this reduces the computational effort greatly.

A CoilDesigner model is developed that can evaluate the performance of the new heat exchangers. This new model can use the air-side performance evaluated earlier and calculate the overall performance of a heat exchanger. In a separate study (Abdelaziz et al., 2008) , it was shown that the conventional correlations for water side heat transfer and pressure drop calculations are valid for the novel heat exchanger geometry that was analyzed in this chapter.

5.5.3 Geometry Representation and Parameterization

Typically all CFD tools follow a three step procedure (Versteeg and Malalasekera, 1995) as follows: (a) Preprocessing (geometry development, meshing and boundary conditions setup), (b) Processing (solving the governing equations) and (c) Post processing (result analysis and plotting). In the geometry development phase, a 2D model (for 2D analysis) or a solid model (for 3D analysis) is developed. For fast performance evaluation in batch mode, the geometry should be parameterized such that by changing a set of key parameters, the shape of the geometry can be tweaked. An example is shown in Figure 5.5. By changing the dimensions a and b, the shape can be changed from a circle to an ellipse and vice-versa.

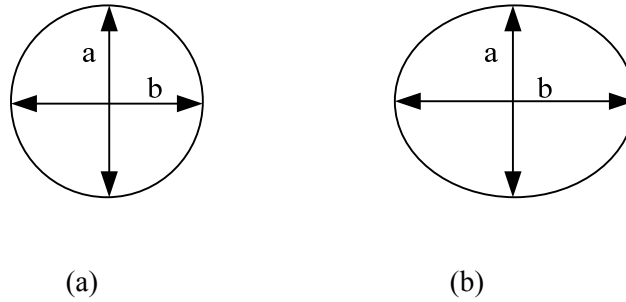


Figure 5.5 Simple shape representation and manipulation

The analyses of these geometries require perimeter and cross section area calculations. While such calculations are trivial for simple shapes like a circle or a square (as shown in Figure 5.6a), these calculations can be very challenging and time consuming for more complex shapes (the ones shown in Figure 5.6b). Therefore a sophisticated method of representation is required for developing geometries.

It is proposed to use non-uniform rational B-splines (NURBS) to represent the different geometries. More details about NURBS can be found in Farin (1999, 2002). The advantages of NURBS are as follows, (a) they can represent practically any type of curve, i.e., smooth or with kinks (sharp edges), (b) they are easy to manipulate i.e. the parameters in the NURBS equations can be changed to change the shape of the curve they represent, and (c) they can be used in CFD geometry development easily, as many popular CFD packages support NURBS.

The use of NURBS will allow us to represent the geometry in a parametric form and could potentially allow the design optimization at the port level. In other words, the optimal port shape could be an aero-foil or an elongated triangle.

Even though it is proposed to use NURBS for representing shapes, one can still use simple shapes such as circles, squares etc. if the HX in consideration warrants it. In the heat exchanger analysis presented in this chapter, the heat exchanger has circular ports and they are specified using a center point along with inner and outer radii.

This geometry aspect is worth mentioning, since when it is coupled with the approach proposed in this chapter, it opens up a new avenue for rapid and streamlined evaluation of novel heat exchanger geometries.

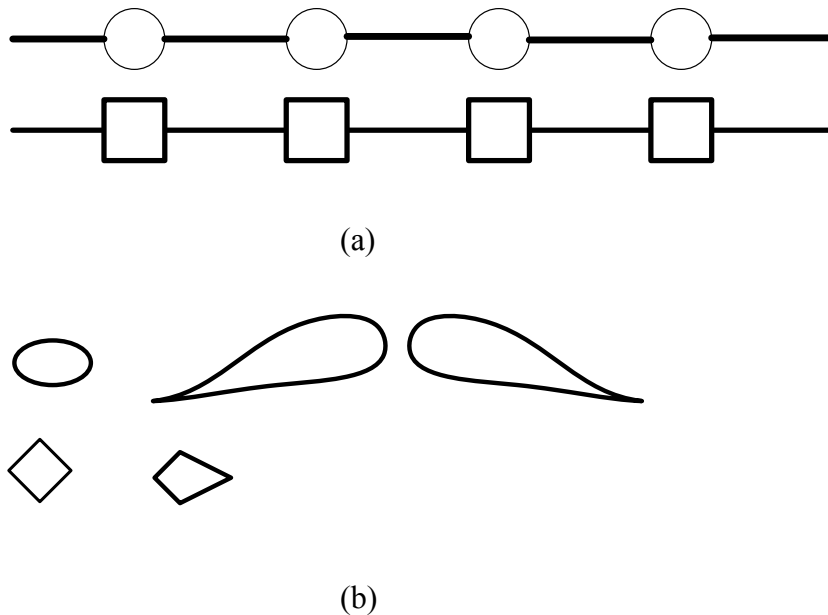


Figure 5.6 Different port shapes, (a) simple ports and (b) complex ports

5.5.4 CFD Analysis

For rapid CFD evaluation of novel geometries, the process of geometry generation, meshing and simulation need to be automated. An automated tool (Radermacher et al., 2007), termed as Parameterized Parallel Computational Fluid

Dynamics (PPCFD) was used to carry out CFD analysis automatically in batch mode. The flow chart for the operation of this PPCFD tool is shown in Figure 5.7.

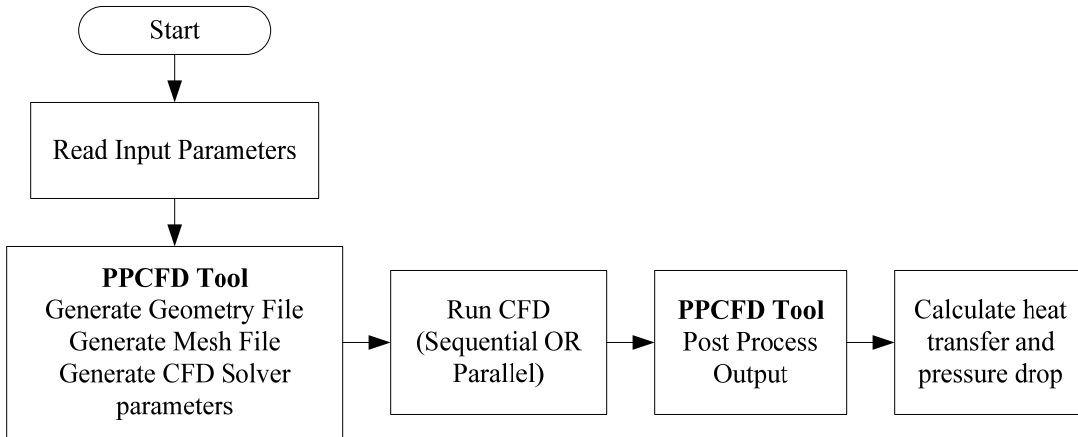


Figure 5.7 Automated CFD evaluations

Conventionally, the geometry generation and the mesh generation steps are performed manually and are the most time consuming. In the new tool these steps have been automated by a computer program that reads input geometry parameters and generates these files. These files then serve as input to the CFD solver. The PPCFD tool itself does not require any user intervention and can generate the outputs of interest, given a set of inputs.

5.5.5 Verification with 3D CFD

In order to gain confidence in the proposed approach, it is imperative that we verify the results obtained using the Hybrid approach with those obtained using detailed 3D CFD analysis. A suitably long segment of the chosen heat exchanger geometry was analyzed using 3D CFD method for a range of heat exchanger dimensions. The length of the HX segment is chosen such that it is greater than the

length of the entrance region. The length of the entrance region can be calculated based on analytical expressions available in the literature. The entrance region needs to be accounted for carefully, since the heat transfer and pressure drop in the entrance region is very different than the one in the fully developed flow region. The same segments (i.e. same length and flow conditions) were analyzed using the new hybrid approach.

The lower and upper bounds for the different design variables were fixed as shown in Table 5.1. Based on these bounds, a test matrix was generated using a 2-level full factorial center augmented design (Myers and Montgomery, 2002). Each of these designs is referred to as a case for identification purposes. The 3D CFD as well as the hybrid approach was applied to these heat exchanger elements. The inlet flow conditions (velocity, pressure and temperature) were fixed. The results are compared based on the predicted air and water side pressure drop and the difference in the air and water temperature across the heat exchanger are shown in Figures 5.8, 5.9 and 5.10.

Figure 5.8 shows the error (difference between 3D CFD and the Hybrid solver) in the predicted air and water side pressure drops. The maximum absolute percent error for air side pressure drop is 23% and that for water is 45%.

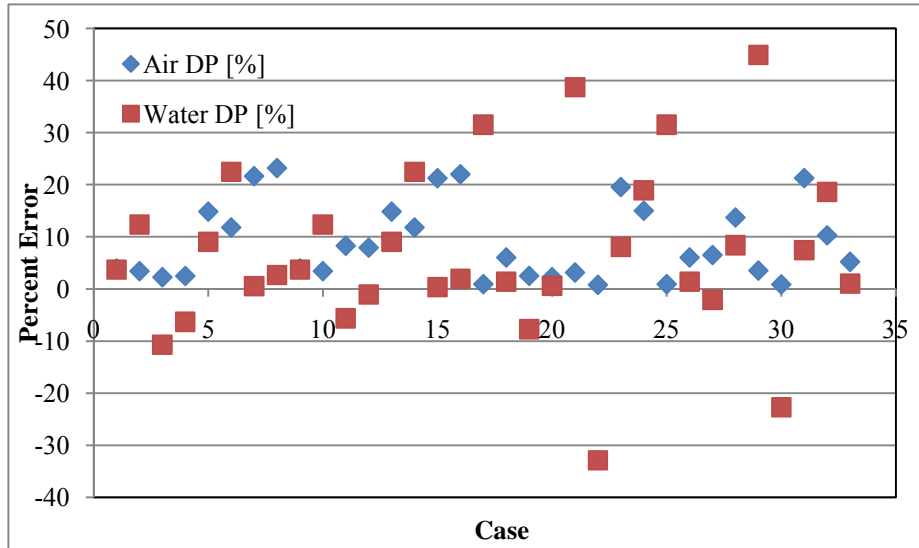


Figure 5.8 Air and water pressure drop errors

Figure 5.9 shows the error in predicted outlet temperatures for air and water. The maximum absolute error for air outlet temperature is 3.5K while that for water is 1.6K. Note that the water side heat transfer coefficient and the pressure drop are calculated using the correlations in CoilDesigner, namely, the Gnielinski correlation (Gnielinski, 1976) for heat transfer and Churchill correlation (Churchill, 1977) for pressure drop.

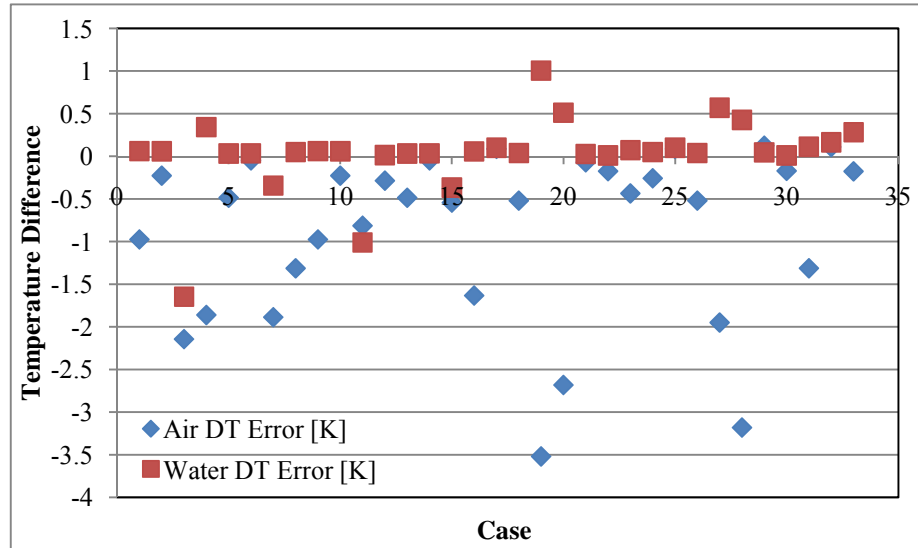


Figure 5.9 Error in predicted outlet temperature

Figure 5.10 shows the same outlet temperature errors, but plotted against the water side Reynolds number (Re). We observe that more of the high errors occur for cases with $Re < 100$. This brings to light the fact that the correlations in CoilDesigner are not applicable for flows with low Reynolds number, pointing to the need for new correlations for use in CoilDesigner. The correlations also do not account for the effect of the entrance region since they were created for fully developed flow. This leads to the conclusion that the hybrid approach can replace 3D CFD calculations for single phase flows for $Re > 100$. This approach was used in subsequent optimization studies. It was also found that the average Re for heat exchanger designs encountered during optimization was greater than 100.

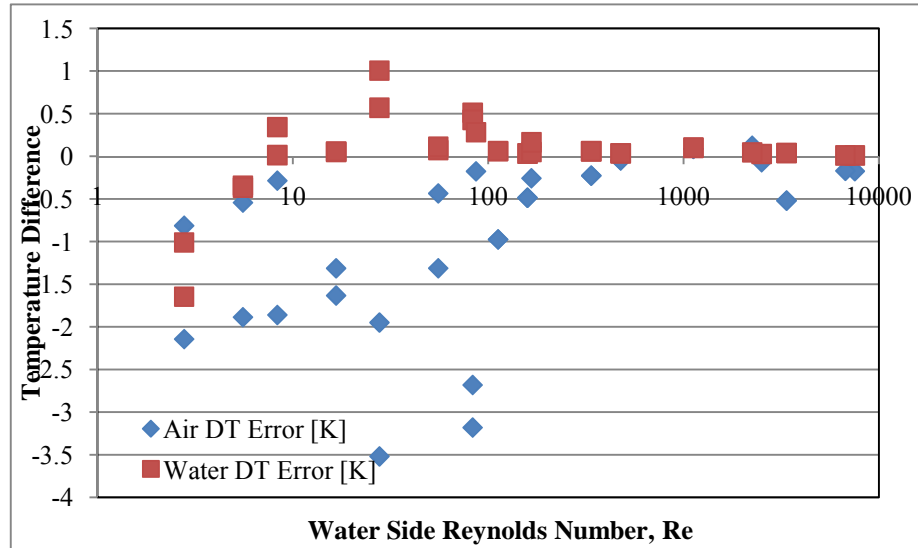


Figure 5.10 Errors in outlet temperature vs. Re

5.5.6 Design Optimization Approach

In general design optimization is carried out via the coupling of an optimizer with a simulation. In this case the simulation is the Hybrid solver proposed in Section 5.5.2. In conventional optimization, we would couple the Hybrid solver along with an optimization algorithm. Based on the design variables of interest, a MOGA is used for optimization. The use of the Hybrid solver with a MOGA still makes the task of optimization computationally prohibitive, since each function call will require a 2D CFD evaluation, which itself takes about 10-60 minutes each. The MOGA will invoke this simulation several thousand times. To reduce this computational burden, a previously developed approximation assisted optimization approach is used. Metamodels are developed for the air side performance (i.e. heat transfer coefficient and pressure drop) as a function of different geometry parameters such as D_{in} , H_s , V_s , v and w . The adaptive DOE approach developed in Chapter 3 are used to build the

metamodels. These metamodels are then coupled with CoilDesigner to evaluate performance of individual heat exchangers.

The design optimization approach is shown in the form of a flow chart in Figure 5.11. The different steps are as follows:

Step-1: Start with concept geometry. In this chapter, the geometry shown in Figure 5.4 is used as the starting geometry.

Step-2: Parameterize Geometry. The important parameters that affect the air side performance of the geometry are identified. This is done by conducting a full-factorial analysis for all parameters of interest followed by analysis using scatter matrix plots.

Step-3: Approximation using PPCFD. In this step, metamodels are developed for air side heat transfer coefficient and pressure drop using the adaptive DOE approach proposed in Chapter 3. The automated tool PPCFD is used for conducting the CFD runs and post processing. Different Kriging correlations are evaluated for a best fit and Kriging metamodels are developed for air HTC and DP.

Step-4: Optimization. In this step, a MOGA is used to optimize the design of the heat exchanger. The objective is to find optimal heat exchangers which provide a given heat load for minimum air-side pressure drop and minimum HX volume. CoilDesigner is used to assemble heat exchangers and the metamodels developed in Step-3 are used to assess the air side performance.

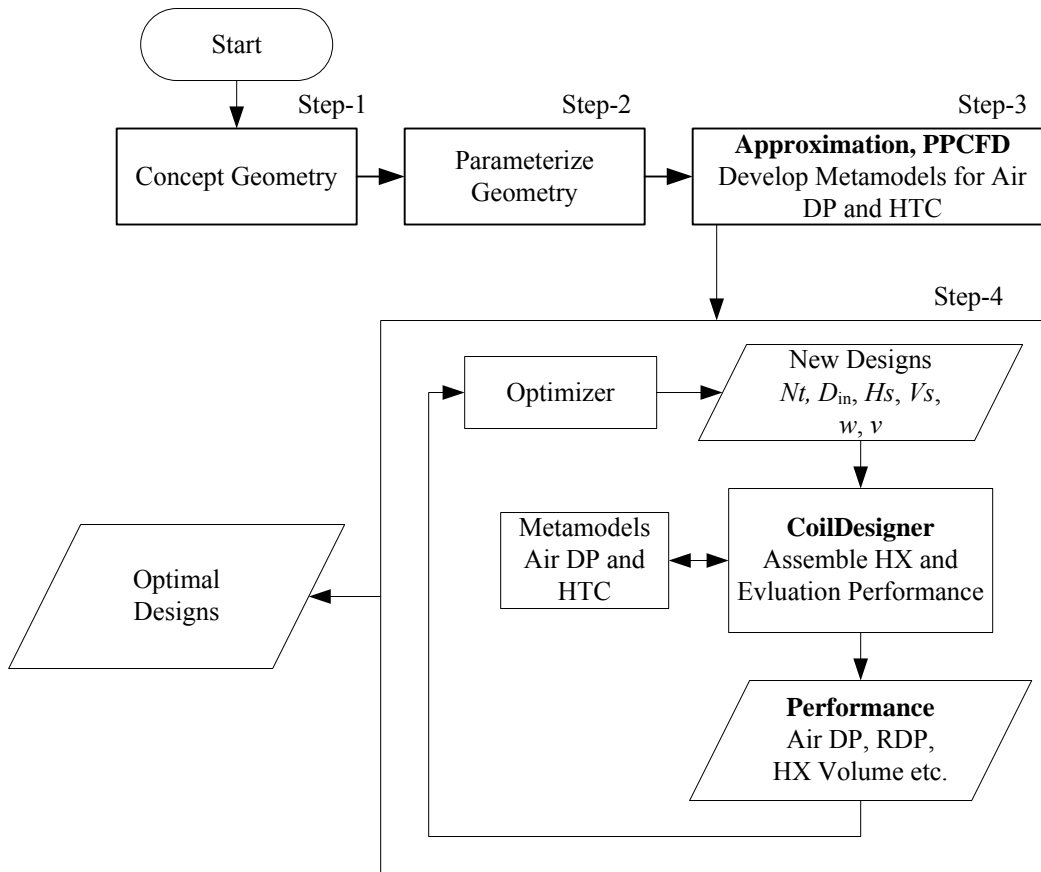


Figure 5.11 Proposed design optimization approach for novel heat exchangers

The result of Step-4 is a set of Pareto optimal heat exchanger designs that deliver a specified heat load. The optimization objectives chosen for analysis in this dissertation are air side pressure drop and HX volume, but any other heat exchanger performance parameter can be used.

5.6 Application of Single Response Adaptive DOE

In this section, the procedure and the results for the application of single response adaptive DOE method (see Chapter 3) to heat exchanger design optimization is presented.

5.6.1 Design Variables

The input variables used to build the metamodel and their limits are given in Table 5.1. The outer diameter, the tube thickness and the leading and the trailing edges are a function of the inner diameter. This was based on prior analysis, but can be readily changed. Thus accounting for inner diameter also accounts for outer diameter, thickness and edges. The vertical and horizontal spacing needs to be accounted for, since it has a direct influence on the air-side heat transfer and pressure drop. The horizontal spacing also has an influence on the number of parallel ports a particular design will have. The depth was chosen such that the minimum number of ports is 1 and maximum number of ports is 41. Since the limits imposed on the inner diameter differ by an order of magnitude, it is imperative to have the limits on the other design variables scale accordingly. The velocity limit was chosen based on the velocity limits for conventional air-conditioning applications. All design variables mentioned below are normalized to the interval [0, 1] when used in DOE and metamodel development.

Table 5.1 Design variables for metamodel

Design Variable	Lower Limit	Upper Limit
Inner diameter, D_{in}	0.1mm	1mm
Horizontal spacing, H_s [mm]	$1.5 \times D_{out}$	$6.0 \times D_{out}$
Vertical spacing, V_s [mm]	$2 \times D_{out}$	$4 \times D_{out}$
Depth, w [mm]	Function of D_{in}	Function of D_{in}
Air velocity, v [m/s]	1.0	3.0

5.6.2 Metamodel Development – SFCVT Method

The SFCVT method with the SO formulation presented in Eq. (3.9) was used. The DOE was carried out separately for the two responses viz., Air DP and Air HTC. Based on preliminary approximation studies, it was found that approximately 200 points were needed to achieve MAS of more than 75 with an acceptability threshold of 10%. The initial design comprising of 100 points was generated using the MED method and the SFCVT method was used to sample 100 additional points. Kriging with logarithmic response (to avoid negative values during prediction) was used to develop the metamodel and a set of 250 randomly generated test points was used to verify the metamodel. The results of this verification are shown in Figures 5.12 and 5.13.

Figure 5.12a shows the RMSE, MAE and MAS for Air DP and HTC and Figure 5.12b shows the RRMSE and RMAE for Air DP and HTC. It can be observed that more than 80% of the test points were predicted within 10% of the true value. From Figure 5.12b, we see that the maximum absolute prediction error was 23% for Air DP and 33% for Air HTC. These large errors were for cases for which the CFD simulation did not converge.

Figure 5.13, shows the box plot for the verification errors, and we see that the median errors values are close to 0. Based on these verification results, the resulting

metamodels were found to be acceptable. These metamodels were then used for optimization.

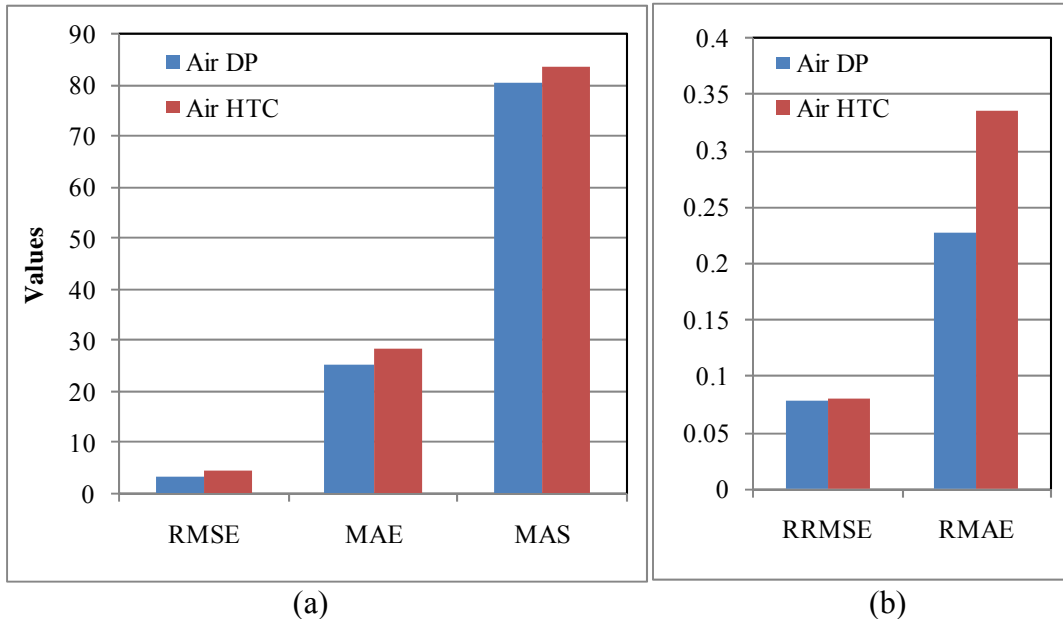


Figure 5.12 Metamodel verification results for Air DP and HTC

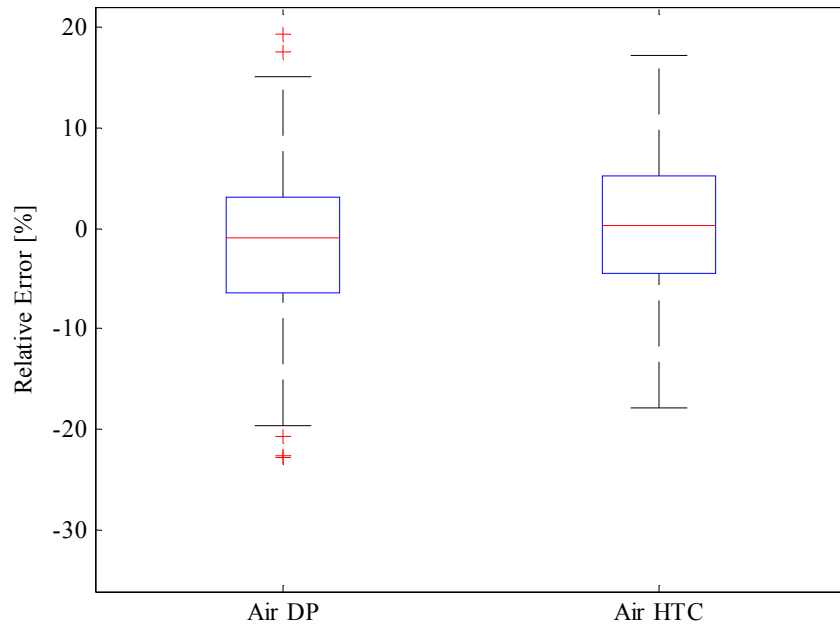


Figure 5.13 Metamodel verification for Air DP and HTC, relative errors

5.6.3 Metamodel Development- MSFCVT Method

Multiresponse metamodels were also developed using the MSFCVT method presented in Chapter 4. The MSFCVT method with the formulation presented in Eq. (4.2) was used. The method parameters were the same as the one used in the development of the SFCVT metamodel, i.e., 100 points in initial design, 100 adaptively sampled points, with 5 new points selected per stage. The same random sample of 250 point was used for metamodel verification. The results are shown in Figure 5.14.

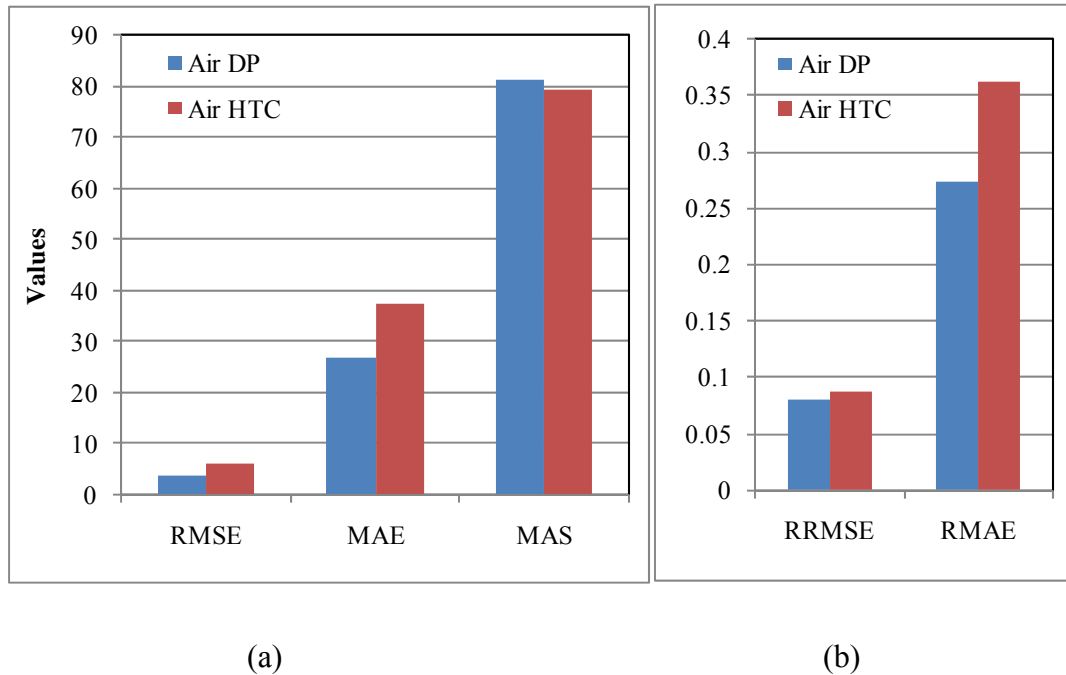


Figure 5.14 MSFCVT method verification for air DP and HTC, (a) RMSE, MAE and MAS, (b) RRMSE and RMAE

From Figure 5.14a, we can see that the approximately 80% of the verification points were predicted within $\pm 10\%$ of the actual value for both air HTC and DP. The maximum absolute error in predicted air DP is 27% and for HTC is 36%. These errors occurred for cases that had convergence issues during CFD simulations. Comparing

the metamodel performance with that obtained from SFCVT method, we observe that the MSFCVT method yields similarly performing metamodels but with a fewer number of total function calls, i.e., 300 vs. 200.

5.7 Design Optimization

5.7.1 Problem Formulation

Based on the performance evaluation criteria discussed earlier, the objective of the design problem was to find new heat exchanger design which has minimum air-side pressure drop and minimum volume, but still has the same heat duty/capacity as a 1 kW air-to-water micro channel heat exchanger.

For a fair comparison, the refrigerant side pressure drop (RDP) was constrained to be 1.5 times that of the microchannel heat exchanger used in the comparison. The optimization problem can be mathematically represented as:

$$\begin{aligned}
 & \min_{HX} ADP, V \\
 & \text{s.t.} \\
 & Q = 1\text{kW} \\
 & ADP < ADP_{\max} \\
 & RDP < RDP_{\max} \\
 & HX \equiv [Nt, D_{in}, Hs, Vs, w, v]
 \end{aligned} \tag{5.1}$$

where, ADP is the air-side pressure drop, V is the HX volume, Q is the heat load, ADP and RDP are the air and the refrigerant side pressure drops (respectively), ADP_{max} and RDP_{max} are the limits on ADP and RDP. Note that Nt is the number of parallel tubes in the heat exchanger and is discrete variable, while D_{in}, Hs, Vs, w, v are all continuous. The MOOP represented by Equation 5.1 was solved using a MOGA.

The relevant problem parameters and constraint limits are shown in Table 5.2. The parameters used for MOGA are given in Table 5.3.

Table 5.2 Optimization problem parameters

Parameter	Value
Heat Load Q , minimum	1kW
Heat Load Q , maximum	1.1 kW
ADP_{max}	100 Pa
RDP_{max}	1kPa
Air inlet temperature	300K
Water inlet temperature	350K
Air flow rate	0.025 kg/s
Water flow rate	0.025 kg/s

Table 5.3 MOGA Parameters

Parameter	Value
GA Population Size	100
GA Population Replacement	10
GA Max Iterations	500
Continuous Variable bit length	10

The metamodels obtained from the SFCVT method for air HTC and DP, described in Section 5.6.2, were used in the CoilDesigner calculations for predicting the coil performance. The resulting Pareto set comprising of 60 designs is shown in Figure 5.15. It can be observed that all the Pareto solutions have an air side pressure drop less than that of the baseline microchannel coil. There are 37 designs better than the baseline microchannel in terms of HX volume with the best heat exchanger having a 44% less volume than the baseline HX. All these heat exchangers have a heat load of 1 kW within +10%. The better designs also have an average of 61% less material volume and hence weight.

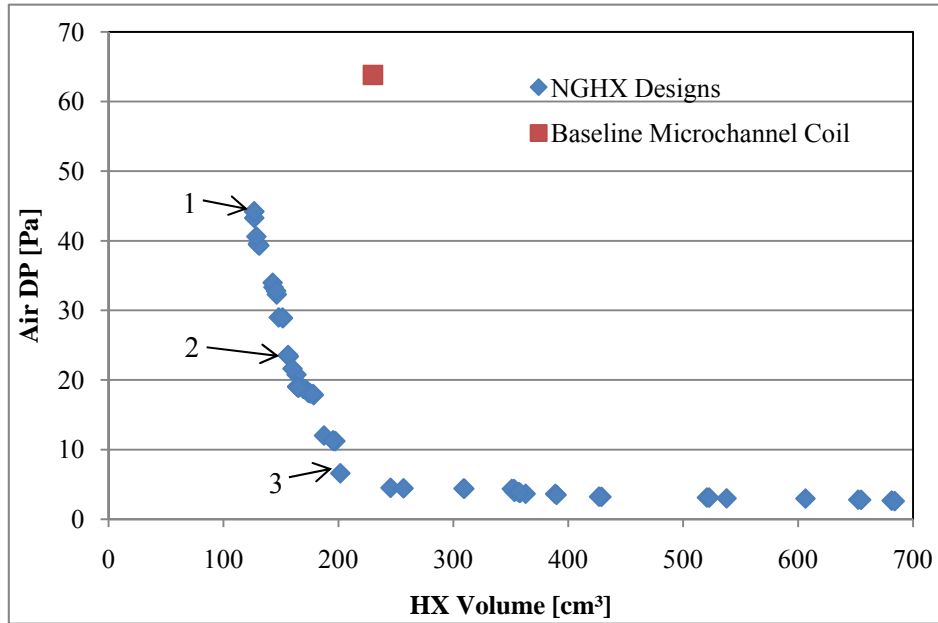


Figure 5.15 Pareto solutions for NGHX approximation assisted optimization

The details of three sample designs are shown in Table 5.4, along with HX volume, air pressure drop and material volume. The designs shown are the ones which are better than the baseline microchannel coil. We observe that the new designs offer a significant reduction in heat exchanger volume and the air side pressure drop compared to baseline coil for the same application performance.

Table 5.4 Sample Pareto solutions

Pareto Design	Normalized Design Variables						HX Vol. [cm ³]	Air DP [Pa]	Matl. Vol. [cm ³]
	Nt	D_{in}	Hs	Vs	w	ν			
1	162	0.316	0.265	0.0039	0.180	0.749	126.6	44.2	14.52
2	176	0.344	0.252	0.0127	0.164	0.427	156.1	23.5	17.79
3	188	0.367	0.020	0.0918	0.164	0.003	201.6	6.6	22.72
Baseline Micro-channel	NA						230.0	63.8	37.3

Figure 5.16 shows the data represented in Table 5.4. The three sample Pareto designs are shown in the main plot along with their relative volume (inset figure) compared to the baseline microchannel coil volume.

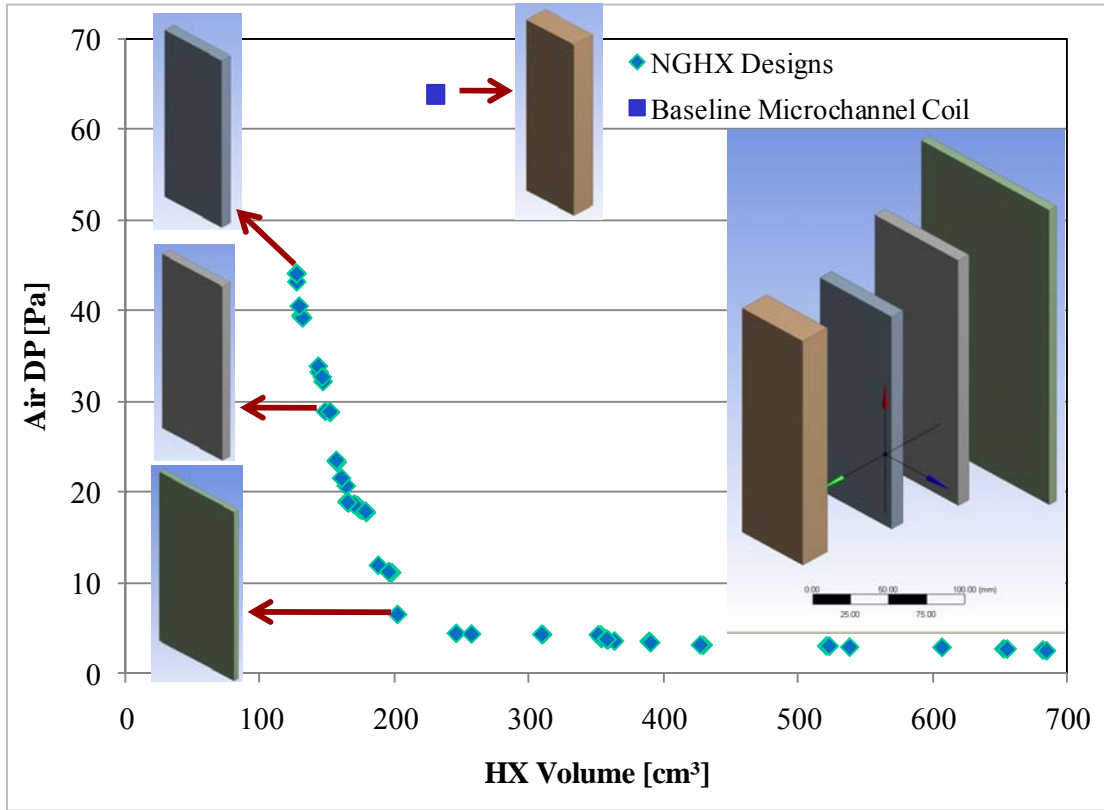


Figure 5.16 Sample Pareto designs and their relative volume compared to the baseline microchannel coil volume

5.7.2 Pareto Optimal Designs – Approximation Perspective

In this section we analyze the Pareto optimal results to evaluate how good the results obtained using approximation assisted optimizations are.

The above optimization was carried out using metamodels for the air side performance of the HX segment. It is imperative that for all Pareto solutions we verify the predicted air-side performance with actual CFD runs and then re-calculate

the overall performance of the heat exchanger. The resulting percentage errors in the predicted air side pressure drop and heat transfer coefficients and subsequently the calculated heat load are shown in Figure 5.17. Based on the median values, the air side pressure drop is over predicted by 2.8%, the heat transfer coefficient is under-predicted by 1.5% and subsequently the heat load is under-predicted by 0.91%. From a heat exchanger perspective, the over-prediction of pressure drop and under-prediction of HTC is favorable, since it will give conservative designs. As seen from this figure, there are some outliers for heat load error values, from which 6 designs violate the heat load constraint (i.e. $1000\text{W} \leq Q \leq 1100\text{W}$). 5 out of these 6 points have a heat load of less than 1kW with maximum deviation of 2.3% and one point has heat load more than 1100W with maximum error of 0.5% which is practically insignificant. Nevertheless, we update the Pareto set with the true responses of Air HTC and DP. The two Pareto sets are shown in Figure 5.18 below. They almost overlap.

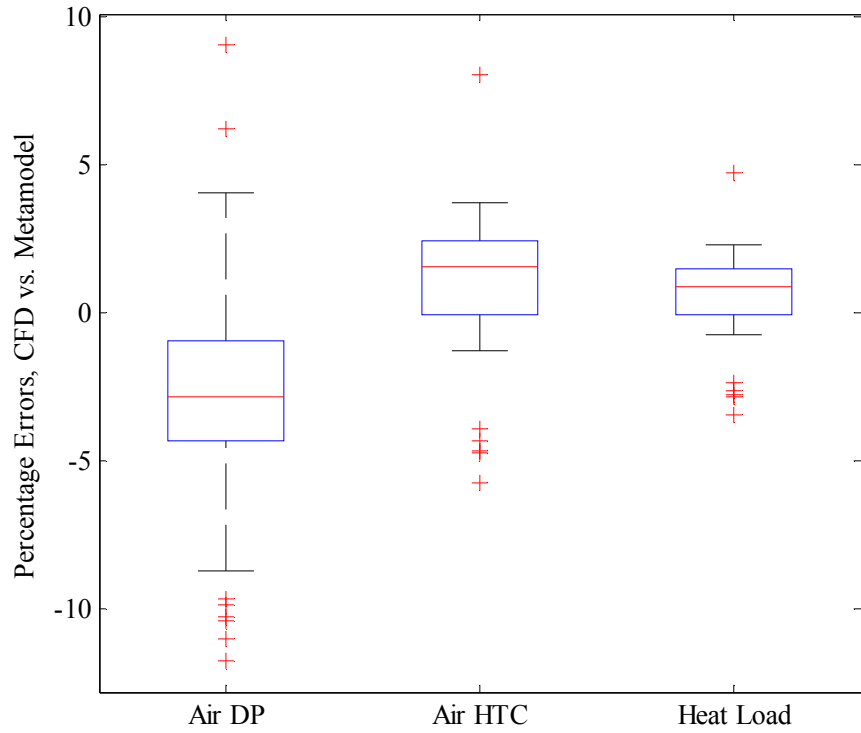


Figure 5.17 CFD vs. Metamodel, percentage errors in predicted performance

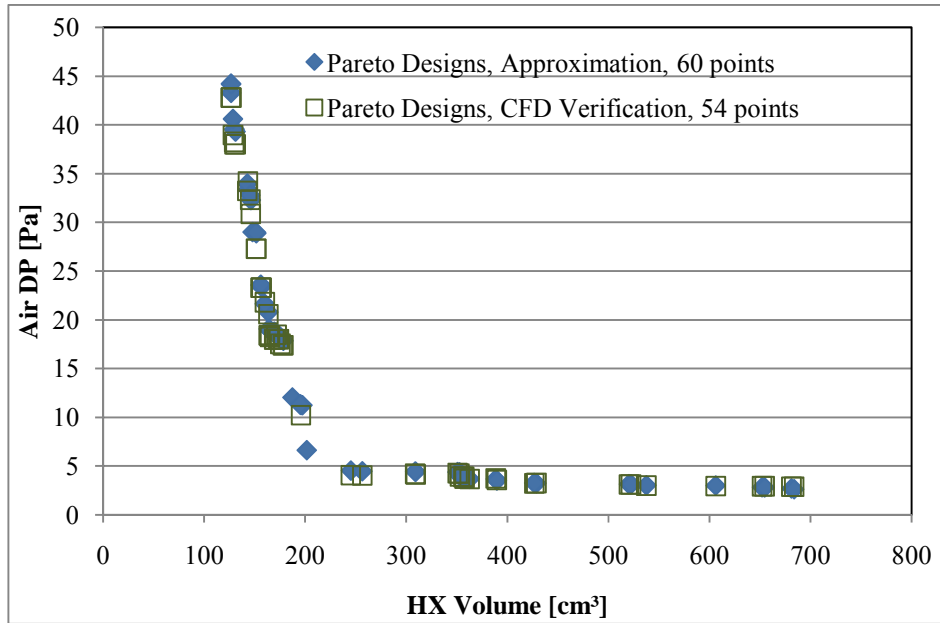


Figure 5.18 Pareto Designs obtained using approximation and verification

5.7.3 Pareto Optimal Designs – Thermodynamic Perspective

In this section we provide insight into the Pareto optimal design from a thermodynamic perspective.

Careful analysis of the design variables corresponding to the Pareto solutions reveals that all of the solutions have the same or close enough normalized inner diameters in the range [0.3,0.40]. This is because the inner diameter has a direct impact on the pressure drop of the refrigerant. MOGA is forced to drive towards the lowest diameter which still satisfies the pressure drop constraint, while other variables such as the horizontal and vertical spacing and velocity take a wide range of values. The HX normalized depth for the Pareto designs was also in a narrow range of [0.16, 0.31]. This is again due to the air side pressure drop constraint. The designs corresponding to smallest vertical spacing also had the corresponding smaller values for velocity, which again is influenced by the air side pressure drop objective.

Overall, we observe that the new heat exchanger geometry is capable of performing better than the current state of the art microchannel (i.e., baseline microchannel coil). This improvement is mainly due to significant compactness of the new geometry. In other words, the new geometry can accommodate more heat transfer area per unit HX volume and per unit HX material volume. The above comparison was carried out for one application, but using the newly developed approach optimal HX designs for other applications (i.e., different fluid inlet conditions and heat load) can be readily obtained. As a final note, it should be pointed out that the above results should be validated experimentally.

5.8 *Summary*

In this chapter, a new approach for the multi-level performance evaluation and design optimization of novel heat exchanger elements is introduced. The objective of developing this approach is to allow streamlined search of novel heat exchanger geometries for air-to-refrigerant heat exchanger applications. Instead of conducting full fledged 3D CFD simulations, the new approach uses 2D CFD techniques coupled with an ε -NTU solver for heat exchanger performance evaluation. This results in over 95% savings in computation time. The 2D CFD is used for air-side performance evaluation of small heat exchanger segment. The ε -NTU solver is then used to assemble these small HX segments or elements to design full scale heat exchangers. The new approach was verified for a range of dimensions for a heat exchanger. The comparison of the results (viz., pressure drop and change in temperature) showed that the new hybrid approach is valid for applications with single phase flows with Reynolds number greater than 100.

Even though, the replacement of 3D CFD with the new approach results in 95% savings of computational effort, the execution time is still prohibitive (~ 1 week for one optimization run). We apply the single response adaptive DOE approach developed in Chapter 3 to this problem, where in we approximate the air performance (DP and HTC) obtained from the 2D CFD calculations. The resulting metamodels for air side DP and HTC had MAS of 80 which was acceptable for the current optimization problem. The fact that MAS of 80 is acceptable is further reinforced by the post-optimization verification results.

The optimization problem was formulated as an MOOP, minimizing the heat exchanger volume and the air side pressure drop while providing a heat load of 1 kW. A conventional state-of-the art microchannel heat exchanger was used as a baseline for comparison. The Pareto optimal designs resulting from the MOOP solution had 37 heat exchanger designs that are better than the baseline heat exchanger, with a volume reduction of 44% and material reduction of 61%. In addition, the computational savings are enormous, since the metamodels can now be used for additional optimization studies with varying constraints etc. The Pareto designs obtained from the approximation assisted optimization were also verified against full CFD calculations. It was found that amongst the Pareto solutions obtained using approximation, 6 designs were infeasible but by a very marginal amount, while all other designs overlap with those obtained after CFD verification.

The inner diameter and the depth of the heat exchangers corresponding to the Pareto solutions were distributed in a very narrow range. The refrigerant side pressure drop constraint was the dominating factor in the choice of inner diameters, while the air side pressure drop objective was the dominating factor for the depth of the heat exchanger. This is because, small inner diameter leads to higher refrigerant side pressure drop and larger depth leads to larger air side pressure drop.

Chapter 6 Conclusion

In this dissertation three research thrusts are presented. The research thrusts are, (a) adaptive DOE approach for single response deterministic computer simulations, (b) adaptive DOE approach for multiresponse deterministic computer simulations and (c) approximation based framework for the performance evaluation and optimization of air-cooled heat exchangers.

This chapter is organized as follows: Section 6.1 provides a summary of the three research thrusts followed by conclusions in Section 6.2. Section 6.3 highlights the main contributions of this dissertation and section 6.4 provides a discussion for potential future research direction.

6.1 Summary

In this section, the three research thrusts are summarized as follows:

- (a) **Adaptive DOE for Single Response:** In Chapter 3 an adaptive DOE method for single response deterministic computer experiments is presented. The proposed approach is based on the notion of tradeoff that needs to be made by a DOE method between allocating samples in sparsely populated regions of the design space versus allocating samples in regions in which the response is most sensitive. The sensitivity of the response in a particular region of the design space is gauged by the calculation of leave one out cross-validation error, while the sparsely sampled regions are tracked through the use of a space –filling criterion. The approach is such

that one point is sampled per stage, though there are provisions for sampling multiple points per stage to take advantage of parallel computing capabilities. The proposed approach is then applied to a suite of test problems compiled as a part of this dissertation.

- (b) Adaptive DOE for Multiple Responses: Chapter 4 extends the approach proposed in Chapter 3 to multiple responses. The problem of adaptive DOE for multiresponse case is posed as a multiobjective optimization problem where the tradeoff is between allocating new samples such that they simultaneously improve the metamodel performance for each of the responses. A multiobjective genetic algorithm is used to solve the optimization problem resulting in a set of Pareto optimal solutions. A level of dominance criteria is introduced to select one point from the Pareto set.
- (c) Approximation Based Framework for Design of Novel Heat Exchangers: In Chapter 5 a new approximation based framework is proposed to evaluate the multi-level performance of air-cooled heat exchangers. An approach that uses 2D CFD coupled with an ϵ -NTU heat exchanger model is developed and termed as the Hybrid solver. This Hybrid solver allows us to achieve the same results as those obtained using a detailed 3D CFD analysis but with an order of magnitude reduction in computational cost. The performance evaluation approach is then coupled with a multi-objective genetic algorithm to find optimal designs for novel air-cooled heat exchanger.

6.2 Conclusions

This section provides some concluding remarks on each research thrust.

6.2.1 Single Response Adaptive DOE

The cross validation based single response adaptive DOE approach outperforms existing adaptive methods such as MSD (Jin, et al., 2002), ACE (Li and Azarm, 2006; Li, 2007) and non-adaptive method such as the MED (Shewry and Wynn, 1987; Koehler and Owen, 1996) method in more than 50% of the test problems. The comparison was based on the median values of the metamodel performance metrics. This observation is supported by the descriptive statistics drawn from the results generated by applying the said approaches to the 24 test problems. In certain cases it was observed that even though the proposed approach does not perform better in terms of RMSE and MAE in comparison to other approaches, it does perform well in terms of the relative predictions, i.e., RRMSE and RMAE. Even though RMSE and MAE are widely used in the literature for comparing metamodel performance, the results in this dissertation show that these measures are not enough to judge a metamodel and as such additional metric such MAS is also used. The metrics of RMSE, MAE, RRMSE, RMAE and MAS are used in this dissertation to compare the performance of different metamodels.

As detailed in Chapter 3, the proposed approach develops a metamodel of LOO errors to predict the regions of high sensitivity in the response space. For certain problems (e.g., test problem P10 in Chapter 3), these intermediate metamodels may not be accurate enough thus resulting in poor sampling which in turn leads to underperforming (compared to non-adaptive method) metamodels. It is important to

objectively evaluate the intermediate metamodels at each stage and if the metamodel is not acceptable, then the adaptive method must switch to a purely space-filling method such as MED. It should be pointed out that the proposed approach aims at sampling for a globally accurate metamodel. Thus, it yields better metamodels for problems with non-symmetric CAMM regions, where as non-adaptive space-filling methods are better suited for test problems with symmetric and highly distributed CAMM regions.

In all the numerical experiments, only the Gaussian correlation was used for the Kriging metamodels. For certain types of problems, this correlation may not be the best correlation and hence during implementation multiple correlations need to be evaluated and the best chosen.

6.2.2 Multiresponse Adaptive DOE

The cross validation based multiresponse adaptive DOE approach outperforms existing adaptive DOE techniques (i.e., DMM method by Li, et al., 2006, MCVV method by Romero, et al., 2006) based on the results published in the literature. The newly developed approach was also applied to a suite of 8 test problems with multiple inputs and multiple responses. Based on the numerical experiments, it was found that the MSFCVT approaches yields comparable or better metamodels for all responses simultaneously when compared with those obtained using the MED (Shewry and Wynn, 1987; Koehler and Owen, 1996) method.

The conclusions drawn for the single response adaptive DOE method in Section 6.2.1 are also applicable to the multiresponse adaptive DOE method.

It was observed at each stage, that MSFCVT simultaneously tried to improve the metamodels for each of the multiple responses. This can sometimes lead to over-improvement in some of the metamodels as observed for Numerical Example-1. At some point during the adaptive DOE phase, the performance of individual metamodels needs to be evaluated and the MSFCVT method needs to focus on the responses with less accurate metamodels. This cannot be carried out in the current implementation, since no assumption about availability of a test sample for verification was made.

6.2.3 Approximation Based Framework for Design of Novel Heat Exchangers

A new approach for multi-level performance evaluation of novel heat exchanger geometries that uses approximation assisted optimization is developed and applied to a real world case study.

The proposed Hybrid approach is valid for single phase flows with $Re > 100$. This is because the correlations in CoilDesigner are not valid in the low Re range. This results in large calculation errors in the water side heat transfer coefficients and pressure drop, which in turn affects the air-side performance, leading to large discrepancies between the heat exchanger performance obtained using a full 3D CFD simulation and those obtained using the hybrid approach.

In the study, individual metamodels were developed for the air side DP and HTC, with 100 initial points and 100 new points for each metamodel, resulting in a total of 300 function evaluations (i.e., initial 100 points were common). The metamodels were verified using 250 randomly generated samples. The resulting MAS was 80.0 for both air HTC and DP. Optimization was carried out with these metamodels and

the results were verified against actual CFD runs. The comparison was surprisingly good with the median prediction errors of 2.8% (over-prediction), 1.5% (under-prediction) and 0.9% (under-prediction) for air DP, HTC and heat load respectively, leading to the conclusion that for multi-level analysis (e.g., simulation at heat exchanger segment level and simulation at the heat exchanger level) a low fidelity, i.e., relatively less accurate metamodel may be acceptable. This is because at the top level, the errors in low level metamodels do not have a significant impact. If an uncertainty analysis can be carried out in early stages of analysis and optimization, it could result in computational savings, since the metamodels need not be highly accurate.

Analysis of the Pareto optimal designs led to the conclusion that the optimization search was dominated by the refrigerant side pressure drop constraint which is a function of the tube inner diameter. All the Pareto solutions had normalized D_{in} in the interval [0.3, 0.4]. Another factor heavily driving the search was the air-side pressure drop objective, which is influenced by the depth of the heat exchanger in the air-flow direction in addition to air velocity and vertical spacing. All Pareto designs had normalized depth in the range [0.16, 0.31].

Based on the promising designs obtained using the proposed approach, it is concluded that this tool will significantly improve the way novel heat exchangers with the proposed and similar geometry are explored.

6.3 Contributions

The main research contributions of this dissertation are:

1. An approach for single response adaptive DOE for deterministic computer simulations has been developed. A new problem formulation is proposed that views adaptive DOE problem as a multiobjective optimization problem. Applicability of the proposed approach has been tested on a broad set of test problems from the literature. It is shown that on an average the proposed approach yields better metamodel for the same number of function calls, than the approaches in the literature.
2. An approach for multiresponse adaptive DOE has been developed. A new multiobjective problem formulation is proposed which makes tradeoffs between the multiple responses. Applicability of the proposed approach is verified by successfully applying it to the test problems from literature. Based on comparison with published results, it is shown that the proposed approach performs better than two other adaptive DOE methods from the literature. It is shown that in multiresponse DOE, there is a tradeoff between allocating points to improve one response vs. another.
3. A new multi-level performance evaluation and optimization approach has been developed for design of novel air-cooled heat exchangers. The approach helps reduce the computation time from a few months to a couple of days, resulting in over 95% savings in computational effort without any practical loss of accuracy in the results. In this approach, the heat exchanger

performance is evaluated not only at the element level, which is the conventional approach, but also at the component level. The component level evaluation tells us upfront as to whether the new geometry can compete with current state of the art heat exchangers. The multi-level performance evaluation approach along with the approach developed in 1 above is used in the development of a multi-objective genetic algorithms based optimization tool for the optimization of novel heat exchanger. The new heat exchanger design has 44% less volume and uses 61% less material compared to current state of the art microchannel heat exchangers. The new heat exchanger design approach is not limited to conventional geometries (e.g. round tubes) and can be applied to non-conventional heat exchanger geometries such as tubes with aero-foil shaped cross section.

6.4 Future Research Directions

The research presented in this dissertation has addressed several shortcomings of adaptive DOE approaches proposed in the literature. In order to make the approach more efficient and less sensitive to initial samples, the following research directions could be pursued:

- (a) The examples shown in this dissertation used the proposed approach to develop metamodels for the entire design space (global metamodels). But the approach can also be used with a restricted design space. One example of such an application is online approximation, where the M/SFCVT method can be used to intelligently sample new points in the regions of expected optima.

- (b) The resource allocation problem, wherein the total number of available function calls is fixed and then the approach should be able to judiciously and objectively allocate samples for initial design, subsequent sequential sampling and for random verification. Moreover, the approach needs to handle this without any prior knowledge of the computer simulation. A preliminary approach is proposed in Section 3.6. But a clever way to evaluating metamodel performance and stalling condition without additional function calls is required.
- (c) In developing the metamodels for the LOO errors, a Gaussian correlation was used. Other correlation options need to be investigated along with any additional tuning. At each stage the best LOO model needs to be developed and since no information about the simulation is known, this points to a trial and error strategy where each type of correlation could be tried and compared.
- (d) In the studies presented, the MED method was used to generate all initial designs. Other space filling techniques such as Latin-hypercubes should be investigated.
- (e) The proposed cross-validation approach can be extended to non-Kriging based metamodels.
- (f) Develop a convenient graphical user interface for the approximation based framework for performance evaluation of heat exchangers, which will allow end-users from the industry to quickly and efficiently evaluate novel heat exchanger geometries.

(g) In Chapter 5, for the geometry under consideration, no significant structural analysis was required. But in real life, new concepts may require careful tradeoff between structural aspect (i.e., material used) and the heat transfer performance giving rise to a multidisciplinary optimization problem possibly a coupled problem. A possible multiobjective collaborative optimization approach such as the one presented in Aute and Azarm (2006) could be implemented as a part of the framework. The use of approximation is a must in such problems since the computational effort increases super linearly with the number of different disciplines involved.

Appendix-A Test Problem Suite

In order to evaluate the general applicability of the approaches proposed in this dissertation, a suite of test problems was compiled. Some of these test problems are based on those found in the literature and used by other researchers (Jin et al., 2002; Li and Azarm, 2006; Romero et al., 2006), while others were devised as a part of this dissertation (see below). The test problems are used to evaluate the following aspects of an adaptive design of experiments approach: (a) scalability to more than two dimensions, and (b) applicability to multi-modal and highly sensitive responses. The remainder of this Appendix provides short background and the literature references for each of the test problems, followed by the equations and the domain of each problem.

Problem P1 and P4 are from Dixon and Szego (1978), P2, P13, P14 and P16 are made up test problems. P5 is Griewank's function (Hedar, 2005), P6 is Himmelblau's function and P7 is the hump function (Floudas et al., 1999), P11 is Rastrigin's function (Hedar, 2005) , P12 is Schwefel's function (Hedar, 2005) and P17 is Coleville function (Hedar, 2005), P15 is the wine bottle function (Van Veldhuizen and Lamont, 1998). Problem P9 is Osio's function (Osio and Amon, 1996), P8 is Sasena's function (Sasena et al., 2000) and P10 is Busby's (Busby et al., 2007) function. Problems P18, P19 and P20 are the scaled 4 dimensional versions of their 2 dimensional counterparts while problems P22, P23 and P24 are scaled to 8 dimensions, i.e., 8 inputs. Problem P21 is the borehole model simulation from Joseph et al., (2008)

Table A.1 Single response test problems

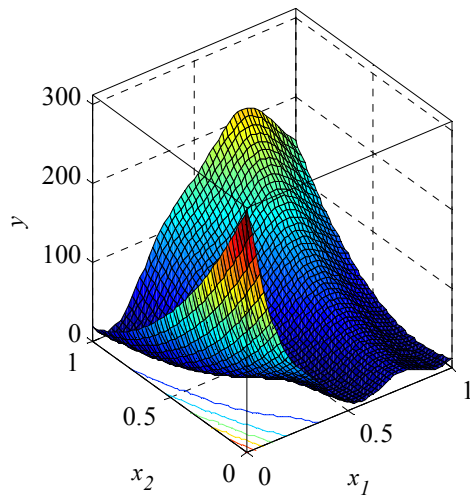
Sr. No.	Problem
1.	<p>P1: Branin Function (Dixon and Szego, 1978)</p> $y = [x_2 - 5.1 \left(\frac{x_1}{2\pi} \right) 2 + \frac{5x_1}{\pi} - 6] 2 + 10 \left(1 - \frac{1}{8\pi} \right) \cos(x_1) + 10$ $x_1 \in [-5, 10], x_2 \in [0, 15]$
2.	<p>P2: Trigonometric Function-1</p> $y = \cos(\sqrt{x_1^2 + x_2^2})$ $x_1, x_2 \in [-5, 5]$
3.	<p>P3: Dixon-Price Function (Hedar, 2005)</p> $y = (x_1 - 1)^2 + \sum_{i=2}^n i(2x_i^2 - x_{i-1})^2$ $x_i \in [-10, 10], i = 1, \dots, n$ $n = 2$
4.	<p>P4: Goldstein-Price (Dixon and Szego, 1978)</p> $y = [1 + (x_1 + x_2 + 1)^2 (19 - 14x_1 + 3x_1^2 - 14x_2 + 6x_1x_2 + 3x_2^2)] [30 + (2x_1 - 3x_2) 2 \times (18 - 32x_1 + 12x_1^2 + 48x_2 - 6x_1x_2 + 27x_2^2)]$ $x_1, x_2 \in [-2, 2]$
5.	<p>P5: Griewank Function (Hedar, 2005)</p> $y = \sum_{i=1}^n \frac{x_i^2}{4000} - \prod_{i=1}^n \cos(x_i / \sqrt{i}) + 1$ $x_i \in [-20, 20], i = 1, \dots, n$ $n = 2$

6.	<p>P6: Himmelblau's Function (Floudas et al., 1999)</p> $y = (x_1^2 + x_2 - 11)^2 + (x_1 + x_2^2 - 7)^2$ $x_1, x_2 \in [-4, 4]$
7.	<p>P7: Hump Function (Floudas et al., 1999)</p> $y = 4x_1^2 - 2.1x_1^4 + \frac{1}{3}x_1^6 + x_1x_2 - 4x_2^2 + 4x_2^4$ $x_1, x_2 \in [-5, 5]$
8.	<p>P8: Sasena's Function (Sasena et al., 2000)</p> $y = 2 + 0.01(x_2 - x_1^2)^2 + (1 - x_1)^2 + 2(2 - x_2) + 7 \sin(0.5x_1) \sin(0.7x_1x_2)$ $x_1, x_2 \in [0, 5]$
9.	<p>P9: Osio's Function (Osio and Amon, 1996)</p> $y = \cos(6(x_1 - 0.5)) + 3.1(x_1 - 0.7) + 2(x_1 - 0.5) + \sin\left(\frac{1}{ x_1 - 0.5 + 0.31}\right) + 0.5x_2$ $x_1, x_2 \in [0, 1]$
10.	<p>P10: Busby's Function (Busby et al., 2007)</p> $y = 7 \frac{\sin(\sqrt{x_1^2 + x_2^2}) + 10^{-7}}{\sqrt{x_1^2 + x_2^2}} + 3 x_1 - x_2 ^{1/2}$ $x_1, x_2 \in [-10, 10]$
11.	<p>P11: Rastrigin's Function (Hedar, 2005)</p> $y = 20 + x_1^2 + x_2^2 - 10(\cos(2\pi x_1) + \cos(2\pi x_2))$ $x_1, x_2 \in [-1, 1]$

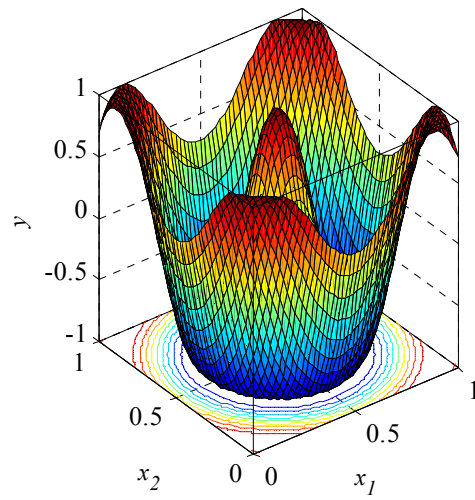
12.	<p>P12: Schwefel Function (Hedar, 2005)</p> $y = 418.9829n - \sum_{i=1}^n (x_i \sin \sqrt{ x_i })$ $x_i \in [-500, 500], i = 1, \dots, n$ $n = 2$
13	<p>P13: Trigonometric Function-2</p> $y = \sin(x_1 + x_2)$ $x_1 \in [0, 2\pi], x_2 \in [0, \pi]$
14.	<p>P14: Trigonometric Function-3</p> $y = \sin(x_1) \cos(x_2)$ $x_1, x_2 \in [-3, 3]$
15.	<p>P15: Wine Bottle Function (Van Veldhuizen and Lamont, 1998)</p> $y = \frac{C+1}{9.32}$ $C = \frac{A^2 + B^2 + 3}{2} + \sin(A^2 + B^2 + 2)$ $A = 6x_1 - 3 \quad ; \quad B = 6x_2 - 3$ $x_1, x_2 \in [0, 1]$
16.	<p>P16: Numerical Function-1</p> $y = x_1 x_2 / (x_1^2 + x_2^2 + 0.1)$ $x_1, x_2 \in [-10, 10]$

17.	<p>P17: Coleville Function (Hedar, 2005)</p> $a_i = x_i - 1, i = 1, \dots, 4$ $y = 100(x_1^2 - x_2)^2 + a_1^2 + a_3^2 + 90(x_3^2 - x_4) + 10.1(a_2^2 + a_4^2) + 19.8a_2a_4$ $x_i \in [-10, 10], i = 1, \dots, 4$
18.	<p>P18: Dixon-Price Function, 4D</p> <p>Same as P3 with n=4</p>
19.	<p>P19: Griewank's Function, 4D</p> <p>Same as P5, with n = 4</p>
20.	<p>P20: Schwefel Function, 4D</p> <p>Same as P12 with n=4</p>
21.	<p>P21: Borehole model (Joseph et al., 2008)</p> $y = \frac{2\pi T_u (H_u - H_l)}{\ln(r / r_w) \left[1 + \frac{2LT_u}{\ln(r / r_w)r_w^2 K_w} + \frac{T_u}{T_l} \right]}$ $r_w \in [0.05, 0.15], r \in [100, 50000]$ $T_u \in [63070, 115600], H_u \in [990, 1110]$ $T_l \in [63.1, 116], H_l \in [700, 820]$ $L \in [1120, 1680], K_w \in [9855, 12045]$
22.	<p>P22: Dixon-Price Function, 8 Dimensions</p> <p>Same as P3, with n=8</p>
23.	<p>P23: Griewank's Function, 8 Dimensions</p> <p>Same as P5, with n = 8</p>
24.	<p>P24: Scwefel's Function, 8D</p> <p>Same as P12 with n=8</p>

On the following pages the respective response surfaces are shown for test problems P1 through P16 with inputs normalized to $[0, 1]$. The normalization is carried out by linearly mapping the ranges of input variables shown in Table A.1 for each input to the interval $[0, 1]$. As an example, in problem P5, the input range of $[-20, 20]$ is changed to $[0, 1]$ by replacing x with $(x+20)/40$. $(x+20)/40$ has the range $[0, 1]$ as shown in the figures.

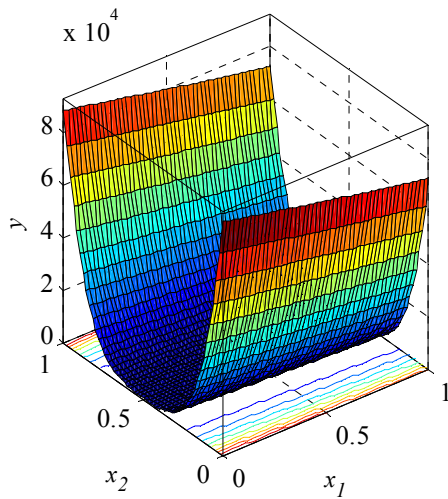


(a)

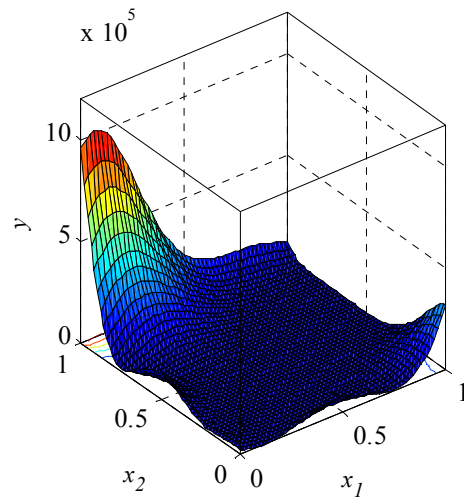


(b)

Figure A.1 Response surface for problem (a) P1 and (b) P2

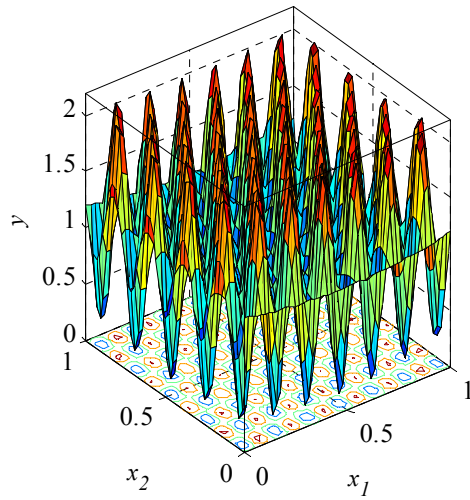


(a)

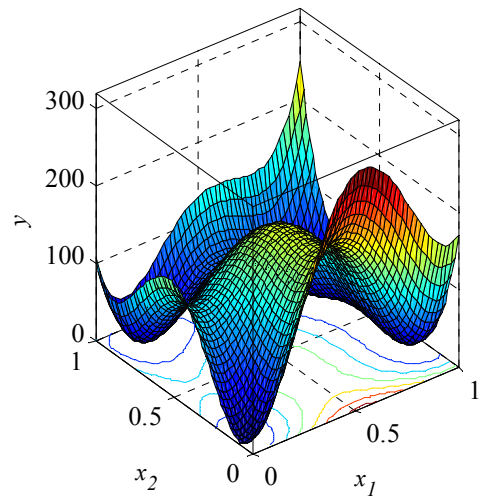


(b)

Figure A.2 Response surface for problem (a) P3 and (b) P4

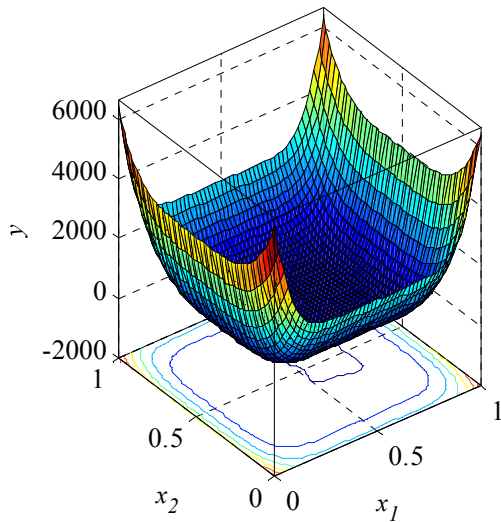


(a)

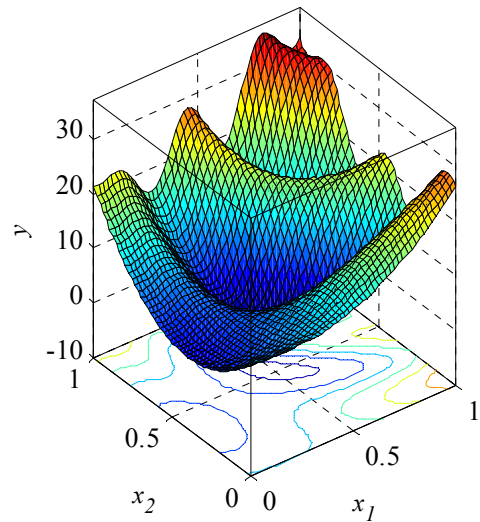


(b)

Figure A.3 Response surface for problem (a) P5 and (b) P6

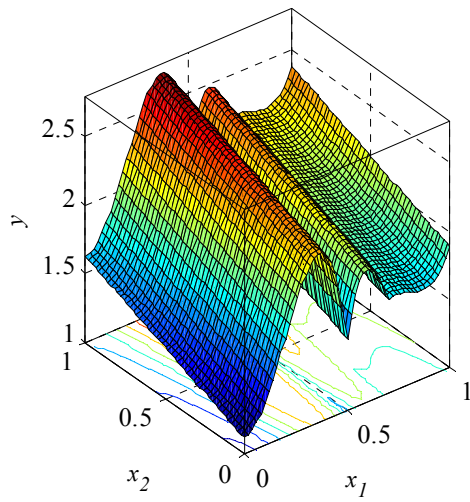


(a)

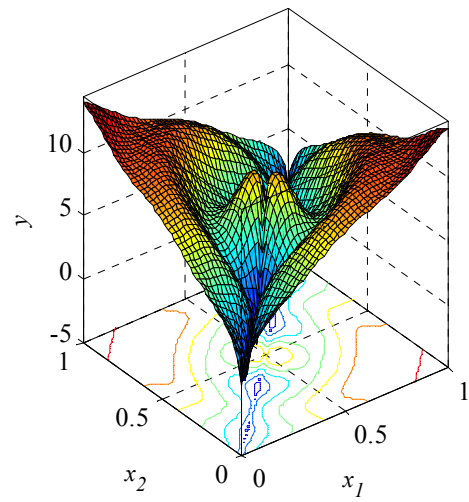


(b)

Figure A.4 Response surface for problem (a) P7 and (b) P8

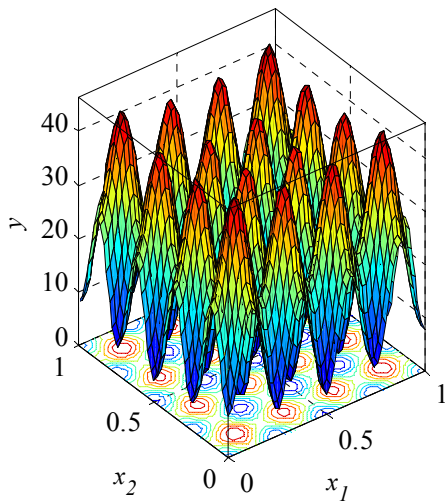


(a)

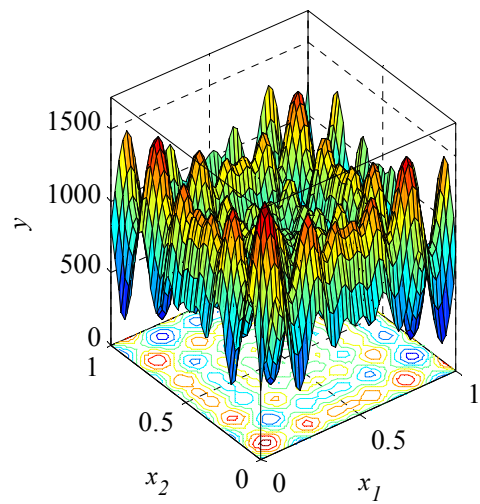


(b)

Figure A.5 Response surface for problem (a) P9 and (b) P10

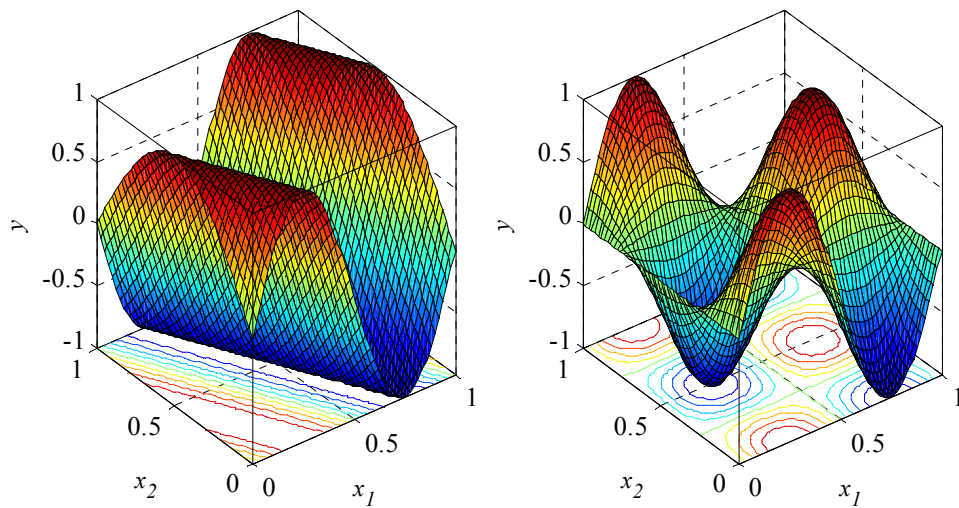


(a)

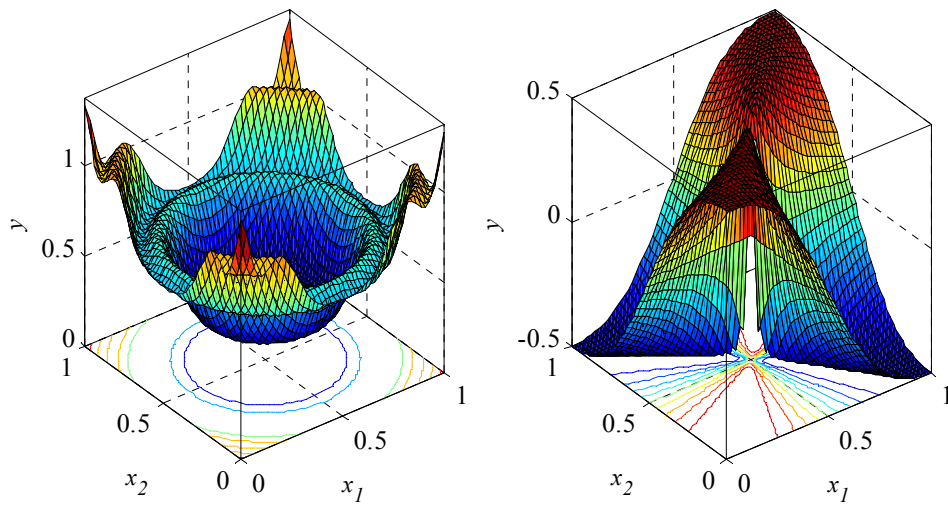


(b)

Figure A.6 Response surface for problem (a) P11 and (b) P12



(a) (b)
Figure A.7 Response surface for problem (a) P13 and (b) P14



(a) (b)
Figure A.8 Response surface for problem (a) P15 and (b) P16

In Table A.2, the multiresponse test problems are described. The multiresponse test problems are basically a combination of the single response test problems used to mimic a multiresponse black-box simulation. The test problems are labeled PM1-PM8. For each response, the corresponding problem number from the single response test suite from Table A.1 is given.

Table A.2 Multiresponse test problems

Sr. No.	Problem
1.	Problem PM1 $y_1 \equiv P17, y_2 \equiv P18$
2.	Problem PM2 $y_1 \equiv P19, y_2 \equiv P20$
3.	Problem PM3 $y_1 \equiv P21, y_2 \equiv P22$
4.	Problem PM4 $y_1 \equiv P23, y_2 \equiv P24$
5.	Problem PM5 $y_1 \equiv P1, y_2 \equiv P6, y_3 \equiv P8, y_4 \equiv P3$
6.	Problem PM6 $y_1 \equiv P4, y_2 \equiv P11, y_3 \equiv P7, y_4 \equiv P10$

7.	Problem PM7 $y_1 \equiv P17, y_2 \equiv P18, y_3 \equiv P19, y_4 \equiv P20$
8.	Problem PM8 $y_1 \equiv P21, y_2 \equiv P22, y_3 \equiv P23, y_4 \equiv P24$

Bibliography

1. Abdelaziz O., Aute V., and Radermacher, R., 2008, "Heat Transfer and Pressure Drop for Laminar Single Phase Fluid Flow in Circular Microchannels," Manuscript Submitted to the *International Journal of Heat and Mass Transfer*.
2. Anderson J. D., 1995, *Computational Fluid Dynamics – The Basics with Applications*, McGraw Hill Inc.
3. ARI Standard 410, 2001, *Standard for Forced-Circulation Air-Cooling and Air-Heating Coils*, Air-Conditioning and Refrigeration Institute.
4. Armstrong, M., 1998, *Basic Linear Geostatistics*, Springer.
5. Aute, V. C., Radermacher, R. and Valiya Naduvath. M., 2004, "Constrained Multiobjective Optimization of an Air-Cooled Condenser," in the *Proceedings of the 10th International Refrigeration & Air-Conditioning Conference at Purdue*, Purdue, Indiana.
6. Aute, V., and Azarm, S., 2006, "A Genetic Algorithms Based Approach for Multidisciplinary Multiobjective Collaborative Optimization," in the *Proceedings of the 11th AIAA/ISSMO Multidisciplinary Analysis and Optimization Conference*, Portsmouth, Virginia.
7. Bakker, T. M. D., 2000, *Design Optimization with Kriging Models*, WBBM Report Series 47, Delft University Press.

8. Busby D., Farmer, C. L., and Iske, A., 2007, "Hierarchical Nonlinear Approximation for Experimental Design and Statistical Data Fitting," *SIAM Journal of Scientific Computing*, Vol. 29, No. 1, pp. 49-69.
9. Charnes, A., Cooper, W., and Ferguson, R., 1955, "Optimal Estimation of executive Compensation by Linear Programming," *Management Science*, Vol. 1 No. 2, pp. 138-151.
10. Chiao, C. H.. and Hamada M. S., 2001, "Analysis of experiments with correlated multiple responses," *Journal of Quality Technology*, Vol. 33, pp. 451-465.
11. Churchill, S.W., 1977, "Frictional equation spans all fluid flow regimes," *Chem. Eng.* 84, 91-92.
12. Clarke, S. M., Griebisch, J. H., and Simpson, T. W., 2005, "Analysis of Support Vector Regression for Approximation of Complex Engineering Analyses," *Journal of Mechanical Design*, Vol. 125, pp. 1077-1087.
13. Coello Coello, A. C., Pulido, G. T., and Lechuga, M. S., 2004, "Handling Multiple Objectives with Particle Swarm Optimization", *IEEE Transactions on Evolutionary Computation*, Vol. 8, No. 3, pp. 256-279
14. Coello Coello, C. A., Lamont, G. B., and Van Veldhuizen, D. A., 2007, *Evolutionary Algorithms for Solving Multi-Objective Problems*, Springer, New York.
15. Cohon, J. L., 1978, *Multiobjective Programming and Planning*, Mathematics in Science and Engineering, Vol. 140, Academic Press.

16. Cox, D. D. and John, S., 1997, "SDO: A Sequential Method for Global Optimization", *Multidisciplinary Design Optimization: State of the Art*, edited by N. Alexandrov and M. Y. Hussaini, SIAM, Philadelphia, pp. 315-329.
17. Cressie, N. A. C., 1993, *Statistics for Spatial Data*, Wiley Series in Probability and Mathematical Statistics.
18. Currin, C., Mitchell, M., Morris, M., Ylvisaker, D., 1988, "A Bayesian Approach to the Design and Analysis of Computer Experiments", *Oak Ridge National Laboratory, Report ORNL-6498*.
19. Currin, C., Mitchell, M., Morris, M., Ylvisaker, D., 1991, "Bayesian Prediction of Deterministic Functions with Applications to the Design and Analysis of Computer Experiments," *Journal of the American Statistical Association*, Vol. 86, pp. 953-963.
20. Das, I., and Dennis, J. E., 1998, "Normal Boundary Intersection: A new method for generating Pareto surface in nonlinear multi-criteria optimization problems," *SIAM Journal of Optimization*, Vol. 8, No. 3, pp. 631-657.
21. Deb, K., 2001, *Multi-Objective Optimization using Evolutionary Algorithms*, Wiley, New York.
22. Deb, K., Agarwal, S., Pratap, A., and Meyarivan, T., 2000, "Fast Elitist Non-dominated Sorting Genetic Algorithm for Multiobjective Optimization: NSGA-II," in *Proceedings of the 6th International Conference on Parallel Problem Solving from Nature (PPSN-VI)*, Paris, France

23. Derringer, G., and Suich, R., 1980, "Simultaneous Optimization of several response variables," *Journal of Quality Technology*, Vol. 12, No. 4, pp. 214-219.
24. Dixon L. C. W., and Szego G. P., 1978, "The Global Optimization Problem: An Introduction," in Dixon, L.C.W. and Szego, G.P., editors, *Toward Global Optimization*, Vol. 2, pp.1-15, North Holland, Amsterdam.
25. Dyn, N., Levin, D., and Rippa, S., 1986, "Numerical Procedures for Surface Fitting of Scattered Data by Radial Basis Function," *SIAM J. of Sci. Stat. Computing*, Vol. 7, No. 2, pp. 639-659.
26. Falco I. D., 1997, "An Introduction to Evolutionary Algorithms and Their Application to the Aerofoil Design problem – Part I: the Algorithms," *von Karman Lecture Series on Fluid Dynamics*, Bruxelles, Belgium.
27. Fang, K. T., Lin, D. K. J., Winkler, P., and Zhang, Y., 2000, "Uniform Design: Theory and Application," *Technometrics*, Vol. 39, No. 3, pp.237-248.
28. Farhang-Mehr A., and Azarm, S., 2005, "Bayesian Metamodeling of Engineering Design Simulations: A Sequential Approach with Adaptation to Irregularities in the Response Behavior," *International Journal for Numerical Methods in Engineering*, Vol. 62, pp. 2104-2126.
29. Farin G. E., 1999, *NURBS: From Projective Geometry to Practical Use*, Published by A. K. Peters.

30. Farin G. E., 2002, *Curves and Surface for Computer Aided Geometric Modeling: A Practical Guide*, Academic Press, Morgan Kaufmann Series in Computer Graphics and Geometric Modeling.
31. Floudas, C. A., Pardalos, P. M., Adjiman, C. S., Esposito W. R., Gumus, Z. H., Harding, S. T., Klepeis J. L., Meyer, C. A., and Schweiger, C. A., 1999, *Handbook of Test Problems in Local and Global Optimization*, Kluwer Academic Publishers.
32. FLUENT 6.2 User Guide, 2005, FLUENT Inc., NH.
33. Fonseca, C. M. and Fleming, P. J., 1993, "Genetic Algorithms for Multiobjective Optimization: Formulation, discussion and generalization," in *Proceedings of the Fifth International Conference on Genetic Algorithms*, pp. 416-423.
34. Fonseca, C. M. and Fleming, P. J., 1998a, "Multiobjective Optimization and Multiple Constraint Handling with evolutionary algorithms – Part I: A unified formulation", *IEEE Transactions on Systems, Man and Cybernetics*, Part A: Systems and Humans, 28(1), pp. 26-37.
35. Fonseca, C. M. and Fleming, P. J., 1998b, "Multiobjective Optimization and Multiple Constraint Handling with evolutionary algorithms – Part II: Application Example", *IEEE Transactions on Systems, Man and Cybernetics*, Part A: Systems and Humans, 28(1), pp. 38-47.

36. Giunta, A. A., Wojtkiewicz, S. F., Eldred, M. S., 2003, "Overview of Modern Design of Experiments Methods for Computational Simulations," *41st Aerospace Sciences Meeting and Exhibit*, AIAA 2003-649, pp. 1-17.
37. Gnielinski, V., 1976, "New equations for heat and mass transfer for turbulent pipe and channel flow," *International Journal of Chemical Engineering*, Vol. 16, No. 2, pp. 359-368.
38. Goel T., Haftka, R. T., Queipo, N. V., and Shyy, W., 2006, "Performance Estimate and Simultaneous Application of Multiple Surrogates," in the *Proceedings of the 11th AIAA/ISSMO Multidisciplinary Analysis and Optimization Conference*, 6-8 September, Portsmouth VA.
39. Goldberg, D. E., 1989, *Genetic Algorithms in Search, Optimization and Machine Learning*, Addison-Wesley.
40. Haimes, Y. Y., Lasdon, L. S. and Wismer, D. A., 1971, "On a bicriterion formulation of the problems of integrated system identification and system optimization," *IEEE Transactions on Systems, Man, and Cybernetics*, Vol. 1, No. 3, pp. 296-297.
41. Hamad, H., 2006, "A New Metric for Measuring Metamodels Quality-of-Fit for Deterministic Simulations," in *Proceedings of the Winter Simulation Conference*, Vol. 3, No. 6, pp. 882-888.
42. Hedar, A. R., 2005, *Test Problems for Unconstrained and Constrained Global Optimization*, Global Optimization Methods and Codes, System Optimization Lab, Kyoto University.

43. Hendrickx, W., Gorissen, D., Dhaene, T., 2006, "Grid Enabled Sequential Design and Adaptive Metamodeling," in the *Proceedings of the 2006 Winter Simulation Conference*.
44. Hilbert, R., Janiga, G., Baron, R., and Thevenin, D., 2006, "Multi-objective Shape Optimization of a Heat Exchanger Using Parallel Genetic Algorithms," *International Journal of Heat and Mass Transfer*, Vol. 49, pp. 2567-2577.
45. Horn, J., Nafploitis, N. and Goldberg, D., 1994, "A niched Pareto genetic algorithm for multi-objective optimization," in *Proceedings of the First IEEE Conference on Evolutionary Computation*, pp. 82-87.
46. Ignizio, J. P., 1976, *Goal Programming and Extensions*, Lexington, MA: Lexington Books.
47. Jiang, H., Aute, V., and Radermacher, R., 2006, 'CoilDesigner: A General Purpose Simulation and Design Tool for Air to Refrigerant Heat Exchangers', *International Journal of Refrigeration*, Vol. 29, No. 4, pp. 601-610.
48. Jin, R., Chen, W., and Sudjianto, A., 2002, "On Sequential Sampling for Global Metamodeling in Engineering Design", *CD-ROM Proceedings of ASME IDETC, Design Automation Conference*, Montreal, Canada.
49. Jin, R., Chen, W., Simpson, T. W., 2001, "Comparative Studies of Metamodeling Techniques Under Multiple Modeling Criteria," *Structural and Multidisciplinary Optimization*, Vol. 23, No. 1. pp, 1-13.

50. Johnson, M. E., Moore, L. M., and Ylvisaker, D., 1990, "Minimax and Maximin Distance Designs," *Journal of Statistics Planning and Inference*, Vol. 26, No. 2, pp. 131-148.
51. Jones, D. R., 2001, "A Taxonomy of Global Optimization Methods Based on Response Surfaces", *Journal of Global Optimization*, Vol. 21, pp. 345-383.
52. Jones, D. R., Schonlau, M., and Welch, W. J., 1998, "Efficient Global Optimization of Expensive Black Box Functions," *Journal of Global Optimization*, Vol. 13, pp. 455-492.
53. Joseph, V. R., Hung, Y. and Sudjianto, A., 2008, "Blind Kriging: A New Method for Developing Metamodels," *Journal of Mechanical Design*, ASME, Vol. 130, pp. 031102-1 – 031102-8.
54. Kalagnanam, J. R., and Diwekar, U. M., 1997, "An Efficient Sampling Technique for Off-Line Quality Control," *Technometrics*, Vol. 39, No. 3, pp.308-319.
55. Kanaris, A. G., Mouza, K. A., and Paras, S. V., 2004, "Designing Novel Compact Heat Exchangers For Improved Efficiency Using a CFD Code," *1st International Conference, From Scientific Computing to Computational Engineering*, 8-10 September, 2004, Athens.
56. Kandlikar, S., Garimella, S., Li, D., Colin, S., and King M., 2006, *Heat Transfer and Fluid Flow in Minichannels and Microchannels*, Elsevier Science.

57. Kays, W. M., and London, A. L., 1984, *Compact Heat Exchangers*, McGraw-Hill, New York.
58. Keeny, R. L., and Raiffa, H., 1976, *Decisions with Multiple Objectives: Preferences and Value Tradeoffs*, New York Wiley.
59. Kleijnen, J. P. C., and van Beers, W. C. M., 2004, "Application-driven sequential designs for simulation experiments: Kriging metamodeling," *Journal of the Operational Research Society*, Vol. 55, No. 8, pp. 876-883.
60. Koehler, J. R., and Owen, A. B., 1996, "Computer Experiments", *Handbook of Statistics*, Vol. 13, Elsevier Science, New York, 1996
61. Koppen, M., Vicente-Garcia, R., and Nockolay, B., 2005, "Fuzzy-Pareto Dominance and Its Application in Evolutionary Multi-objective Optimization," Coello Coello et al., Editors, EMO 2005, pp. 399-412.
62. Lam, C. Q., and Notz, W., 2007, "Comparing Adaptive Designs of Computer Experiments for Global Fit of Response Surfaces," *International Conference on Advances in Interdisciplinary Statistics and Combinatorics*, October 12-14, 2007, NC.
63. Langer, H., Puhlhofer, T., and Baier, H., 2002, "An Approach for Shape and Topology Optimization Integrating CAD Parameterization and Evolutionary Algorithms," in the *Proceedings of the 9th AIAA/ISSMO Symposium on Multidisciplinary Analysis and Optimization*, 4-6 September, 2002, Atlanta Georgia.

64. Li, G., 2007, *Online and Offline Approximations for Population Based Multi-Objective Optimization*, PhD Dissertation 2007, University of Maryland College Park.
65. Li, G., and Azarm, S., 2006, "Maximum Accumulative Error Sampling Strategy for Approximation of Deterministic Engineering Simulations," in *Proceedings of the 11th AIAA/ISSMO Multidisciplinary Analysis and Optimization Conference*, Portsmouth, VA.
66. Li, G., Azarm, S., Farhang-Mehr, A., and Diaz, A. R., 2006, "Approximation of multiresponse deterministic engineering simulations: a dependent metamodeling approach," *Structural and Multidisciplinary Optimization*, Vol. 31, pp.260-269.
67. Lin, Y., Chen, V. C. P., Tsui, K.-L., Mistree F., and Allen J. K., 2004a, "An Sequential Exploratory Experimental Design Method: Development of Appropriate Empirical Models in Design," *ASME Design Engineering Technical Conference*, Salt Lake City, Utah, Paper No. DETC 2004-57527.
68. Lin, Y., Mistree F., Allen J. K., Tsui K., and Chen V. C. P., 2004b, "Sequential Metamodeling in Engineering Design", in *Proceedings of the 10th AIAA/ISSMO Multidisciplinary Analysis and Optimization Conference*, Albany, NY.
69. Lindley, D. V., 1956, "On a measure of the information provided by an experiment," in *The Annals of Mathematical Statistics*, Vol. 27, pp. 986-1005.

70. Lophaven, S. N., Nielsen, H. B., and Søndergaard, J., 2002, "Aspects of the Matlab Toolbox DACE," IMM-TR2002-13, Technical University of Denmark, DK.
71. Makinen, R., Neittaanmaki, J., Periaux, J. and Toivanen, J., 1998, "A Genetic Algorithm for Multiobjective Design Optimization in aerodynamics and electromagnetics," *Computational Fluid Dynamics, Proceedings of the ECCOMAS 98 Conference*, Vol. 2, pp. 418-422, Wiley.
72. Martin, J. D., and Simpson, T. W., 2005, "Use of Kriging Models to Approximate Deterministic Computer Models," *AIAA Journal*, Vol. 43, No. 4, pp. 853-863.
73. MATLAB® The Language of Technical Computing, 2007, User Manual, The MathWorks Inc.
74. McGill, R., Tukey, J. W., and Larsen W. A., 1978, "Variations of Box Plots," *The American Statistician*, Vol. 32, No. 1, pp. 12-16.
75. McKay, M. D., Beckman, R. J., and Conover, W. J., 1979, "A Comparison of Three Methods for Selecting Values of Input Variables in the Analysis of Response from a Computer Code," *Technometrics*, Vol. 21, No. 2, pp. 239-245.
76. Meckesheimer, M., Booker, A. J., Barton, R. R., and Simpson T. W., "Computationally Inexpensive Metamodel Assessment Strategies," 2002, *AIAA Journal*, Vol. 40, No. 10, pp. 2053-2060.
77. Miettinen, K., 1999, *Nonlinear Multiobjective Optimization*, Kluwer.

78. Morini, G. L., 2006, "Scaling Effects for Liquid Flows in Microchannels," *Heat Transfer Engineering*, Vol. 27, No. 4, pp. 64-73.
79. Myers, R. H., and Montgomery, D. C., 2002, *Response Surface Methodology: Process and Product Optimization Using Designed Experiments*, John Wiley & Sons, New York.
80. Nam, D., and Park, C. H., 2000, "Multiobjective Simulated Annealing: A Comparative Study to Evolutionary Algorithms," *International Journal of Fuzzy Systems*, Vol. 2, No. 2, pp. 87—97.
81. Osio, I. G., and Amon, C. H., 1996, "An engineering design methodology with multi-stage Bayesian surrogates and optimal sampling," *Research in Engineering Design*, Vol.8, pp. 189-206.
82. Owen, A., 1992, "Orthogonal Arrays for Computer Experiments, Integration and Visualization," *Statistica Sinica*, Vol. 2, pp.439-452.
83. Park, K., Oh P-K., and Lim, H-J., 2006, "The application of the CFD and Kriging method to an optimization of heat sink," *International Journal of Heat and Mass Transfer*, Vol. 49, pp. 3439-3447.
84. Perez-Segarra, C. D., Lifante, C., Oliet, C., Cadafalch, J., 2002, "CFD studies on fin and tube heat exchanger: critical analysis of the numerical solutions reliability," in the *Proceedings of the Third International Conference on Engineering Computational Technology*, Stirling, Scotland, pp. 81-82.

85. Radermacher, R., and Azarm, S., 2007, "Multi-Objective Optimization of Microscale Heat Exchange Technology," *ONR Thermal Management Program Review*, September 2007.
86. Radermacher, R., and Azarm, S., Abdelaziz O., and Aute, V., 2007, *Next Generation Heat Exchangers Workshop*, May 15, 2007, University of Maryland.
87. Romero, D. A., Amon, C. H., and Finger, S., 2006, "On Adaptive Sampling for Single and Multi-Response Bayesian Surrogate Models," in *Proceedings of the ASME International Design Engineering Technical Conference*, Philadelphia, PA
88. Sacks, J., Welch, W. J., Mitchell, T. J., and Wynn, H. P., 1989, "Design and Analysis of Computer Experiments," *Statistical Science*, Vol.4, No.4, pp. 409–435.
89. Sasena, M. J., 2002, "Adaptive Experimental Design Applied to an Ergonomics Testing Procedure", in *Proceedings of the ASME International Design Engineering Technical Conference*, Montreal, Canada.
90. Sasena, M. J., Papalambros, P. Y., Goovaerts, P., 2000, "Metamodeling Sampling Criteria in Global Optimization Framework", in *Proceedings of the 8th AIAA/USAF/ISSMO Symposium on Multidisciplinary Analysis and Optimization*, Long Beach CA.

91. Schaffler, S., Schultz, R., Weinzierl, K., 2002, "Stochastic Method for the Solution of unconstrained vector optimization problems", *Journal of Optimization Theory and Applications*, Vol. 114, No. 1, pp. 209-222.
92. Schwentker, A., Aute, V., Radermacher, R., and Mercer, K., 2005, "Simulation and Design Tool for Microchannel Heat Exchangers", in the *Proceedings of the Fifth International Conference on Compact, Ultra-compact Heat Exchangers*, British Columbia, Canada.
93. Serafini, P., 1992, "Simulated Annealing for Multiple Objective Optimization Problems," *Proceedings of the 10th International Conference on Multiple Criteria Decision Making*, Taipei, pp. 87-96.
94. Shah, R. K., and Sekulic, D. P., 2003, *Fundamentals of Heat Exchanger Design*, Wiley.
95. Shannon, C. E., 1948, "A Mathematical Theory of Communication", *Bell Technical Journal*, Vol. 27, pp. 379-423 and pp. 623-656
96. Shao, T., and Krishnamurty, S., 2008, "A Clustering-Based Surrogate Model Updating Approach to Simulation-Based Engineering Design," *Journal of Mechanical Design*, Vol. 130, pp. 041101-1 – 041101-13.
97. Shewry, M. C., and Wynn, H. P., 1987, "Maximum Entropy Sampling", *Journal of Applied Statistics*, Vol. 14, pp. 165-170
98. Shukla, P. K., Deb, K., and Tiwari, S., 2005, "Comparing Classical Generating Methods with Evolutionary Multi-Objective Optimization Methods", EMO 2005

99. Simpson, T. W., Peplinski, J. D., Koch, P. N., and Allen, J. K., 2001, "Metamodels for Computer-based Engineering Design: Survey and recommendations", *Engineering With Computers*, Vol. 17, pp 129-150.
100. Singh, V., Aute V., and Radermacher R., 2008, "Numerical Approach for Modeling Air-to-Refrigerant Fin and Tube Heat Exchanger with Tube to Tube Heat Transfer," *International Journal of Refrigeration*, Article in Press, doi:10.1016/j.ijrefrig.2008.03.013.
101. Srinivas, N, and Deb, K., 1994, "Multiobjective Optimization Using Nondominated Sorting in Genetic Algorithms," *Evolutionary Computation*, Vol. 2, No. 3, pp. 221-248.
102. Steuer, R. E., 1986, *Multiple Criteria Optimization: Theory, Computation and Application*, New York, Wiley.
103. Taguchi, G., (1987), *System of Experimental Design*, Edited by Don Clausing, American Supplier Institute, Dearborn, MI, 1987.
104. Timmel, G., 1980, "Ein stochastisches suchverfahren zur bestimmung der optimalen kombinationen bei statistischen polzkriteriellen optimierungsaufgaben", *Wiss. Z. TH. Illmenau*, Vol. 6, pp. 159-174.
105. Van Veldhuizen, D. A. and Lamont, G B., 1998, "Multiobjective Evolutionary Algorithms Research: A History and Analysis," *Technical Report TR-98-03*, Air Force Institute of Technology, Wright-Patterson AFB, OH.

106. Ver Hoef, J. M. and Cressie, N., 1993, "Multivariable spatial prediction," *Journal of Mathematical Geology*, Vol. 25, No.2, p. 219-240
107. Versteeg, H. K. and Malalasekera, W., 1995, *An Introduction to Computational Fluid Dynamics: The Finite Volume Method*, Longman Scientific and Technical.
108. Wang, G. G., and Shan, S., 2007, "Review of Metamodeling Techniques in Support of Engineering Design Optimization", *Journal of Mechanical Design*, April 2007, Vol. 129, No. 4, pp. 369-463.
109. Watson, A. G., and Barnes, R. J., 1995, "Infill Sampling Criteria to Locate Extremes," *Mathematical Geology*, Vol. 27, No. 5, pp. 589-608.
110. Webb, R. L., and Kim, N. H., 2005, *Principles of Enhanced Heat Transfer*, Taylor and Francis.
111. Zitzler, E. and Thiele, L., 1998, "An Evolutionary Algorithm for Multiobjective Optimization: The Strength Pareto Approach", *Technical Report 43*, Zurich, Switzerland: Computer Engineering and Networks Laboratory (TIK), Swiss Federal Institute of Technology (ETH).